ENDOGENOUS LIPID CHEMOATTRACTANTS AND EXTRACELLULAR MATRIX PROTEINS INVOLVED IN DEVELOPMENT OF *MYXOCOCCUS XANTHUS*

by

PATRICK DAVID CURTIS

(Under the Direction of Lawrence J. Shimkets)

ABSTRACT

The soil bacterium *Myxococcus xanthus* is a model organism to study multicellular development and biofilm formation. When starved, swarms of *M. xanthus* cells aggregate into a multicellular architecture called a fruiting body, wherein cells differentiate into metabolically dormant myxospores. Fruiting body formation requires directed cell movement and production of an extracellular matrix (ECM) to facilitate cell-contact dependent motility (Social motility), and biofilm formation. *M. xanthus* displays chemotaxis towards phospholipids derived from its membrane containing the rare fatty acid 16:1ω5c. This study demonstrates that 16:1ω5c is primarily found at the *sn*-1 position within the major membrane phospholipid, phosphatidylethanolamine (PE), which is contrary to the established dogma of fatty acid localization in Gram-negative bacteria. Additionally, 16:1ω5c at the *sn*-1 position stimulates chemotaxis stronger than 16:1ω5c located at the *sn*-2 position. These results suggest that the endogenous lipid chemoattractants may serve as a self-recognition system. Chemotaxis towards a self-recognition marker could facilitate movement of cells into aggregation centers. Lipid chemotaxis is dependent on the ECM-associated zinc metalloprotease FibA, suggesting that the ECM may harbor protein components of extracellular signaling pathways. Protein components

of prokaryotic biofilms are largely unexplored. Twenty one putative ECM-associated proteins were identified, including FibA. Many are novel proteins. A large portion of the putative ECM proteins have lipoprotein secretion signals, unusual for extracellular proteins. An MXAN4860 *pilA* mutant displays a 24 hour delay in fruiting body formation and sporulation compared to the *pilA* parent, indicating that MXAN4860 functions in the FibA-mediated developmental pathway previously described. The ECM provides the main connective network between cells in fruiting bodies and biofilms, and the proteins identified here may be components of novel signaling pathways controlling communal cellular behavior.

INDEX WORDS: *Myxococcus xanthus*, Lipid Chemotaxis, Biofilm, Extracellular Matrix, Hypothetical Proteins, Development

# ENDOGENOUS LIPID CHEMOATTRACTANTS AND EXTRACELLULAR MATRIX PROTEINS INVOLVED IN DEVELOPMENT OF *MYXOCOCCUS XANTHUS*

by

PATRICK DAVID CURTIS

B.S., Purdue University, 2001

A Dissertation Submitted to the Graduate Faculty of The University of Georgia in Partial Fulfillment of the Requirements for the Degree

DOCTOR OF PHILOSOPHY

ATHENS, GEORGIA

2007

ENDOGENOUS LIPID CHEMOATTRACTANTS AND EXTRACELLULAR MATRIX PROTEINS INVOLVED IN DEVELOPMENT OF *MYXOCOCCUS XANTHUS*

by

PATRICK DAVID CURTIS

Major Professor: Lawrence J. Shimkets

Committee: Russell W. Carlson
Harry A. Dailey
Timothy R. Hoover
Eric V. Stabb

Electronic Version Approved:

Maureen Grasso
Dean of the Graduate School
The University of Georgia
May 2007

## DEDICATION

I dedicate this work to my mother, Diane M. Curtis. She has been a source of encouragement, inspiration and support my entire life, no matter the field or endeavor I put myself to. This is for you, Mom.

ACKNOWLEDGEMENTS

First off I must thank my P.I. Larry Shimkets. His guidance and patience has helped me become to the scientist I am today. I can see his stamp on my thought processes and approach to the scientific method, and I understand why he is well respected not just in the myxobacterial community, but the scientific community at large. I also must thank him for putting up with me during the middle when things got rough, for sticking with me until I emerged on the other side. I would also like to thank my committee members Russ Carlson, Harry Dailey, Tim Hoover and Eric Stabb, who helped me to write better, helped me to apply for postdoctoral positions, helped to refocus and reapply my research each year, and provided moral support, often in the form of Packer games.

I also thank the past and present members of the Shimkets lab for their training and support from day 1 in the lab. In particular I must acknowledge Pam Bonner, who was my compatriot, sympathizer, empathizer, psychologist, shoulder-to-lean-on, sister in practice if not blood, and friend for 5 years. Without the people of the lab, I would not have made it as far as I did.

To my friends in and out of the department, thank you for making my time here special and full of fond memories. Thank you to the members of my class, in particular James Henriksen who has been my brew partner, philosophical foil, person to argue with like the 80 year-old grumpy men we were born as, and my best friend. Thanks to Turner Classic movies for keeping me sane the first three years, Blizzard Entertainment for keeping me sane the last three years, and ABC Package and The Shroom for keeping me sane at sporadic points in between.

TABLE OF CONTENTS

Page

LIST OF TABLES

Page

LIST OF FIGURES

Page

# CHAPTER 1

# INTRODUCTION AND LITERATURE REVIEW: METABOLIC PATHWAYS RELEVANT TO PREDATION, SIGNALING, AND DEVELOPMENT[1]

[1] Curtis, P.D. and Shimkets, L.J. Submitted to Myxobacteria III, ASM Press

## Introduction

Genome analysis offers the ability to examine the central metabolism of organisms from a perspective that, while holistic in information content, lacks the accuracy of conclusions derived from sound biochemical and genetic analysis. Shadows of possibilities emerge that only silhouette necessary experimentation. Conversely, biochemical and genetic analyses are incomplete without the genomic knowledge. Here, previously determined biochemical and genetic data are analyzed through the scope of genomic analysis, with particular attention to catabolic and anabolic pathways involved in the basic biology of the myxobacteria.

Genomic annotation was based upon the completed *M. xanthus* genome (Goldman *et al.*, 2006). Metabolic pathways were examined by homology searching using the amino acid sequence for well-characterized enzymes. Metacyc <http://metacyc.org/> contains a compilation of most known pathways, enzymes and genes and has a pathway analysis for *M. xanthus* which was often used as a reference point (Caspi *et al.*, 2006). A limitation of this analysis is its reliance on the annotation conducted by The Institute for Genome Research (TIGR). To reduce problems with annotation errors, all pathways in the chapter were also annotated by hand using BLASTp. Two considerations were used in assigning a function to a putative protein sequence, amino acid identity with known members of the Enzyme Commission (EC) class (>30%) and Cluster of Orthologous Groups (COG) determination by TIGR. A strong hit satisfies both criteria. Gene/protein names adopted below are derived primarily from homologs found in *E. coli* K12 when applicable. This policy deviates from TIGR, which names the genes/proteins after the closest named homolog in the database and does not specify the origin of the name. As with any homology-based search, the results should be considered 'putative' until gene knockouts and enzyme assays confirm the identity and function of the

homolog. The word “putative” is avoided for the sake of brevity, but it should be understood that the proposed pathways simply represent the most likely candidates based on current knowledge.

The first portion of this article entitled ‘Catabolic pathways’ deals with the catabolism of amino acids and lipids as they are the principal carbon and energy sources derived from prey bacteria. The second portion of this article, entitled ‘Anabolic pathways’, highlights the synthesis of lipids because of their unusual chemical structures in myxobacteria, and also the spore-specific components trehalose and ether lipids.

## Catabolic Pathways

Most myxobacteria, including *Myxococcus xanthus*, can catabolize prey microorganisms. *M. xanthus* utilizes amino acids and lipids as carbon and energy sources, incorporates purines and pyrimidines via salvage pathways, but fails to utilize sugars (Bretscher and Kaiser, 1978; Hemphill and Zahler, 1968a, b; Lau *et al.*, 2002; Loebeck and Klein, 1956). The literature supporting these assertions is extensive and will not be reviewed. Rather, genomic evidence for specific pathways involved in assimilation and catabolism will be provided.

Most of the research examining the sources of energy for the myxobacteria have focused on the assimilation of amino acids, not without reason (Bretscher and Kaiser, 1978; Dworkin, 1962). The average *E. coli* cell is composed of roughly 55% dry weight protein (Neidhardt and Umbarger, 1996), by far the largest macromolecule component of the cell. Though lipids represent a much smaller fraction of the total cell mass [9%, (Neidhardt and Umbarger, 1996)], their energetic content is considerable. The catabolism of serine to $CO_2$ will yield approximately 11 ATP, while the catabolism of a 16:0 fatty acid to $CO_2$ will yield approximately 80 ATP. Therefore, both cellular fractions represent rich sources of energy.

**Amino Acid Catabolism**

In most cases there is excellent agreement between the presence of a particular amino acid catabolic pathway, and the ability of that amino acid to stimulate growth in defined and minimal media. The pathways are listed below according to amino acid, roughly in alphabetical order.

**Alanine.** *M. xanthus* uses alanine dehydrogenase for catabolism of L-alanine.

**L-alanine + $NAD^+$ + $H_2O$ → pyruvate + NADH + ammonia**

EC 1.4.1.1
alanine dehydrogenase
MXAN4146

L-alanine can also be converted to D-alanine for use in peptidoglycan biosynthesis using alanine racemase (EC 5.1.1.1, Alr, MXAN7160). D-alanine may be catabolized to pyruvate using the iron-containing alcohol dehydrogenase MXAN5629.

**Arginine.** *M. xanthus* contains many pathways for catabolizing arginine so it is surprising that arginine has not been exploited as a major component in minimal and defined media (Bretscher and Kaiser, 1978). Collectively these pathways produce L-glutamate, putrescine (and hence other polyamines), L-proline, and succinate. The bulk of the arginine degradation in *E. coli* is carried out by the arginine succinyltransferase (AST) pathway, which is found in many Proteobacteria that use arginine as a sole carbon source. This pathway is not present in *M. xanthus*, which may explain the lack of importance for arginine in minimal media.

Several arginine catabolic pathways use arginase to hydrolyze L-arginine. Different organisms have variations of the arginase pathway depending on the fate of the catabolic

products. The classical arginase pathway yields L-glutamate. There is weak homology for arginase, (26-31% amino acid identity), but beyond that the pathway is conserved in *M. xanthus*.

**L-arginine → L-ornithine → L-glutamate γ-semialdehyde**
EC 3.5.3.1 arginase MXAN4431
EC 2.6.1.13 ornithine amino transferase MXAN7377

**L-glutamate γ-semialdehyde → pyrroline 5-carboxylate → L-glutamate**
Spontaneous
EC 1.5.1.12 1-pyrroline-5-carboxylate dehydrogenase MXAN5891

There is a branch in this pathway as ornithine cyclodeaminase (EC 4.3.1.12, MXAN7463) converts L-ornithine to L-proline.

The arginine decarboxylase pathway produces putrescine as an intermediate for synthesis of other polyamines, and succinate as an end product.

**L-arginine → agmatine → putrescine → 4-amino-butyraldehyde**
EC 4.1.1.19 arginine decarboxylase MXAN2742
EC 3.5.3.11 agmatinase MXAN4431
EC 2.6.1.29 putrescine transaminase MXAN3014 or MXAN7377

**4-amino-butyraldehyde → 4-aminobutyrate → succinate semialdehyde**
EC 1.2.1.19 γ-aminobutyraldehyde dehydrogenase MXAN0921
EC 2.6.1.19 4-aminobutyrate transaminase MXAN3014

**succinate semialdehyde → succinate**
EC 1.2.1.16 succinate semialdehyde dehydrogenase MXAN2844

*E. coli* has two forms of arginine decarboxylase. Constitutively-expressed SpeA is used for the biosynthesis of putrescine, while inducibly-expressed AdiA is used for arginine catabolism. Interestingly, there is no homolog for AdiA but there is strong homology for a SpeA in *M. xanthus*. All the other elements of the pathway to degrade arginine to succinate exist,

suggesting that SpeA plays a dual role in biosynthesis of putrescine and catabolism of arginine. *M. xanthus* contains 2 homologs of *E. coli* transaminase YgiG (MXAN3014 and MXAN7377). *E. coli* uses at least three different enzymes to catalyze the last reaction, Sad, AldA, and GabD. There are many homologs of each in *M. xanthus*, and though MXAN2844 is annotated as succinate semialdehyde dehydrogenase, there are other possibilities.

**Asparagine/Aspartate.** *E. coli* K12 has three different types of L-asparaginases to deaminate asparagine, two of which are present in *M. xanthus*. *E. coli* aspartase (EC 4.3.1.1) removes the nitrogen from aspartate to produce fumarate but there is no evidence for this enzyme in *M. xanthus*. Instead *M. xanthus* appears to use a version of this pathway found in some Gram-positive bacteria and mammals to produce phosphoenolpyruvate.

**L-asparagine → L-aspartate + α-ketoglutarate → oxaloacetate + L-glutamate**

EC 3.5.1.1
L-asparaginase I
MXAN5198
L-asparaginase II
MXAN1160

EC 2.6.1.1
aspartate aminotransferase
MXAN3386

**Oxaloacetate + GTP → phosphoenolpyruvate + GDP + $CO_2$**

EC 4.1.1.32
Phosphoenolpyruvate carboxykinase
MXAN1264

**Cysteine.** Two pathways are known for the catabolism of L-cysteine to pyruvate; at least one may exist in *M. xanthus*. In *E. coli* two desulfhydrases convert L-cysteine to pyruvate in a single step. Tryptophanase (TnaA, also used in tryptophan catabolism) does not appear to have a homolog in *M. xanthus*. MetC, β-cystathionase (also used in methionine synthesis), has four homologs in *M. xanthus*: MXAN2035, MXAN0969, MXAN0970, and MXAN1955. Of these, MXAN2035 shares the most homology with the bacterial and yeast genes.

**L-cysteine + $H_2O$ → pyruvate + ammonia + $H_2S$**

EC 4.4.1.1
L-cysteine desulfhydrase
MXAN2035

The oxidation of cysteine to 3-sulfinoalanine and eventually to pyruvate is the major route of cysteine catabolism in mammals. The first step in this pathway involves cysteine dioxygenase (EC 1.13.11.20). There is weak homology for this enzyme in *M. xanthus* (MXAN4718). The remaining enzyme in the pathway, aspartate amino transferase (MXAN3386), is likely to be present (see catabolism of asparagine/aspartate).

**Glutamine/Glutamate.** Two enzymes convert L-glutamine to L-glutamate: glutaminase and glutamate synthase. The biochemical properties of the two major *E. coli* glutaminases (EC 3.5.1.2) have been studied in detail but the genes encoding them have not been identified. Two putative glutaminase genes have been described in *E. coli*, *ybaS* and *yneH*, however neither has a homolog in *M. xanthus*. Nor is there a homolog of human glutaminase C. A number of amidotransferases, such as anthranilate synthetase, have glutaminase activity and may contribute to glutamine catabolism.

The biochemistry and genetics of glutamate synthase is known from a variety of bacteria. Glutamate synthase (EC 1.4.1.13) catalyzes the transamination of α-ketoglutarate to produce two glutamates. The *Klebsiella aerogenes* enzyme consists of a single 175 kDa protein whereas the *E. coli* enzyme consists of 53 kDa and 135 kDa subunits. *M. xanthus* has adjacent genes encoding two subunits like those in *E. coli*, MXAN3917 and MXAN3918.

One of the major catabolic pathways for glutamate involves deamination to α-ketoglutarate by glutamate dehydrogenase. This is a key reaction in the catabolism of arginine,

glutamine, histidine and proline, all of which produce glutamate as an intermediate. Glutamate dehydrogenase catalyzes a reversible reaction that can be either anabolic or catabolic depending on the conditions and the organism. *M. xanthus* glutamate dehydrogenase (GdhA) is MXAN5873. Mammalian glutamate dehydrogenase uses both $NAD^+$ and $NADP^+$ as cofactors (EC 1.4.1.3). Most prokaryotic enzymes can use either $NAD^+$ (EC 1.4.1.2) or $NADP^+$ (EC 1.4.1.4). The TIGR annotation gives the *M. xanthus* enzyme as EC 1.4.1.3, suggesting this enzyme may use both cofactors.

The primary pathway for the use of L-glutamate as a carbon source in *E. coli* is transamination of oxaloacetate to form L-aspartate and α-ketoglutarate by AspC.

**L-glutamine** → **L-glutamate** → **L-aspartate**
**+ α-ketoglutarate** **+ oxaloacetate** **+ α-ketoglutarate**

| EC 1.4.1.13 | EC 2.6.1.1 |
|---|---|
| glutamate synthase | aspartate aminotransferase |
| MXAN3917, large subunit<br>MXAN3918, small sununit | MXAN3386 |

Aspartate aminotransferase (EC 2.6.1.1) resembling that of a *Bacillus* species is found in the *M. xanthus* genome, MXAN3386, and is dramatically different from the *E. coli* AspC. AspA (EC 4.3.1.1), which produces fumarate from L-aspartate by deamination, appears to be absent suggesting that the aspartate is directed toward the synthesis of the aspartate family of amino acids or catabolized to oxaloacetate and phosphoenolpyruvate (see asparagine/aspartate).

Glutamate can also enter the TCA cycle as succinate using the three-step glutamate decarboxylase pathway in which the final two steps are identical to those for putrescine degradation (see arginine).

**L-glutamate** → **4-aminobutyrate** → **succinate semialdehyde** → **succinate**

| EC 4.1.1.15 | EC 2.6.1.19 | EC 1.2.1.16 |
|---|---|---|
| glutamate decarboxylase | 4-aminobutyrate aminotransferase | succinate semialdehyde dehydrogenase |
| MXAN6783 | MXAN3014 | MXAN2844 |

There is also evidence for a second bacterial pathway for catabolizing glutamate to succinate

**L-glutamate → α-ketoglutarate → S-succinyl-dihyrolipoamide → succinyl-CoA**

| EC 2.6.1.1 | EC 1.2.4.2 | EC 2.3.1.61 |
|---|---|---|
| aspartate aminotransferase | 2-oxoglutarate dehydrogenase | 2-oxoglutarate dehydrogenase |
| MXAN3386 | MXAN6035, E1 component | MXAN6036, E2 component |

**succinyl-CoA → succinate**

EC 6.2.1.5
succinyl-CoA synthase
MXAN3542, α subunit
MXAN3541, β subunit

**Glycine.** Glycine plays a key role in C1 anabolism through the generation of the C1 donor $N^{10}$-formyl-tetrahydrofolate. All elements of the pathway are present in *M. xanthus* with the exception of the anaerobic formate dehydrogenase. These results suggest that the pathway is strictly anabolic unless another route exists for oxidation of formate.

Four polypeptides are involved in the glycine cleavage pathway, GcvHPT and LpdA, with the first three genes forming an operon in both *E. coli* and *M. xanthus*.

**Glycine + tetrahydrofolate → 5, 10-methylene-tetrahydrofolate**

EC 1.4.4.2 and EC 2.1.2.10
glycine dehydrogenase, MXAN3042
tetrahydrofolate aminomethyltransferase
MXAN3041, MXAN3040, MXAN6341

**5, 10-methylene-tetrahydrofolate → 5,10-methenyl-tetrahydrofolate**

EC 1.5.1.15
methylenetetrahydrofolate dehydrogeanse
MXAN1095

**5,10-methenyl-tetrahydrofolate → $N^{10}$-formyl-tetrahydrofolate**

EC 3.5.4.9
methenyl tetrahydrofolate cyclohydrolase
MXAN2226

**$N^{10}$-formyl-tetrahydrofolate + phosphate + ADP → formate + tetrahydrofolate + ATP**

EC 6.3.4.3
formate tetrahydroformate ligase
MXAN0175

**Histidine.** *M. xanthus* may catabolize L-histidine to L-glutamate. The first three enzymes in the pathway have strong *M. xanthus* homologs but here the trail runs dry. *B. subtilis* uses EC 3.5.3.8 for the last step, but evidence for this enzyme in *M. xanthus* is lacking. *Pseudomonas* uses two enzymes for the last step, EC 3.5.3.13 and EC 3.5.1.68, to remove ammonia and formate sequentially. The first of these has a homolog in the *M. xanthus* genome (formiminoglutamate deiminase, MXAN1010), but a homolog of the formate hydrolase is not apparent.

**L-histidine → urocanate → 4-imidazolone-5-propionate**

| EC 4.3.1.3 | EC 4.2.1.49 |
|---|---|
| histidine ammonia lyase | urocanase |
| MXAN3465 | MXAN4343 |

**4-imidazolone-5-propionate → N-formimine-L-glutamate → L-glutamate**

| EC 3.5.2.7 | ?? |
|---|---|
| imidazolone-5-propionatase | |
| MXAN4345 | |

**Isoleucine/Leucine/Valine.** The branched chain amino acids are unique in that they are essential for growth in all *M. xanthus* isolates that have been examined and are also essential for secondary metabolite production in myxobacteria and other organisms (Bretscher and Kaiser, 1978). Catabolism of these amino acids appears directed primarily at their use as primers for the synthesis of branched chain fatty acids (see Lipid Biogenesis, pg. 25). The key enzyme in this process is the branched chain keto acid dehydrogenase (BCKAD) complex, also known as Esg in *M. xanthus*, which catalyzes the oxidative decarboxylation of the branched-chain $\alpha$-keto acids derived from leucine, isoleucine and valine. In mammals the complex consists of 12 branched-chain $\alpha$-ketoacid dehydrogenase (E1) subunits and 6 dihydrolipoyl dehydrogenase (E3) subunits

noncovalently associated with a core of 24 dihydrolipoyl transacylase (E2) components. A BCKAD kinase inactivates the complex by phosphorylation of alpha subunits of the heterotetrameric ($\alpha 2ß2$) E1 component; BCKAD phosphatase removes phosphates to activate the complex. The complex is present in *M. xanthus* though there is no evidence for regulation by covalent modification.

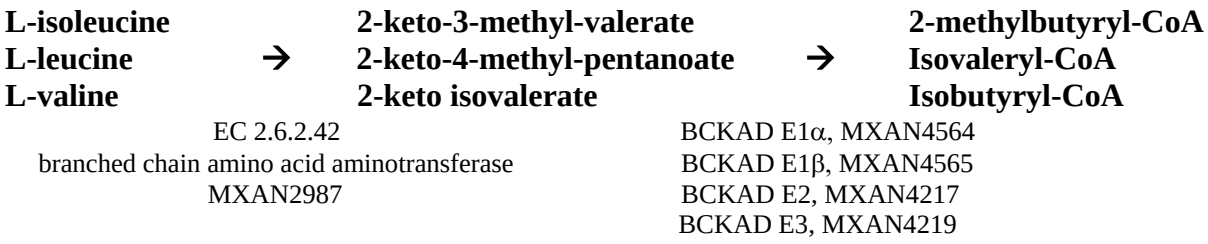


**Lysine.** At least 9 pathways are known for the catabolism of lysine that vary in the initial products. The genes are known for only three of these pathways. In *E. coli*, lysine is decarboxylated to cadaverine by IdcC or CadA, neither of which is apparently present in *M. xanthus*. In plants and animals, lysine is oxidized to saccharopine using a unique dehydrogenase that we did not find in *M. xanthus*. In fungi, lysine is degraded to glutarate following acetylation of the 6 amino group with a unique lysine $N^6$ acetyltransferase, which is also missing in *M. xanthus*. Therefore it is not clear whether lysine is catabolized.

**Methionine.** The methionine catabolic pathway is similar to that observed in mammals and involves the synthesis of S-adenosyl-L-methionine for transmethylation reactions and then hydrolysis of adenosine to produce homocysteine. Homocysteine forms a branch point in the pathway and may either be recycled to L-methionine, using the vitamin B12-dependent methionine synthase (not shown), or degraded to succinate.

**L-methionine → *S*-adenosyl-L-methionine → *S*-adenosyl-homocysteine**

EC 2.5.1.6 — methionine adenosyltransferase — MXAN6517

EC 2.1.1.73 — DNA methyltransferase — MXAN3598

***S*-adenosyl-homocysteine → homocysteine → L-methionine**

EC 3.3.1.1 — *S*-adenosylhomocysteine hydrolase — MXAN6516

EC 2.1.1.13 — methionine synthase — MXAN1971

**Homocysteine → cystathionine → 2-oxobutanoate → propionyl CoA**

EC 4.2.1.22 — cystathionine β-synthase — MXAN2041

EC 4.4.1.1 — cystathionine γ-lyase — MXAN3917

no EC number or gene

**propionyl CoA → (S)-methyl-malonyl-CoA → (R)-methyl-malonyl-CoA**

EC 6.4.1.3 — propionyl-CoA carboxylase — MXAN1111, α subunit; MXAN1113, β subunit

EC 5.1.99.1 — no gene associated with activity

**(R)-methyl-malonyl-CoA → succinyl-CoA**

EC 5.4.99.2 — methylmalonyl-CoA mutase — MXAN2263, α subunit; MXAN2264, β subunit

**Phenylalanine/Tyrosine.** Only a single aerobic phenylalanine/tyrosine catabolic pathway is known. In this pathway phenylalanine is catabolized to tyrosine by phenylalanine 4-hydroxylase (EC 1.14.16.1, MXAN5127) and eventually to succinate. While homologs for genes involved in some later steps are found in *M. xanthus*, no homolog for the second step in the catabolic pathway (EC 2.6.1.5, tyrosine aminotransferase) is found. In *M. xanthus* $^{14}$C-labelled phenylalanine is converted to tyrosine and the excess tyrosine secreted into the growth medium (Hemphill and Zahler, 1968a), suggesting that this pathway is, indeed, blocked at the first step of tyrosine catabolism.

**L-phenylalanine → L-tyrosine**

EC 1.14.16.1 — phenylalanine 4-hydroxylase — MXAN5127

**Proline.** There is a single pathway for degradation of proline that involves the sequential action of proline dehydrogenase and 1-pyrroline-5-carboxylate dehydrogenase to produce glutamate. In bacteria the two enzyme domains are usually encoded by a single gene whereas in eukaryotes they are separate genes. *M. xanthus* appears to have separate and unlinked genes encoding these proline degradation enzymes.

**L-proline → 1-pyrroline 5-carboxylate → L-glutamate**

| EC 1.5.99.8 | EC 1.5.1.12 |
|---|---|
| proline dehydrogenase | 1-pyrroline-5-carboxylate dehydrogenase |
| MXAN7405 | MXAN5891 |

**Serine.** L-serine is deaminated to pyruvate and ammonia in *E. coli* by three homologous serine deaminases, but only one is found in *M. xanthus*.

**L-serine → pyruvate + ammonia**

EC 4.3.1.17
serine deaminase
MXAN6186

**Threonine.** L-threonine can be converted to many metabolites by pathways whose biochemistry has far surpassed the genetics. All the known pathways begin with either deamination to 2-oxobutanoate or oxidation to 2-amino-3-oxobutanoate. In *M. xanthus* the former reaction appears to be present while the latter reaction is doubtful. 2-oxobutanoate is then catabolized to cystathionine, an intermediate in methionine catabolism that can be used to generate succinate, methionine or pyruvate (see Methionine).

**L-threonine → 2-oxobutanoate + cysteine + ammonia → cystathionine**

| EC 4.3.1.19 | EC 4.4.1.1 |
|---|---|
| threonine dehydratase | cystathionine γ-lyase |
| MXAN5874 | MXAN2035 |
| threonine deaminase | |
| MXAN6186 | |

**Tryptophan.** There are seven known pathways for the catabolism of tryptophan. The biochemistry has been examined more extensively than the genetics due to the fact that various products of tryptophan are plant hormones, dyes, or putrid byproducts of cheese production. The simplest pathway is the conversion of tryptophan to pyruvate and indole in a single step by tryptophanase. This pathway is intriguing as indole induces spore formation in *Stigmatella* and may be a cell-cell signal (Stamm *et al.*, 2005). Neither a homolog of this enzyme nor any enzymes in the other pathways were detected in *M. xanthus*. Additionally, no tryptophanase homolog could be found in the *Stigmatella aurantiaca* genome. Some parts of a eukaryotic catabolic pathway are found, but genes encoding several of the enzymes of the pathway are missing.

In summary, genomic evidence suggests that *M. xanthus* is missing pathways for catabolism of seven amino acids: leucine, isoleucine, valine, phenylalanine, tyrosine, tryptophan and lysine. The absence of catabolic pathways for leucine, isoleucine and valine is not surprising given that *M. xanthus* is auxotrophic for these amino acids (Bretscher and Kaiser, 1978), and also uses them in fatty acid biosynthesis (see Lipid Biogenesis, pg. 25). Catabolism of these amino acids may strain branched chain fatty acid synthesis, which appears to be necessary for development (Toal *et al.*, 1995). The absence of phenylalanine/tyrosine, tryptophan and lysine catabolic pathways is a mystery. It is interesting to note that of the mixture of amino acids that comprise the A signal (an early developmental signal), leucine, isoleucine, phenylalanine, tyrosine and tryptophan account for 63% of the A signal activity (Kuspa *et al.*, 1992).

**Purine and pyrimidine salvage.**

A variety of labeling and analog toxicity studies indicate that purines and pyrimidines are efficiently salvaged in *M. xanthus*, and these will not be reviewed here (Hemphill and Zahler, 1968a; Tsai and Westby, 1978). *M. xanthus* has a suite of purine and pyrimidine salvage pathways comparable to what is found in *E. coli* with several options for converting nucleobases and nucleosides into nucleotides. The preferred method of nucleoside and deoxynucleoside salvage in *E. coli* is to first remove the (deoxy)ribose moiety from the (deoxy)nucleoside, then use a phosphoribosyltransferase to create the nucleotide monophosphate. *E. coli* can also transport the (deoxy)nucleosides and then phosphorylate them.

Adenosine and deoxyadenosine are salvaged through deamination to inosine/deoxyinosine (EC 3.5.4.4, Add, MXAN1519) and hydrolysis to hypoxanthine (purine nucleoside phosphorylase, DeoD, MXAN2306). Guanosine and deoxyguanosine are hydrolyzed to guanine (purine nucleoside phosphorylase, DeoD, MXAN2306). Phosphoribosyltransferases were found for adenine (EC 2.4.2.7, Apt, MXAN5352) and uracil (EC 2.4.2.9, Upp, MXAN0124). *E. coli* has two additional phosphoribosyltransferases both of which function on hypoxanthine and guanine. The *M. xanthus* homolog appears to be more closely related to one with a bias for hypoxanthine (EC 2.4.2.-, Hyp, MXAN5070), but it should be assumed from labeling studies that *M. xanthus* can utilize guanine as well.

Uridine and cytidine are phosphorylated to UMP/CMP by uridine kinase (EC 2.7.1.48, Udk, MXAN4159). Thymidine and thymine nucleotides are deoxy compounds with no ribonucleotide counterparts; thymidine is phosphorylated to TMP by thymidine kinase (EC 2.7.1.21, Tdk, MXAN5072). Deoxycytidine is deaminated to deoxyuridine and either degraded to uracil or and phosphorylated to deoxyUMP by thymidine kinase (EC 2.7.1.21, Tdk,

MXAN5072) then converted to TMP by thymidylate synthase (EC 2.1.1.45, ThyA, MXAN5942).

It should be noted from the genomic studies here and from previous labeling studies (Hemphill and Zahler, 1968a), that the main fate of exogenous purines/pyrimidines is incorporation into nucleic acids and not degradation for energy generation.

**Lipid Catabolism.**

Lipid oxidation has been demonstrated by $^{14}C$ labeling experiments in *M. virescens* (Loebeck and Klein, 1956) and methyloleate feeding in *M. xanthus* (Lau *et al.*, 2002). The principle, but not sole, source of lipids in prey bacteria are the phospholipids, which may be hydrolyzed by four classes of lipases in *M. xanthus*: phospholipase D, patatins, α/β hydrolases and GDSL lipases. Phospholipase D (MXAN6753) removes the head group leaving phosphate at the *sn*-3 position on the glycerol backbone. Fatty acids are located at the *sn*-1 and *sn*-2 position in phospholipids. Three classes of lipases generate glycerol and fatty acids (Moraleda-Muñoz and Shimkets, 2007). Both are robust carbon sources although glycerol utilization by *M. xanthus* has not been reported. Interestingly, most lipase homologs identified here are not predicted to have *sn* position-specific activity, perhaps indicating their importance for catabolism over lipid signaling.

**Lipases.** Patatins were originally identified as the major storage protein in potato, but biochemical characterization revealed fatty esterase activity, usually on compounds containing a single fatty acyl chain (Galliard, 1971). MXAN3852 contains the conserved active site, the oxyanion hole, and other features that suggest it may be catalytically functional. Three other

patatin homologs are present in *M. xanthus*, but may be missing motifs necessary for catalytic function. MXAN3852 is only expressed during starvation, and deletion results in no phenotype with regards to aggregation and sporulation on TPM agar (Moraleda-Muñoz and Shimkets, 2007). On CF agar there is a 24 hour delay to both aggregation and sporulation, and the fruiting bodies are unusually large and amorphous.

The α/β hydrolases contain an eight stranded β sheet (stabilized by intervening α helices) formed of two antiparallel β strands followed by six parallel β strands (Ollis *et al.*, 1992). Many α/β hydrolases are proteases, but at least two putative α/β hydrolases in *M. xanthus* are likely lipases. MXAN5522 (a triacyl glycerol lipase acting on all three *sn* positions) is located directly upstream of a lipase chaperone homolog (MXAN5523). Lipases often have chaperones to prevent catalytic activity until they are secreted. This lipase is expressed during both vegetative growth and development (Moraleda-Muñoz and Shimkets, 2007). Interestingly, it shows a sharp spike of expression 24 hours into development. Deletion of MXAN5522 results in 3-fold increased spore yield on both TPM and CF. While there is no defect in aggregation on TPM, this strain aggregates 24 hours faster than WT on CF (Moraleda-Muñoz and Shimkets, 2007). A possible explanation for the increased rate of sporulation in this strain may be that it is unable to utilize storage lipids for energy, thereby starving faster than normal. MXAN4638 is a putative lysophopholipase, which removes the fatty acid from lysophospholipids. Interestingly, disruption of the gene upstream and operonic with MXAN4638 generates an A motility defect (Youderian *et al.*, 2003).

*M. xanthus* contains two GDSL lipase homologs (MXAN5500 and MXAN4569), which are general bacterial lipases that liberate fatty acids from either *sn* position in phospholipids. The C-terminal domain is a β barrel porin that forms a pore in the outer membrane through which the

N-terminal catalytic domain is secreted, and ultimately anchors the lipase facing away from the membrane. Both *M. xanthus* homologs lack the C-terminal anchoring domain. There is one report of a GDSL lipase anchored to the membrane by an N-terminal acylation (Klingsbichel, 1996), and though MXAN4569 appears to have an acylation signal, MXAN5500 does not. The lack of an anchoring domain may be an indication that MXAN5500 diffuses away from the cell. Deletion of MXAN4569 has no effect on aggregation or sporulation on TPM (Moraleda-Muñoz and Shimkets, 2007). On CF, aggregation shows a mild fruiting body morphology defect and sporulation proceeds approximately 24 hours faster than WT.

The lipases from MXAN3852, MXAN5522 and MXAN4569 were all tested *in vitro* against various tagged lipid derivatives to elucidate fatty acyl chain specificity. All lipases showed preferences for short acyl chains and had the highest activity for two carbon chain lengths.

**β Oxidation**. Fatty acids are usually degraded by β oxidation, where two-carbon acetate units are sequentially removed from the carboxyl end of the fatty acid also known as the Δ terminus, as opposed to the methyl end or ω terminus (for review see (Clark and Cronan, 1996)).

This process resembles fatty acid elongation in reverse. FadL (MXAN7040) translocates the free fatty acid across the outer membrane, which is then translocated across the inner membrane and esterified to a CoA moiety by FadD (Weimar *et al.*, 2002). *M. xanthus* contains as many as 10 FadD homologs (EC 6.2.1.3, the most likely homologs are MXAN1573, MXAN7148, MXAN0216 and MXAN0225). Next, a *trans* double bond is introduced 2 carbons from the Δ terminus ($\Delta^2$) by FadE. While the *M. xanthus* FadE (EC 1.3.99.3) homologs are not clear, MXAN3795 and MXAN3797 are conspicuous possibilities as they appear to be in an

operon with MXAN3791, an AtoB homolog. Also interesting is MXAN6989, which encodes a peptide with strong homology to the C terminus of FadE and appears to be in an operon with FadA and FadB homologs.

Next, water is substituted into the double bond to create a β-hydroxy fatty acyl-CoA which is oxidized to a β-keto group. Both these reactions are performed by the multifunctional fatty acid oxidation complex β subunit FadB. Additionally, FadB epimerizes D-β-hydroxy fatty acyl CoA to L-β-hydroxy fatty acyl-CoA for further processing. *M. xanthus* contains two FadB homologs (EC 1.1.1.35, MXAN5371 and MXAN6987). Upon generation of the β-keto fatty acyl-CoA, the fatty acid oxidation complex α subunit (FadA) cleaves the chain at the β-keto group by adding a CoA moiety, creating acetyl-CoA and the fatty acyl-CoA truncated by two carbons. *M. xanthus* contains two FadA homologs, (EC 2.3.1.16) MXAN5372 and MXAN6988 that are located next to FadB homologs. This β oxidation cycle continues until there are only 4 carbons left on the fatty acid chain when the chain is hydrolyzed to two acetyl-CoA units by AtoB (EC 2.3.1.9, MXAN3791 and MXAN5135).

For fatty acids with unsaturations at odd numbers of carbons from the carboxyl terminus, FadB isomerizes the *cis*-$\Delta^3$ double bond to *trans*-$\Delta^2$. Fatty acids with unsaturations at even numbers of carbons from the carboxyl terminus are reduced by 2,4-dienoyl-CoA reductase (EC 1.3.1.34, FadH, MXAN3389). This enzyme reduces the second double bond of the *trans*-$\Delta^2$, *cis*-$\Delta^4$ intermediate to *trans*-$\Delta^2$ fatty acyl-CoA, which is further oxidized by the FadE and the unsaturated fatty acid degradation pathway (Hubbard *et al.*, 2003).

Like *E. coli*, *M. xanthus* contains two sets of both major β oxidation pathway enzymes, FadA and FadB. In *E. coli* one set functions under aerobic conditions while the other set works under anaerobic conditions (Campbell *et al.*, 2003). While *M. xanthus* is a strict aerobe, it is

possible that the cells may encounter periods where energy generation is needed under oxygen limiting conditions, such as the interior of a fruiting body where free fatty acids may be a plentiful energy source. Expression studies would help determine if/when each set of β oxidation enzymes is expressed.

**α oxidation.** α oxidation removes a single carbon from the fatty acid (Caspi *et al.*, 2006) and has been demonstrated in *S. aurantiaca* (Dickschat *et al.*, 2005). Molecular oxygen is added to a free fatty acid to create β-hydroperoxy-fatty acid by the fatty acid α dioxygenase (EC 1.11.13.-, MXAN5217). This molecule spontaneously degrades, though it can be facilitated by the dioxygenase (Hamberg *et al.*, 2002), to either a β-hydroxy-fatty acid, or a fatty aldehyde with a loss of $CO_2$ and $H_2O$. The fatty aldehyde dehydrogenase (EC 1.2.1.3, MXAN6986) oxidizes the aldehyde to the acid and in the process reduces NAD to NADH. α oxidation only generates one NADH as opposed to the several generated as a result of β oxidation. Despite the two homologs, α oxidation was not observed in radiolabeling studies with *M. xanthus* (Bode *et al.*, 2005). In peas, α oxidation is only observed during seed germination, indicating a situational role for this pathway (Saffert *et al.*, 2000). By analogy, perhaps α oxidation is important during *M. xanthus* spore germination.

**ω oxidation.** During ω oxidation the last carbon in a chain is converted to a carboxyl group, creating fatty acids from alkanes and dicarboxylates from fatty acids. *M. xanthus* does not appear to have a homolog of the ω fatty acid oxidase.

**Carbohydrate Utilization.**

*M. xanthus* and most myxobacteria (with the exception of *Sorangium* and *Byssophaga* species) cannot grow on carbohydrates (Bretscher and Kaiser, 1978; Watson and Dworkin, 1968). Prey bacteria are not particularly enriched in carbohydrates (*E. coli* contains 2.5% glycogen (Neidhardt and Umbarger, 1996)), yet carbohydrates are energy rich and are available in the rhizosphere. The ability of *M. xanthus* to utilize carbohydrates is examined in two parts: carbohydrate assimilation by the phosphotransferase system and carbohydrate metabolism by glycolysis.

**Phosphotransferase system.** While sugars can be internalized through each of the major types of transport systems, the phosphotransferase system (PTS) is specific to carbohydrates and should be an indicator of carbohydrate utilization. The PTS pathway begins with the transfer of a phosphoryl group from phosphoenolpyruvate (PEP) to Enzyme I (EI). This phosphoryl group is then transferred to HPr, which then transfers the phosphoryl group, sometimes through another carrier protein, to the permease composed of IIA, IIB, IIC and sometimes IID subunits, which phosphorylate the transported carbohydrate. *M. xanthus* has homologs of all the PTS components neatly located in an operon (EI, MXAN6530; HPr, MXAN6531; and IID-A, MXAN6532-5). In *E. coli*, EI and HPr are common components of all PTS and substrate specificity is conferred by the sugar specific II proteins. Unlike *E. coli*, which has over a dozen sets of II proteins, *M. xanthus* has only one, but it is homologous with the *E. coli* system that has the broadest substrate range.

The *M. xanthus* system is a Class 4 PTS [for a review see (Postma *et al.*, 1993)], due to the presence of a IID homolog, most closely resembling the mannose PTS in *E. coli*. The *M. xanthus* system has separate IIA and IIB subunits like the PTS systems in *Klebsiella pneumoniae* and *Bacillus subtilis* (Postma *et al.*, 1993). The *M. xanthus* IIA and IIB homologs have the conserved His10 and His175 residues involved in the phosphorelay (Erni *et al.*, 1987). Therefore, at this level of analysis *M. xanthus* has all the necessary components for a functional PTS system.

The most homologous system is the *E. coli* mannose PTS system, which transports 8 different sugars: mannose, *N*-acetylglucosamine, glucosamine, fructose, 2-deoxyglucose, glucose, trehalose, and methyl α-glucoside (Postma *et al.*, 1996). Many of these have been examined as growth substrates in defined and minimal media for *M. xanthus* without success (Bretscher and Kaiser, 1978). *N*-acetylglucosamine has been used in peptidoglycan labeling studies with poor incorporation (L. Shimkets, unpublished). As PTS is dependent on the availability of PEP, perhaps the cellular level of phosphoenolpyruvate is in short supply under the conditions examined for transport to occur. Another possibility is that the PTS system may only be expressed under specific conditions. As the system is predicted to transport trehalose, a possible link with germination exists as the spore-specific sugar trehalose is first secreted then disappears (see section entitled Trehalose, pg. 39).

**Glycolysis.** Monosaccharides are used for exopolysaccharide, peptidoglycan and lipopolysaccharide biosynthesis. Additionally, *M. xanthus* produces glycogen (a homopolysaccharide of glucose monomers joined with α-1,4-linkages and α-1,6 branches) during early to middle stationary phase growth (Nariya and Inouye, 2003). Glycogen is a

common carbon and energy storage polymer in many bacteria. Monosaccharides are produced by gluconeogenesis, which uses many of the glycolysis enzymes in reverse

Glycolysis has three kinase reactions not involved in gluconeogenesis: those performed by glucokinase, phosphofructokinase and pyruvate kinase. For the first step in glycolysis, glucose must be phosphorylated to glucose-1-phosphate. Extracellular glucose can be phosphorylated by the PTS system (see above), though activity has not been demonstrated in *M. xanthus*. While intracellular glucose is phosphorylated by glucokinase, there are no recognizable glucokinase homologs in the genome, and glucokinase activity was not observed in *M. xanthus* (Watson and Dworkin, 1968). Glycogen is consumed in *E. coli* by removing glucose monomers from the non-reducing end of the chain as glucose-1-phosphate by glycogen phosphorylase GlgP (Alonso-Casajus *et al.*, 2006). No glycogen phosphorylase homolog is found in the genome.

The second unique kinase step, that performed by phosphofructokinase, has been carefully studied (Nariya and Inouye, 2002). *M. xanthus* has a phosphofructokinase (EC 2.7.1.11, Pfk, MXAN6373). The activity of Pfk is modulated by phosphorylation of Thr-226 by the protein serine/threonine kinase Pkn4 (Nariya and Inouye, 2002). Additionally, the kinase activity of Pkn4 is controlled by a regulatory protein MkapB and may be involved in a larger signaling network (Nariya and Inouye, 2005). Deletion of phosphofructokinase leads to elevated glycogen levels and decreased spore production (Nariya and Inouye, 2003). Spore production can be restored by supplying the mutant with exogenous pyruvate, which is then presumably catabolized by the TCA cycle.

The third unique kinase step is missing. Although *M. xanthus* contains two pyruvate kinase homologs (EC 2.7.1.40, Pyk, MXAN3514 and MXAN6299), enzymatic activity was not found in cell or spore extract (Watson and Dworkin, 1968). Pyruvate kinase is necessary for

development in *S. aurantiaca* and binds indole, a known sporulation inducer in that organism (Stamm *et al.*, 2005).

Glycogen produced during stationary phase is consumed prior to sporulation, consumption of glycogen is necessary for efficient sporulation, and consumption of glycogen is linked to the regulated activity of phosphofructokinase (Nariya and Inouye, 2003). These results indicate that glycolysis occurs during development. However, the source of phosphorylated glucose for glycolysis is unclear as no glycogen phosphorylase homolog is found in the genome, and the later and critical glycolysis reaction perfomed by pyruvate kinase has not been detected. Additionally, during development monosaccharides are needed for trehalose (see Trehalose, pg. 39) and exopolysaccharide biosynthesis, suggesting competing destinations for glucose in the cell.

An interesting hypothesis is that the glycolytic pathway is functioning incompletely during development. The reaction following phosphofructokinase cleaves fructose-1,6-bisphosphate into glyceraldehydes-3-phosphate and dihydroxyacetone phosphate. Dihydroxyacetone phosphate may be used in ether lipid biosynthesis (see Ether Lipids, pg. 36), compounds only found in *M. xanthus* during development. This unconventional use of glycolysis may explain the unusual method of enzymatic regulation of phosphofructokinase. Further testing, specifically during development, is required to determine if *M. xanthus* is fully using a glycolysis pathway.

## Anabolic Pathways

Lacking space in this chapter to focus on all aspects of anabolism we chose to focus on unusual cell envelope molecules and spore-specific products. Over the years the structural components

of the myxobacterial cell envelope have been examined. Lipids are by far the most structurally divergent group of macromolecules relative to other Proteobacteria and may perform roles in cell signaling (Curtis *et al.*, 2006; Downard and Toal, 1995; Kearns *et al.*, 2001). In the following sections we discuss phospholipids and ceramides. Steroids and polyketides are discussed in chapter 14. Additionally the synthesis and fate of the spore-specific carbohydrate trehalose is examined.

**Lipid Biogenesis.**

While phospholipids perform a basic structural role, the fatty acid diversity of myxobacteria is extraordinary and exceeds that necessary for structural purposes. While most Proteobacteria have 3-5 different fatty acids (Cronan and Rock, 1996), vegetative *M. xanthus* cells contain at least 18 different fatty acids (Curtis *et al.*, 2006; Kearns *et al.*, 2001). Within *M. xanthus* phospholipids, fatty acids can have straight chains or branched chains, and either type can be saturated or unsaturated. The principle phospholipid in *M. xanthus*, phosphatidylethanolamine (PE), deviates markedly from PE species of other Proteobacteria in that it contains unsaturated fatty acids at the *sn*-1 position, which appear to have a role in cell signaling (Curtis *et al.*, 2006). In this section, phospholipid (and ceramide) biosynthesis is examined with attention to sources of structural diversity.

**Fatty acid primer synthesis.** The biosynthesis of fatty acids begins with the generation of a primer that is extended in a series of repetitive cycles to form the fatty acid. For straight chain fatty acids with even numbers of carbons the primer is acetyl-CoA. The branched chain fatty acids are the most abundant fatty acids in *M. xanthus*. The primers for branched chain fatty acids

are derived from the branched chain amino acids (see isoleucine/leucine/valine in amino acid catabolism for detail). Fatty acids derived from leucine comprise the iso-odd fatty acid family, those derived from isoleucine the anteiso-odd family, and those derived from valine comprise the iso-even family. In the first step of branched chain primer synthesis, the amine group is removed producing the α-ketoacid branched chain derivative (EC 2.6.1.42, IlvE, MXAN2987). The α-ketoacids are decarboxylated and attached to CoA by the BCKAD complex to form the primer. Myxobacterial BCKAD enzymes may have more pronounced substrate specificities than usual. Deuterium labeled leucine was incorporated into fatty acids of both *M. xanthus* and *S. aurantiaca*, whereas little labeled valine was incorporated (Bode *et al.*, 2005); concordantly, the most abundant branched chain fatty acids in these two organisms are the iso-odd fatty acids (Dickschat *et al.*, 2005; Kearns *et al.*, 2001; Ware and Dworkin, 1973). In *Streptomyces*, incorporation of valine into iso-even fatty acids was equal to leucine into iso-odd fatty acids (Cropp *et al.*, 2000).

Transposon insertions in the *M. xanthus* genes encoding E1α and E1β subunits (*esg* locus) block development within the first 5 hours (Downard *et al.*, 1993). These mutants show decreased amounts of branched chain fatty acids and increased levels of the fatty acid 16:1ω5c (Curtis *et al.*, 2006; Kearns *et al.*, 2001). It is possible that branched chain fatty acids are necessary for the generation of a chemical signal required for development or for extracellular matrix production (Kim *et al.*, 1999), which is essential for fruiting body formation (Behmlander and Dworkin, 1991; Lu *et al.*, 2005; Yang *et al.*, 2000).

Both *M. xanthus* and *S. aurantiaca* have a second, novel system for branched chain primer synthesis. Acetate is incorporated into isovaleryl-CoA, the primer for iso-odd fatty acids, using a shunt from the mevalonate pathway for isoprenoid biosynthesis (Bode *et al.*, 2006a;

Mahmud *et al.*, 2002). In the mevalonate pathway, three acetate units are used to construct HMG-CoA, which is reduced to mevalonic acid. In the proposed shunt, HMG-CoA is decarboxylated and dehydrated to 3-methylbut-3-enol-CoA, which is then isomerized to 3,3-dimethylacrylyl-CoA and finally reduced to isovaleryl-CoA. HMG-CoA decarboxylase and dehydratase activity has been demonstrated in cell free extracts of the *S. aurantiaca* BCKAD mutant (Mahmud *et al.*, 2005), and labeled 3,3-dimethylacrylate was shown to be incorporated into the branched chain fatty acids of both *S. aurantiaca* and *M. xanthus* BCKAD deficient strains (Mahmud *et al.*, 2002). No evidence has been found that this pathway functions in the wild type under vegetative conditions. However, this pathway does function during fruiting body formation, presumably to supply isovaleryl-CoA when leucine is limited (Bode *et al.*, 2006b).

**Fatty Acid Elongation**. Fatty acid elongation is a repetitive process (Figure 1-1) that extends the fatty acid two carbons per cycle (Cronan and Rock, 1996). The initial step is the condensation of the primer, or the primer extended by previous cycles, with malonyl-ACP. The condensation step can be performed by ketoacyl-ACP synthase I (KAS I, FabB), KAS II (FabF) or KAS III (FabH). In the process, the terminal carboxylic acid of malonyl-ACP leaves resulting in a β-ketoacyl-ACP. FabB is necessary for initiating extension of growing unsaturated fatty acid chains but can also extend saturated chains. FabF is required for thermal regulation of fatty acid saturation. FabH perform the first condensation of the primer with malonyl-ACP. In the next step the β-carboxyl group is reduced to a hydroxyl group with FabG. Then the molecule is dehydrated with FabA or FabZ resulting in a *trans*-$\Delta^2$ double bond. The sole product of FabZ-mediated dehydration is the *trans*-$\Delta^2$ compound. While FabA generates *trans*-$\Delta^2$ double bonds

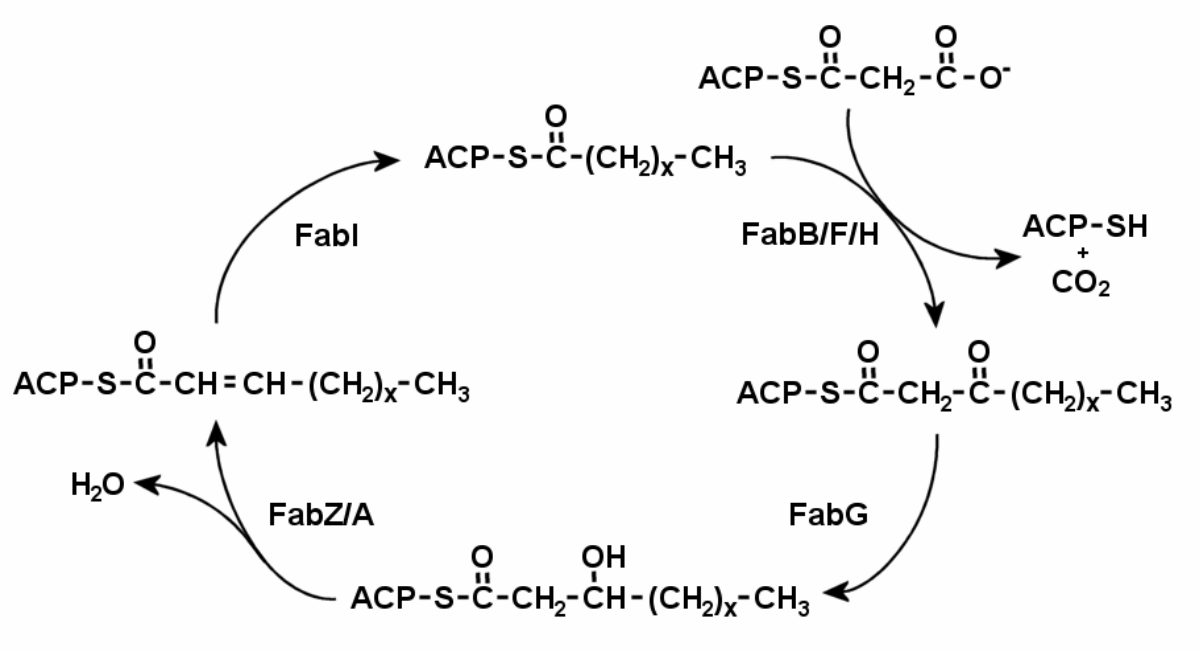


**Figure 1-1.** Fatty acid biosynthesis is a cyclic process. Condensation of malonyl-ACP with the growing chain by FabB, FabF or FabH results in chain extension by two carbons. The β-keto group is reduced to a β-hydroxyl group by FabG, which is then dehydrated to a *trans*-$\Delta^2$ unsaturated bond by FabZ or FabA. This bond is reduced to full saturation by FabI, or isomerized to *cis*-$\Delta^3$ and preserved in later chain extension to create unsaturated fatty acids.

as well, it can also isomerize the double bond to *cis*-$\Delta^3$, which is preserved in later cycles by FabB to create unsaturated fatty acids. FabA, while active on saturated chains, is inactive on unsaturated chains. Therefore, while FabA initiates unsaturated fatty acid biosynthesis by creating the *cis* double bond, it is FabZ that extends unsaturated fatty acids (Heath and Rock, 1996). Finally, the *trans*-$\Delta^2$ double bond is reduced with FabI to create a saturated carbon chain.

The *M. xanthus* fatty acid elongation machinery is spectacularly redundant. There are multiple homologs for almost every enzyme. MXAN4772-4768 contains homologs of *plsX*, *fabD* (malonyl transacetylase which transfers the malonyl group from a CoA moiety to an ACP), *fabG*, *acpP* (acyl carrier protein), and *fabF* (Figure 1-2). This cluster is organized similarly to the *E. coli* fatty acid biosynthetic cluster (*plsX*, *fabH*, *fabD*, *fabG*, *acpP* and *fabF*) with the notable absence of *fabH*. Also, the *rpmF* gene is upstream of this cluster in *E. coli*, but transcribed in the same orientation. A second operon (MXAN6392-6401) contains homologs of *acpP*, *fabZ*, a β-lactamase, *fabF*, *fabF*, *fabZ*, *fabG*, *fabG*, *fabF* and *fabF* (Figure 1-3).

In total there are at least three FabZ/A homologs (two in the clusters and one elsewhere) and five FabF/B homologs. Homology alone cannot distinguish FabZ from FabA nor FabF from FabB as the *M. xanthus* proteins diverge greatly from other characterized homologs. The extraordinary redundancy may relate to the immense fatty acid diversity.

Though many of these enzymes have yet to be characterized, the function for one fatty acid biosynthetic enzyme has been elucidated. The enzyme encoded by a *fabH* gene MXAN0853 is the major FabH for initiating straight chain fatty acids (Bode *et al.*, 2006a). A mutant of MXAN0853 has severely reduced levels of straight chain fatty acids while branched chain fatty acids collectively increase in compensation. Residual levels of straight chain fatty acids are produced through the activity of an unknown FabH using butyryl-CoA as the primer.

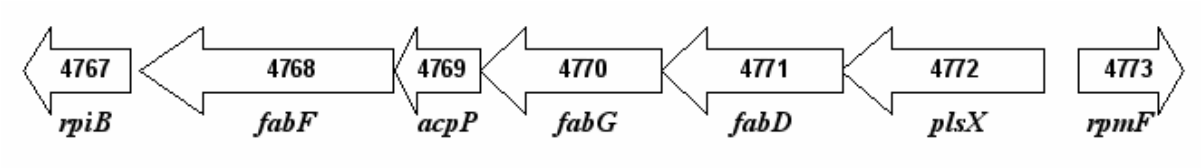


**Figure 1-2.** A putative fatty acid biosynthesis operon in *M. xanthus*. The operon begins with *plsX* (MXAN4772), *fabD* (MXAN4771), *fabG* (MXAN4770), *acpP* (MXAN4769) and *fabF* (MXAN4768). This operon closely resembles the fatty acid operon found in *E. coli*. They differ in that the *E. coli* operon contains *fabH* after *plsX* and the *rpmF* gene upstream of the operon is transcribed in the same direction as opposed to the opposite orientation found in *M. xanthus*.

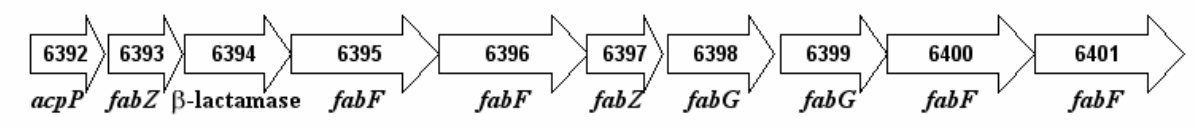


**Figure 1-3.** A second putative fatty acid biosynthesis cluster operon in *M. xanthus*. The operon contains 10 genes (MXAN6392-6401): *acpP*, *fabZ*, a β-lactamase, *fabF*, *fabF*, *fabZ*, *fabG*, *fabG*, *fabF* and *fabF*.

Other *fabH* genes MXAN0215 and MXAN7353 were also disrupted, but had no effect on fatty acid composition.

In. *E. coli*, unsaturated fatty acids are made as part of the fatty acid elongation cycle. FabA introduces *cis* double bonds at many places during fatty acid extension, but FabB extends a specific molecule thereby creating only one unsaturated fatty acid. It is unclear how unsaturated fatty acids are made in *M. xanthus*. The multiple FabA/Z and FabF/B homologs in *M. xanthus* could generate the different unsaturated fatty acids (Curtis *et al.*, 2006; Kearns *et al.*, 2001). In cyanobacteria and *Bacillus*, unsaturated fatty acids are generated by desaturases that introduce double bonds into fatty acids at specific points from the Δ end. Most of the points of unsaturation found in *M. xanthus* fatty acids can be introduced by just two desaturases ($\Delta^5$ and $\Delta^{11}$ position desaturases, (Curtis *et al.*, 2006)), and the *M. xanthus* genome contains many desaturase homologs. Only trace amounts of 16:1ω6/7 contradict the desaturase hypothesis.

Fatty acid diversity in *S. aurantiaca* is due to nontraditional combinations of pathways. Supplementing the *S. aurantiaca* BCKAD mutant with isovalerate enriched for both iso-odd and iso-even fatty acids when it would be predicted to enrich for only iso-odd (Dickschat *et al.*, 2005), consistent with the use of α oxidation during *de novo* fatty acid synthesis. *S. aurantiaca* fed with labeled iso17:0 produced labeled iso16:0, iso15:0, iso14:0, iso13:0 and iso11:0 products, consistent with the use of α and β fatty acid oxidation. Labeled iso17:0 was also found as iso15:1, suggesting that unsaturation is introduced into the pre-formed fatty acid by a desaturase. It is unclear whether desaturase activity accounts for the major portion of unsaturated fatty acids as the points of unsaturation would require many different desaturases. For example, iso17:1 includes ω4, ω5, ω6 and ω7 isomers, which would require the action of four separate desaturases. Alternatively, α and β oxidation of fatty acids may increase diversity.

Clearly, fatty acid biosynthesis of *S. aurantiaca* is not a unidirectional, cyclic pathway but involves both extension and retraction with possible intermediate desaturation.

**Phospholipid Biosynthesis**. During phospholipid biosynthesis, the newly formed fatty acyl chains are attached to glycerol-3-phosphate to create phosphatidic acid, then the head group is added (Cronan and Rock, 1996). First, a fatty acid is esterified to the *sn*-1 position by glycerol-3-phosphate acyltransferase (PlsB). *M. xanthus* contains two homologs of this essential enzyme (EC 2.3.1.15, MXAN3288 (PlsB1) and MXAN1675 (PlsB2)), neither of which is essential, suggesting that both are functional (Curtis *et al.*, 2006). While the *sn*-1 position in *E. coli* is occupied solely by saturated fatty acids (unless the cells are cold shocked) (Cronan and Rock, 1996), *M. xanthus* has predominantly unsaturated fatty acids at *sn*-1 (Curtis *et al.*, 2006). It would appear that both PlsB1 and PlsB2 can use unsaturated fatty acids as elimination of either enzyme does not eliminate *sn*-1 unsaturated fatty acids from PE. PlsB1 appears to have a slight preference for longer chain fatty acids as PE species containing 17 carbon fatty acids decrease in a mutant lacking this enzyme (Curtis *et al.*, 2006).

In the second step 1-acyl-*sn*-glycerol-3-phosphate acyltransferase (PlsC) adds a fatty acid to the *sn*-2 position of 1-acyl-*sn*-glycerol-3-phosphate to generate phosphatidic acid. Five PlsC homologs have been identified (EC 2.3.1.51, PlsC1, MXAN3330; PlsC2, MXAN3969; PlsC3, MXAN5578; PlsC4, MXAN0955; PlsC5, MXAN0147). Disruption of the genes encoding PlsC2, PlsC4 and PlsC5 resulted in almost no detectable change to the membrane, suggesting that either those genes are not necessary for phospholipid biosynthesis or that there is functional redundancy (Curtis *et al.*, 2006).

**Glycerol 3- phosphate → 1-acyl-*sn*-glycerol-3-phosphate → phosphatidic acid**

| EC 2.3.1.15 | EC 2.3.1.51 |
|---|---|
| glycerol-3-phosphateacyltransferase | 1-acyl-*sn*-glycerol-3-phosphate acyltransferase |
| MXAN3288 | MXAN3330, MXAN3969, |
| MXAN1675 | MXAN5578, MXAN0955, MXAN0147 |

Finally the head groups are synthesized on phosphatidic acid. Radiolabeling studies indicate that 76% of the *M. xanthus* phospholipid is PE, while phosphatidylglycerol (PG) comprises 9% and cardiolipin 1% (Orndorff and Dworkin, 1980). The relative amounts of PE, PG and cardiolipin in the *M. xanthus* membrane fall along predicted lines for the Proteobacteria. However, relative to *E. coli*, the outer membrane of *M. xanthus* is unusually rich in PE resulting in a lower buoyant density (Orndorff and Dworkin, 1980; Simunovic *et al.*, 2003).

Phosphatidylethanolamine is derived by first charging phosphatidic acid with CMP to create CDP-diacyl glycerol, then exchanging CMP with serine to create phosphatidylserine, which is decarboxylated to PE. The first step is catalyzed by phosphatidate cytidylyltransferase (EC 2.7.7.41, CdsA, MXAN2556). While no clear phosphatidylserine synthase homolog was found to mediate the serine substitution, there is a homolog for the terminal enzyme phosphatidylserine decarboxylase (EC 4.1.1.65, Psd, MXAN3724).

The CDP-diacyl glycerol intermediate is also used for PG synthesis. A glycerol-3-phosphate molecule is substituted for CMP to create phosphatidylglycerolphosphate, which is then dephosphorylated to create PG. Two PG molecules are condensed (with one glycerol as a leaving group) to synthesize cardiolipin. Glycerol-3-phosphate substitution is performed by phosphatidylglycerol phosphate synthase (EC 2.7.8.5, PgsA, MXAN4626). Homologs for the PgpA and PgpB phosphatidylglycerolphosphate phosphatases were not evident, but *M. xanthus* contains a cardiolipin synthase homolog (EC 2.7.8.-, Cls, MXAN0537).

Phosphatidylinositol (PI) has not been detected in *M. xanthus* despite extensive examination (Orndorff and Dworkin, 1980), but has been found in other myxobacteria. PI accounts for 18-25% of *S. aurantiaca* phospholipid (Caillon *et al.*, 1983) and 7% of *M. fulvus* phospholipid (Kleinig, 1972). Phospholipase C-mediated hydrolysis of PI generates phosphorylated inositol signaling molecules in eukaryotic organisms. Interestingly, release of phosphorylated inositol was observed during aggregation of *S. aurantiaca* (Benaissa *et al.*, 1994). *M. xanthus* appears to have some elements of inositol metabolism. Three genes in a cluster are predicted to involve inositol in some fashion. The protein predicted by MXAN0450 has >30% identity to a CDP-diacylglycerol – inositol 3-phosphatidyltransferase from *Bacteroides thetaiotaomicron*, but does not match a COG. MXAN0451 may encode an inositophosphorylceramide synthase, which would add inositol to a ceramide. The predicted protein has 28% identity to the enzyme from *Issatchenkia orientalis* but also does not match a COG. The clearest homolog of the cluster is MXAN0452, encoding a *myo*-inositol-1-phosphate synthase (EC 5.5.1.4, MXAN0452) that converts glucose-6-phosphate to inositol-1-phosphate. However, the production and fate of inositol in *M. xanthus* is unknown.

**Ceramide and Sphingolipid Biosynthesis**. Ceramides are long-chain 1,3-dihydroxy-2-amino bases with amide-attached fatty acids. While they have not yet been examined in *M. xanthus*, multiple forms have been found in *Cystobacter fuscus* (Eckau *et al.*, 1984) and *M. stipitatus* (Stein and Budzikiewicz, 1988). Ceramides regulate many cellular functions such as cell proliferation, differentiation, apoptosis and the inflammatory response in eukaryotes [for a review, see (Hannun, 1994)]. The structural diversity among the myxobacterial ceramides is immense. There is variation in the length, branching and unsaturation in the acyl backbones of

both the sphinganine base and amide linked fatty acid. The head groups also offer another level of structural diversity as the ceramides found in *M. stipitatus* had phosphoethanolamine at the sphinganine-1 position while those found in *C. fuscus* had no additional attachment. How this diversity is produced and what role it plays in the life cycle of these organisms is presently unclear but potentially relevant to the developmental cycle.

## Spore-specific products

The culmination of fruiting body development is the production of dormant, heat resistant spores. Little is known about the structure of the spore and even less is known about the contribution of the envelope components to dormancy and germination. Aside from the spore coat proteins, which have been studied in some detail and will not be discussed here, two other spore-specific products are known: ether lipids and trehalose. Annotation of the genome revealed some clear candidates for the biosynthetic pathways for both of these spore-specific products. It should now be possible to make mutations in the relevant genes and assess their contributions to the construction and durability of the spore.

**Ether Lipid Biosynthesis.** Though ester linkages are the most common linkages in bacterial PE, myxobacterial phospholipids also contain alkyl ether linkages, with an ether bond between the acyl chain and glycerol backbone, and alk-1-enyl linkages where the ether link is followed by a double bond between the first two carbons on the acyl chain (Figure 1-4).

Phospholipids containing ether-linked chains (ether lipids) are prevalent in myxobacteria. Only 28% of *S. aurantiaca* PE is the traditional diacyl form, while 38% is alkyl-acyl form and 34% is dialkyl. *S. aurantiaca* PG is 36% diacyl, 50% alkyl-acyl and 14% dialkyl, while all of

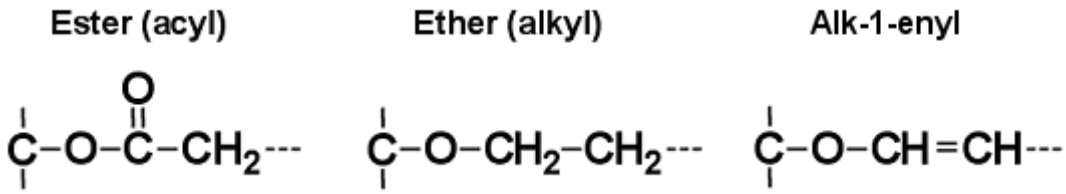


**Figure 1-4.** Acyl chains can be linked to the glycerol backbone of certain lipids in three ways. First is the ester linkage; this is the most common linkage type. Second is the ether linkage, requiring a fatty alcohol instead of a fatty acid. Third is the alk-1-enyl linkage, where an unsaturation immediately follows the ether bond.

the phosphatidylinositol (PI) is in the dialkyl form (Caillon *et al.*, 1983). *M. fulvus* PE is 84% diacyl, 2% alkyl-acyl and 14% alk-1-enyl-acyl (Kleinig, 1972). The PI in this organism is 71% diacyl, 22% alkyl-acyl and 7% alk-1-enyl-acyl.

*M. xanthus* produces two ether lipids during development (Ring *et al.*, 2006). Perhaps more surprising given the immense fatty acid diversity of *M. xanthus* PE, only the branched chain fatty acid iso15:0 is found in ether-linked lipids. The first is phosphatidylethanolamine with iso15:0 at the *sn*-1 position in an alk-1-enyl linkage, and iso15:0 ester-linked at the *sn*-2 position (this compound is referred to as VEPE). The second compound is an unusual neutral lipid, with iso15:0 ester-linked to the *sn*-1 and *sn*-2 positions, while iso15:0 fatty acid is ether-linked to the *sn*-3 position (compound referred to as TG-1). Both VEPE and TG-1 are highly enriched in myxospores. Ether lipids are more stable to environmental stresses and may improve the spore resistance properties. Mutants unable to synthesize branched chain fatty acids are developmentally defective, but can be complimented by adding exogenous TG-1. Interestingly, several mutants blocked at multiple points of development accumulate VEPE to the same levels as wild type, but have reduced levels of TG-1, suggesting that TG-1 synthesis may be tied to developmental signaling.

Ether lipid synthesis in eukaryotic organisms begins by transferring a fatty acyl chain to the *sn*-1 position of dihydroxyacetone phosphate (DHAP) [for a review, see (Nagan and Zoeller, 2001)]. A fatty alcohol is then exchanged for the fatty acid, creating the ether linkage. The *sn*-2 keto group is reduced to an alcohol and the second fatty acid is attached. The phosphate group is removed and the PE head group attached from CDP-ethanolamine. *M. xanthus* contains homologs of some of the eukaryotic enzymes.

The first few steps of ether lipid synthesis in *M. xanthus* may be accomplished by MXAN1675 and MXAN1676. MXAN1675 (PlsB2) is a unique gene fusion containing a fatty acid reductase at the N-terminus and a glycerol-3 phosphate acyltransferase at the C-terminus (Curtis *et al.*, 2006). As such, the C-terminal domain could create 1-acyl-glycerol-3-phosphate and the N-terminal domain could generate the fatty alcohol from a fatty acyl CoA. Interestingly, while bacterial fatty acid reduction requires two separate enzymes (Reiser and Somerville, 1997), eukaryotic fatty acid reductases are able to reduce fatty acids to fatty alcohols with one enzyme (Metz *et al.*, 2000; Moto *et al.*, 2003), and the N-terminal portion of PlsB2 more closely resembles eukaryotic enzymes. The fatty alcohol exchange step may be performed by the 1-alkyldihydroxyacetone 3-phosphate synthase (EC 2.5.1.26) homolog MXAN1676 (45% amino acid identity to the human counterpart). As the human enzyme uses a DHAP backbone as opposed to the bacterial G3P backbone, oxidation of the G3P *sn*-2 alcohol to a keto group may be necessary for 1-alkydihydroxyacetone 3-phosphate synthase function. While there is a reductase in the cluster (MXAN1674), another possibility is *M. xanthus* SocA (MXAN5208), which is the first enzyme reported to reduce the *sn*-2 alcohol of a lysophospholipid (Avadhani *et al.*, 2006).

**Trehalose Biosynthesis.** Trehalose is composed of two glucose monomers with an α 1-1 linkage and confers resistance to osmotic stress (Styrvold and Strom, 1991), heat, and desiccation (Crowe *et al.*, 1984). Given these properties, it is not surprising that trehalose is found in the spores and cysts of a variety of organisms, including *M. xanthus* (Crowe *et al.*, 1984; McBride and Ensign, 1987a, b; McBride and Zusman, 1989). The biosynthesis of trehalose involves two steps. In the first step glucose-6-phosphate is condensed with UDP-D-

glucose by trehalose-6-phosphate synthase (EC 2.4.1.15, OtsA, MXAN1192) to create trehalose-6-phosphate (Caspi *et al.*, 2006). Then the phosphate is removed by trehalose-6-phosphate phosphatase. There is no clear *M. xanthus* homolog of this enzyme, though another phosphatase may perform this function. Trehalose accumulation in *M. xanthus* requires SigD, a sigma factor necessary for stationary phase survival and development (Ueki and Inouye, 1998). In the absence of SigD, trehalose synthesis is severely limited in myxospores.

The fate of trehalose in *M. xanthus* is the mystery. In both glycerol spores and fruiting body spores, 75% of the trehalose disappears within the first 2.5 hours of germination (McBride and Zusman, 1989). Approximately 25% of trehalose is released into the medium but eventually consumed by the germinating spores. In *E. coli*, trehalose is degraded to glucose by a periplasmic trehalase; no homolog exists in *M. xanthus*. Trehalase activity was not detected in spore extracts and the glucose concentration was not elevated. In fact, the germinating spores were unable to utilize exogenously added glucose (McBride and Zusman, 1989).

## Summary

The complexity of the myxobacteria is not limited to patterns of behavior, but is etched into the fabric of the large and diverse genome. The small sampling of metabolic pathways examined here lead to the following conclusions:

1. Despite the fact that *M. xanthus* is thought to subsist primarily on the protein component of prey cells, catabolic pathways for seven amino acids are absent.

2. Pathways are found to salvage purines and pyrimidines for incorporation into nucleic acids.

3. *M. xanthus* contains many lipases, some of which have relevance in aggregation and sporulation, and released fatty acids are likely catabolized by β oxidation in *M. xanthus*.

4. Although *M. xanthus* has homologs for a functional PTS system and both produces and consumes glycogen, it appears that there is no fully-functioning glycolysis pathway. Genome analysis has not solved the mystery of *M. xanthus* sugar metabolism.

5. Lipid biogenesis is spectacularly complex, and the source of unsaturated fatty acids in *M. xanthus* is unknown, though there is evidence that desaturases may be involved. Fatty acid biogenesis in *S. aurantiaca* is even more astounding as it uses α and β oxidation to generate fatty acid diversity.

6. Myxobacteria produce ether lipids, unusual for prokaryotes.

7. While *M. xanthus* produces the spore-protectant trehalose, it is unclear how this compound is degraded, even though evidence clearly demonstrates degradation during spore germination.

**Purpose**

The movement of thousands of cells into a fruiting body necessitates temporal and spatial intercellular signaling. *M. xanthus* lacks the well characterized quorum sensing mechanisms for Gram negative and Gram positive bacteria and instead uses different types of signaling mechanisms. Three signaling systems of interest to this study are lipid chemotaxis, extracellular matrix (ECM)-dependent signaling, and pilus-dependent signaling. Lipid chemotaxis involves the alteration of motile behavior in response to lipids derived from its own membrane, resulting in net movement of cells up lipid gradients (Bonner *et al.*, 2005; Kearns *et al.*, 2000; Kearns *et al.*, 2001; Kearns *et al.*, 2002). ECM-dependent signaling and pilus-dependent signaling are two branches of a pathway governing development. ECM-dependent signaling requires the ECM-associated zinc metalloprotease FibA (Bonner *et al.*, 2006), and pilus-dependent signaling requires the presence of the Type IV pilus structural monomer PilA, or an extended pilus; pilus

retraction is not required (Black *et al.*, 2006; Bonner *et al.*, 2006). Loss of either PilA or FibA does not inhibit development, but development is abolished in the double mutant. These results argue that PilA mediates a pilus-dependent developmental signaling pathway, FibA controls an ECM-dependent pathway, and given that development is abolished only when the pathways are disrupted in the same strain, each pathway is a branch of a larger pathway. The goal of this dissertation is to enhance our understanding of these signaling processes.

Previous work has identified some extracellular and intracellular protein components of lipid chemotaxis (Bonner *et al.*, 2005; Kearns *et al.*, 2000; Kearns *et al.*, 2002), and linked the chemotactic signal to the rare fatty acid 16:1ω5c found in the *M. xanthus* membrane (Kearns *et al.*, 2001). However, the exact nature of the endogenous signal(s) is unknown. Alterations in the lipid profile due to mutation have deleterious effects on development (Toal *et al.*, 1995). Profiling lipids in the *M. xanthus* membrane may not only reveal aspects of the lipid chemotactic signal, but also how the changes in the lipid profile impact development. In this work mass spectrometry was used to profile *M. xanthus* membrane phosphatidylethanolamine (PE), with particular emphasis on the locations of unsaturated bonds in fatty acids and fatty acid localization within PE molecules. Additionally, mutagenesis of genes encoding PE biosynthetic enzymes was used to generate altered PE profiles, and PE extracted from mutants with different profiles was used in chemotaxis excitation assays to determine characteristics of the endogenous lipid signal(s). The results show that 16:1ω5c is primarily located at the *sn*-1 position in *M. xanthus* PE. Chemotaxis assays suggest that 16:1ω5c at the *sn*-1 position is more important for excitation than the same fatty acid at the *sn*-2 position. The combination of a rare fatty acid at an unusual position argues that the lipid signal is specific to the organism and the chemotactic response functions in changing behavior based upon the recognition of other *M. xanthus* cells.

Lipid chemotaxis is dependent on the catalytic activity of FibA, suggesting that the lipid signal may function in the FibA-mediated developmental pathway. The Dif chemotaxis sensory system is necessary for lipid chemotaxis (Bonner *et al.*, 2005), though it also functions in controlling ECM biogenesis possibly through the pilus-mediated signaling pathway (Black and Yang, 2004; Black *et al.*, 2006). Strains carrying mutations in *dif* genes are unable to develop (Lancero *et al.*, 2002; Shimkets, 1986), arguing the Dif system may be an integration point for the FibA- and PilA mediated branches. While these portions of the pathway have been described, other extracellular proteins are unknown; identification and characterization of ECM-associated proteins may identify new components of the pathway. Additionally, proteomic analysis of extracellular matrix proteins from biofilm producing organisms has not been reported. This type of analysis could provide new insights into mechanisms of signaling in biofilms. In this work proteins associated with the ECM were identified using mass spectrometry. Nearly all the genes encoding putative ECM proteins were disrupted in the wild type, *pilA* and *fibA* strains, and the mutants generated were tested for defects in fruiting body formation and sporulation. The results suggest that i) the ECM is enriched in proteins of novel function, and ii) the protein encoded by MXAN4860 functions in the FibA-mediated pathway.

Little is known in prokaryotes about how uniform cellular groups are able to coordinate temporal and special events to create novel three-dimensional architectures. By expanding the knowledge of extracellular signaling mechanisms in *M. xanthus* it may be possible to learn how multiple signaling events are integrated to coordinate social behavior.

**Acknowledgments.**

The authors wish to thank Nilesh Patel, James Henriksen, and Zhengchang Su for help with the genome annotation. This material is based upon work supported by the National Science Foundation under Grant No. 0343874 to L. Shimkets.

**References**

Alonso-Casajus, N., Dauvillee, D., Viale, A.M., Munoz, F.J., Baroja-Fernandez, E., Moran-Zorzano, M.T., Eydallin, G., Ball, S., and Pozueta-Romero, J. (2006) Glycogen phosphorylase, the product of the *glgP* Gene, catalyzes glycogen breakdown by removing glucose units from the nonreducing ends in *Escherichia col*i. *J Bacteriol* **188**: 5266-5272.

Avadhani, M., Geyer, R., White, D.C., and Shimkets, L.J. (2006) Lysophosphatidylethanolamine is a substrate for the short-chain alcohol dehydrogenase SocA from *Myxococcus xanthus*. *J Bacteriol* **188**: 8543-8550.

Behmlander, R.M., and Dworkin, M. (1991) Extracellular fibrils and contact-mediated cell interactions in *Myxococcus xanthus*. *J Bacteriol* **173**: 7810-7820.

Benaissa, M., Vieyres-Lubochinsky, J., Odeide, R., and Lubochinsky, B. (1994) Stimulation of inositide degradation in clumping *Stigmatella aurantiaca*. *J Bacteriol* **176**: 1390-1393.

Black, W.P., and Yang, Z. (2004) *Myxococcus xanthus* chemotaxis homologs DifD and DifG negatively regulate fibril polysaccharide production. *J Bacteriol* **186**: 1001-1008.

Black, W.P., Xu, Q., and Yang, Z. (2006) Type IV pili function upstream of the Dif chemotaxis pathway in *Myxococcus xanthus* EPS regulation. *Mol Microbiol* **61**: 447-456.

Bode, H.B., Dickschat, J.S., Kroppenstedt, R.M., Schulz, S., and Müller, R. (2005) Biosynthesis of iso-fatty acids in myxobacteria: Iso-even fatty acids are derived by alpha-oxidation from iso-odd fatty acids. *Journal of the American Chemical Society* **127**: 532-533.

Bode, H.B., Ring, M.W., Kaiser, D., David, A.C., Kroppenstedt, R.M., and Schwar, G. (2006a) Straight-chain fatty acids are dispensable in the myxobacterium *Myxococcus xanthus* for vegetative growth and fruiting body formation. *J Bacteriol* **188**: 5632-5634.

Bode, H.B., Ring, M.W., Schwar, G., Kroppenstedt, R.M., Kaiser, D., and Muller, R. (2006b) 3-Hydroxy-3-methylglutaryl-coenzyme A (CoA) synthase is involved in biosynthesis of isovaleryl-CoA in the myxobacterium *Myxococcus xanthus* during fruiting body formation. *J Bacteriol* **188**: 6524-6528.

Bonner, P.J., Xu, Q., Black, W.P., Li, Z., Yang, Z., and Shimkets, L.J. (2005) The Dif chemosensory pathway is directly involved in phosphatidylethanolamine sensory transduction in *Myxococcus xanthus*. *Mol Microbiol* **57**: 1499-1508.

Bonner, P.J., Black, W.P., Yang, Z., and Shimkets, L.J. (2006) FibA and PilA act cooperatively during fruiting body formation of *Myxococcus xanthus*. *Mol Microbiol* **61**: 1283-1293.

Bretscher, A.P., and Kaiser, D. (1978) Nutrition of *Myxococcus xanthus*, a fruiting myxobacterium. *J Bacteriol* **133**: 763-768.

Caillon, E., Lubochinsky, B., and Rigomier, D. (1983) Occurrence of dialkyl ether phospholipids in *Stigmatella aurantiaca* DW4. *J Bacteriol* **153**: 1348-1351.

Campbell, J.W., Morgan-Kiss, R.M., and Cronan, J.E., Jr. (2003) A new *Escherichia coli* metabolic competency: growth on fatty acids by a novel anaerobic beta-oxidation pathway. *Mol Microbiol* **47**: 793-805.

Caspi, R., Foerster, H., Fulcher, C.A., Hopkinson, R., Ingraham, J., Kaipa, P., Krummenacker, M., Paley, S., Pick, J., Rhee, S.Y., Tissier, C., Zhang, P., and Karp, P.D. (2006) MetaCyc: a multiorganism database of metabolic pathways and enzymes. *Nucleic Acids Res* **34**: D511-516.

Clark, D.P., and Cronan, J.E. (1996) Two-Carbon Compounds and Fatty Acids as Carbon Sources. In *Escherichia coli and Salmonella*. Neidhardt, F.C., Curtiss, R., Ingram, J.L., Lin, E.C.C., Low, K.B. and Magasanik, B. (eds). Washington D.C.: American Society for Microbiology Press, pp. 343-357.

Cronan, J.E., and Rock, C.O. (1996) Biosynthesis of Membrane Lipids. In *Escherichia coli and Salmonella*. Neidhardt, F.C., Curtiss, R., Ingram, J.L., Lin, E.C.C., Low, K.B. and Magasanik, B. (eds). Washington D.C.: American Society for Microbiology Press, pp. 612-636.

Cropp, T.A., Smogowicz, A.A., Hafner, E.W., Denoya, C.D., McArthur, H.A., and Reynolds, K.A. (2000) Fatty-acid biosynthesis in a branched-chain alpha-keto acid dehydrogenase mutant of *Streptomyces avermitilis*. *Can J Microbiol* **46**: 506-514.

Crowe, J.H., Crowe, L.M., and Chapman, D. (1984) Infrared spectroscopic studies on interactions of water and carbohydrates with a biological membrane. *Arch Biochem Biophys* **232**: 400-407.

Curtis, P.D., Geyer, R., White, D.C., and Shimkets, L.J. (2006) Novel lipids in *Myxococcus xanthus* and their role in chemotaxis. *Environ Microbiol* **8**: 1935-1949.

Dickschat, J.S., Bode, H.B., Kroppenstedt, R.M., Müller, R., and Schulz, S. (2005) Biosynthesis of iso-fatty acids in myxobacteria. *Org Biomol Chem* **3**: 2824-2831.

Downard, J., Ramaswamy, S.V., and Kil, K.S. (1993) Identification of *esg*, a genetic locus involved in cell-cell signaling during *Myxococcus xanthus* development. *J Bacteriol* **175**: 7762-7770.

Downard, J., and Toal, D. (1995) Branched-chain fatty acids: the case for a novel form of cell-cell signalling during *Myxococcus xanthus* development. *Mol Microbiol* **16**: 171-175.

Dworkin, M. (1962) Nutritional requirements for vegetative growth of *Myxococcus xanthus*. *J Bacteriol* **84**: 250-257.

Eckau, H., Dill, D., and Budzikiewicz, H. (1984) Novel ceramides from *Cystobacter fuscus* (Myxobacterales). *Zeitschrift Fur Naturforschung C-a Journal of Biosciences* **39**: 1-9.

Erni, B., Zanolari, B., and Kocher, H.P. (1987) The mannose permease of *Escherichia coli* consists of three different proteins. Amino acid sequence and function in sugar transport, sugar phosphorylation, and penetration of phage lambda DNA. *J Biol Chem* **262**: 5238-5247.

Galliard, T. (1971) The enzymic deacylation of phospholipids and galactolipids in plants. Purification and properties of a lipolytic acyl-hydrolase from potato tubers. *Biochem J* **121**: 379-390.

Goldman, B.S., Nierman, W.C., Kaiser, D., Slater, S.C., Durkin, A.S., Eisen, J.A., Ronning, C.M., Barbazuk, W.B., Blanchard, M., Field, C., Halling, C., Hinkle, G., Iartchuk, O., Kim, H.S., Mackenzie, C., Madupu, R., Miller, N., Shvartsbeyn, A., Sullivan, S.A., Vaudin, M., Wiegand, R., and Kaplan, H.B. (2006) Evolution of sensory complexity recorded in a myxobacterial genome. *Proc Natl Acad Sci U S A* **103**: 15200-15205.

Hamberg, M., Ponce de Leon, I., Sanz, A., and Castresana, C. (2002) Fatty acid alpha-dioxygenases. *Prostaglandins Other Lipid Mediat* **68-69**: 363-374.

Hannun, Y.A. (1994) The sphingomyelin cycle and the second messenger function of ceramide. *J Biol Chem* **269**: 3125-3128.

Heath, R.J., and Rock, C.O. (1996) Roles of the FabA and FabZ beta-hydroxyacyl-acyl carrier protein dehydratases in *Escherichia coli* fatty acid biosynthesis. *J Biol Chem* **271**: 27795-27801.

Hemphill, H.E., and Zahler, S.A. (1968a) Nutrition of *Myxococcus xanthus* FBa and some of its auxotrophic mutants. *J Bacteriol* **95**: 1011-1017.

Hemphill, H.E., and Zahler, S.A. (1968b) Nutritional induction and suppression of fruiting in Myxococcus xanthus FBa. *J Bacteriol* **95**: 1018-1023.

Hubbard, P.A., Liang, X., Schulz, H., and Kim, J.J. (2003) The crystal structure and reaction mechanism of *Escherichia coli* 2,4-dienoyl-CoA reductase. *J Biol Chem* **278**: 37553-37560.

Kearns, D.B., Campbell, B.D., and Shimkets, L.J. (2000) *Myxococcus xanthus* fibril appendages are essential for excitation by a phospholipid attractant. *Proc Natl Acad Sci U S A* **97**: 11505-11510.

Kearns, D.B., Venot, A., Bonner, P.J., Stevens, B., Boons, G.-J., and Shimkets, L.J. (2001) Identification of a developmental chemoattractant in *Myxococcus xanthus* through metabolic engineering. *Proc Natl Acad Sci U S A* **98**: 13990-13994.

Kearns, D.B., Bonner, P.J., Smith, D.R., and Shimkets, L.J. (2002) An extracellular matrix-associated zinc metalloprotease is required for dilauroyl phosphatidylethanolamine chemotactic excitation in *Myxococcus xanthus*. *J Bacteriol* **184**: 1678-1684.

Kim, S.H., Ramaswamy, S., and Downard, J. (1999) Regulated exopolysaccharide production in *Myxococcus xanthus*. *J Bacteriol* **181**: 1496-1507.

Kleinig, H. (1972) Membranes from *Myxococcus fulvus* (*Myxobacterales*) containing carotenoid glucosides. I. Isolation and composition. *Biochim Biophys Acta* **274**: 489-498.

Klingsbichel, E. (1996) Esterase EstA from *Pseudomonas marginata*: heterologous expression, biological, biochemical, and biocatalytical characterization. Graz: Technical University of Graz.

Kuspa, A., Plamann, L., and Kaiser, D. (1992) Identification of heat-stable A-factor from *Myxococcus xanthus*. *J Bacteriol* **174**: 3319-3326.

Lancero, H., Brofft, J.E., Downard, J., Birren, B.W., Nusbaum, C., Naylor, J., Shi, W., and Shimkets, L.J. (2002) Mapping of *Myxococcus xanthus* social motility *dsp* mutations to the *dif* genes. *J Bacteriol* **184**: 1462-1465.

Lau, J., Frykman, S., Regentin, R., Ou, S., Tsuruta, H., and Licari, P. (2002) Optimizing the heterologous production of epothilone D in *Myxococcus xanthus*. *Biotechnol Bioeng* **78**: 280-288.

Loebeck, M.E., and Klein, H.P. (1956) Substrates for *Myxococcus virescens* with special reference to eubacterial fractions. *J Gen Microbiol* **14**: 281-289.

Lu, A., Cho, K., Black, W.P., Duan, X.Y., Lux, R., Yang, Z., Kaplan, H.B., Zusman, D.R., and Shi, W. (2005) Exopolysaccharide biosynthesis genes required for social motility in *Myxococcus xanthus*. *Mol Microbiol* **55**: 206-220.

Mahmud, T., Bode, H.B., Silakowski, B., Kroppenstedt, R.M., Xu, M., Nordhoff, S., Hofle, G., and Müller, R. (2002) A novel biosynthetic pathway providing precursors for fatty acid biosynthesis and secondary metabolite formation in myxobacteria. *J Biol Chem* **277**: 32768-32774.

Mahmud, T., Wenzel, S.C., Wan, E., Wen, K.W., Bode, H.B., Gaitatzis, N., and Müller, R. (2005) A biosynthetic pathway to isovaleryl-CoA in myxobacteria: The involvement of the mevalonate pathway. *Chembiochem* **6**: 322-330.

McBride, M.J., and Ensign, J.C. (1987a) Metabolism of endogenous trehalose by *Streptomyces griseus* spores and by spores or cells of other actinomycetes. *J Bacteriol* **169**: 5002-5007.

McBride, M.J., and Ensign, J.C. (1987b) Effects of intracellular trehalose content on *Streptomyces griseus* spores. *J Bacteriol* **169**: 4995-5001.

McBride, M.J., and Zusman, D.R. (1989) Trehalose accumulation in vegetative cells and spores of Myxococcus xanthus. *J Bacteriol* **171**: 6383-6386.

Metz, J.G., Pollard, M.R., Anderson, L., Hayes, T.R., and Lassner, M.W. (2000) Purification of a jojoba embryo fatty acyl-coenzyme A reductase and expression of its cDNA in high erucic acid rapeseed. *Plant Physiol* **122**: 635-644.

Moraleda-Muñoz, A., and Shimkets, L.J. (2007) Lipolytic enzymes in *Myxococcus xanthus*. *Submitted*.

Moto, K., Yoshiga, T., Yamamoto, M., Takahashi, S., Okano, K., Ando, T., Nakata, T., and Matsumoto, S. (2003) Pheromone gland-specific fatty-acyl reductase of the silkmoth, *Bombyx mori*. *Proc Natl Acad Sci U S A* **100**: 9156-9161.

Nagan, N., and Zoeller, R.A. (2001) Plasmalogens: biosynthesis and functions. *Prog Lipid Res* **40**: 199-229.

Nariya, H., and Inouye, S. (2002) Activation of 6-phosphofructokinase via phosphorylation by Pkn4, a protein Ser/Thr kinase of *Myxococcus xanthus*. *Mol Microbiol* **46**: 1353-1366.

Nariya, H., and Inouye, S. (2003) An effective sporulation of *Myxococcus xanthus* requires glycogen consumption via Pkn4-activated 6-phosphofructokinase. *Mol Microbiol* **49**: 517-528.

Nariya, H., and Inouye, S. (2005) Modulating factors for the Pkn4 kinase cascade in regulating 6-phosphofructokinase in *Myxococcus xanthus*. *Mol Microbiol* **56**: 1314-1328.

Neidhardt, F.C., and Umbarger, H.E. (1996) Chemical Composition of *Escherichia coli*. In *Escherichia coli and Salmonella*. Neidhardt, F.C., Curtiss, R., Ingram, J.L., Lin, E.C.C., Low, K.B. and Magasanik, B. (eds). Washington D.C.: American Society for Microbiology Press, pp. 13-16.

Ollis, D.L., Cheah, E., Cygler, M., Dijkstra, B., Frolow, F., Franken, S.M., Harel, M., Remington, S.J., Silman, I., Schrag, J., and et al. (1992) The alpha/beta hydrolase fold. *Protein Eng* **5**: 197-211.

Orndorff, P.E., and Dworkin, M. (1980) Separation and properties of the cytoplasmic and outer membranes of vegetative cells of *Myxococcus xanthus*. *J Bacteriol* **141**: 914-927.

Postma, P.W., Lengeler, J.W., and Jacobson, G.R. (1993) Phosphoenolpyruvate:carbohydrate phosphotransferase systems of bacteria. *Microbiol Rev* **57**: 543-594.

Postma, P.W., Lengeler, J.W., and Jacobson, G.R. (1996) Phosphoenolpyruvate:Carbohydrate Phosphotransferase Systems. In *Escherichia coli and Salmonella*. Neidhardt, F.C., Curtiss, R., Ingram, J.L., Lin, E.C.C., Low, K.B. and Magasanik, B. (eds). Washington D.C.: American Society for Microbiology Press, pp. 1149-1174.

Reiser, S., and Somerville, C. (1997) Isolation of mutants of *Acinetobacter calcoaceticus* deficient in wax ester synthesis and complementation of one mutation with a gene encoding a fatty acyl coenzyme A reductase. *J Bacteriol* **179**: 2969-2975.

Ring, M.W., Schwar, G., Thiel, V., Dickschat, J.S., Kroppenstedt, R.M., Schulz, S., and Bode, H.B. (2006) Novel iso-branched ether lipids as specific markers of developmental sporulation in the myxobacterium *Myxococcus xanthus*. *J Biol Chem* **281**: 36691-36700.

Saffert, A., Hartmann-Schreier, J., Schon, A., and Schreier, P. (2000) A dual function alpha-dioxygenase-peroxidase and NAD(+) oxidoreductase active enzyme from germinating pea rationalizing alpha-oxidation of fatty acids in plants. *Plant Physiol* **123**: 1545-1552.

Shimkets, L.J. (1986) Role of cell cohesion in *Myxococcus xanthus* fruiting body formation. *J Bacteriol* **166**: 842-848.

Simunovic, V., Gherardini, F.C., and Shimkets, L.J. (2003) Membrane localization of motility, signaling, and polyketide synthetase proteins in *Myxococcus xanthus*. *J Bacteriol* **185**: 5066-5075.

Stamm, I., Lottspeich, F., and Plaga, W. (2005) The pyruvate kinase of *Stigmatella aurantiaca* is an indole binding protein and essential for development. *Mol Microbiol* **56**: 1386-1395.

Stein, J., and Budzikiewicz, H. (1988) Bacterial Components .36. ceramide-1-phosphoethanolamines from *Myxococcus stipitatus*. *Zeitschrift Fur Naturforschung Section B-a Journal of Chemical Sciences* **43**: 1063-1067.

Styrvold, O.B., and Strom, A.R. (1991) Synthesis, accumulation, and excretion of trehalose in osmotically stressed *Escherichia coli* K-12 strains: influence of amber suppressors and function of the periplasmic trehalase. *J Bacteriol* **173**: 1187-1192.

Toal, D.R., Clifton, S.W., Roe, B.A., and Downard, J. (1995) The *esg* locus of *Myxococcus xanthus* encodes the E1α and E1β subunits of a branched-chain keto acid dehydrogenase. *Mol Microbiol* **16**: 177-189.

Tsai, W.C., and Westby, C.A. (1978) Synthesis and salvage of purines during cellular morphogenesis of *Myxococcus xanthus*. *J Bacteriol* **136**: 582-587.

Ueki, T., and Inouye, S. (1998) A new sigma factor, SigD, essential for stationary phase is also required for multicellular differentiation in *Myxococcus xanthus*. *Genes Cells* **3**: 371-385.

Ware, J.C., and Dworkin, M. (1973) Fatty acids of *Myxococcus xanthus*. *J Bacteriol* **115**: 253-261.

Watson, B.F., and Dworkin, M. (1968) Comparative intermediary metabolism of vegetative cells and microcysts of *Myxococcus xanthus*. *J Bacteriol* **96**: 1465-1473.

Weimar, J.D., DiRusso, C.C., Delio, R., and Black, P.N. (2002) Functional role of fatty acyl-coenzyme A synthetase in the transmembrane movement and activation of exogenous long-chain fatty acids. Amino acid residues within the ATP/AMP signature motif of *Escherichia coli* FadD are required for enzyme activity and fatty acid transport. *J Biol Chem* **277**: 29369-29376.

Yang, Z., Ma, X., Tong, L., Kaplan, H.B., Shimkets, L.J., and Shi, W. (2000) *Myxococcus xanthus dif* genes are required for biogenesis of cell surface fibrils essential for social gliding motility. *J Bacteriol* **182**: 5793-5798.

Youderian, P., Burke, N., White, D.J., and Hartzell, P.L. (2003) Identification of genes required for adventurous gliding motility in *Myxococcus xanthus* with the transposable element *mariner*. *Mol Microbiol* **49**: 555-570.

# CHAPTER 2

# NOVEL LIPIDS IN *MYXOCOCCUS XANTHUS* AND THEIR ROLE IN CHEMOTAXIS[1]

[1] Curtis, P.D., Geyer, R., White, D.C. and Shimkets, L.J. (2006) *Environ Microbiol* **8**, 1935-1949
Reprinted here with permission of publisher.

**Abstract**

Organisms that colonize solid surfaces, like *Myxococcus xanthus*, use novel signaling systems to organize multicellular behavior. Phosphatidylethanolamine (PE) containing the fatty acid 16:1ω5 ($\Delta^{11}$) elicits a chemotactic response. The phenomenon was examined by observing the effects of PE species with varying fatty acid pairings. Wild type *M. xanthus* contains 17 different PE species under vegetative conditions and 19 at the midpoint of development; 13 of the 17 have an unsaturated fatty acid at the *sn*-1 position, a novelty among Proteobacteria. *M. xanthus* has two glycerol-3-phosphate acyltransferase (PlsB) homologs which add the *sn*-1 fatty acid. Each produces PE with 16:1 at the *sn*-1 position and supports growth and fruiting body development. Deletion of *plsB1* (MXAN3288) results in more dramatic changes in PE species distribution than deletion of *plsB2* (MXAN1675). PlsB2 has a putative N-terminal eukaryotic fatty acid reductase domain and may support both ether-lipid synthesis and PE synthesis. Disruption of a single *sn*-2 acyltransferase homolog (PlsC, of which *M. xanthus* contains five) results in minor changes in membrane PE. Derivatization of purified PE extracts with dimethyldisulfide was used to determine the position of the double bonds in unsaturated fatty acids. The results suggest that $\Delta^5$ and $\Delta^{11}$ desaturases may create the double bonds after synthesis of the fatty acid. PE enriched for 16:1 at the *sn*-1 position stimulates chemotaxis more strongly than PE with 16:1 enriched at the *sn*-2 position. It appears that the deployment of a rare fatty acid (16:1ω5) at an unusual position (*sn*-1) has facilitated the evolution of a novel cell signal.

## Introduction

In nature many bacteria are attached to surfaces where they are subject to different physical stresses than planktonic cells. As a consequence, surface dwelling bacteria often employ distinctive mechanisms, including different motility motors, chemical signals and sensory transduction mechanisms. A model surficial organism is *Myxococcus xanthus*, a soil-dwelling δ-proteobacterium with a complex life cycle. Vegetative cells travel in swarms, feeding on other bacteria. When starved, cells aggregate into large fruiting bodies and then differentiate into spores. During development, swarms of *M. xanthus* maintain significant species purity (Fiegna and Velicer, 2005), even in a complex soil microbial community, through mechanisms that are as yet unknown. Lipid signals may be important. *M. xanthus* cells respond chemotactically to purified *M. xanthus* membrane phosphatidylethanolamine (PE) (Kearns and Shimkets, 1998), containing the fatty acid 16:1ω5 (Kearns *et al.*, 2001b). This response is dependent on the presence of the extracellular matrix and has only been observed under starvation conditions, suggesting developmental relevance. Chemotaxis is also promoted by PE containing 18:1ω9 (Kearns and Shimkets, 1998), a fatty acid not found in *M. xanthus* (Kearns *et al.*, 2001b) but common in prey bacteria such as *Escherichia coli* (Cronan and Rock, 1996). The response to PE containing 18:1ω9 uses a different sensory pathway from the 16:1ω5 response and may be involved in sensing prey (Bonner *et al.*, 2005; Kearns *et al.*, 2000).

Mutations that alter the fatty acid composition of the membrane can have dramatic effects on development. For example, mutation of the genes encoding the E1α and E1β subunits of the branched-chain keto-acid dehydrogenase complex (BCKAD) (involved in the synthesis of branched-chain fatty acids) decreases the abundance of branched-chain fatty acids, with a subsequent rise in unsaturated fatty acids (Toal *et al.*, 1995). These mutants are deficient in

fruiting body formation and sporulation. Partial restoration of branched-chain fatty acid synthesis by feeding cells isovalerate improves fruiting body formation and sporulation (Toal *et al.*, 1995). These results argue that a balance of fatty acids is necessary to maintain the complex life cycle of the organism.

PE is usually the most abundant phospholipid in Proteobacterial membranes. Its biosynthesis starts with the addition of an acyl chain (fatty acid) at the *sn*-1 position of glycerol-3-phosphate by glycerol-3-phosphate acyltransferase PlsB (Cronan and Rock, 1996). The second acyl chain is added at the *sn*-2 position by PlsC (1-acyl-*sn*-glycerol-3-phosphate acyltransferase), forming phosphatidic acid. A serine molecule is added to the phosphate group, forming phosphatidylserine, which is then decarboxylated to create the phosphatidylethanolamine. The fatty acid diversity of PE molecules is due in part to the activities of the PlsB and PlsC acyltransferases and in part to the pool of available fatty acids.

In this work the molecular diversity of membrane PE was examined in wild type and mutant strains, showing that *M. xanthus* contains significant amounts of unsaturated fatty acids at the *sn*-1 position. Mixtures of PE molecules enriched in *sn*-1 16:1 are stronger attractants than molecules with *sn*-2 16:1. This effect is associated with 16:1ω5 as it is the major monounsaturated fatty acid in *M. xanthus*.

**Experimental Procedures**

**Strains and growth conditions**. *M. xanthus* wild-type strain DK1622 (Kaiser, 1979), and mutant strains LS2300 (*plsB1*; MXAN3288), LS2301 (*plsB2*; MXAN1675), JD300 (Downard and Toal, 1995), LS2305 (*plsC2*; MXAN3969), LS2306 (*plsC4*; MXAN0955) and LS2307 (*plsC5*; MXAN0147) were grown at 32$^{o}$C in CYE [1.0% Bacto Casitone, 0.5% Difco

yeast extract, 10 mM 3-[*N*-morpholino]propanesulfonic acid (MOPS), pH 7.6 and 0.1% $MgSO_4$] broth with vigorous shaking (Campos *et al.*, 1978). Cultures were grown on plates containing CYE with 1.5% Difco agar. To induce development, 7.5 ml of 5 x $10^9$ cells $ml^{-1}$ were plated on TPM agar [10 mM Tris (hydroxymethyl) aminomethane HCl, 8 mM $MgSO_4$, 1 mM $KHPO_4$-$KH_2PO_4$, 1.5% Difco agar, pH 7.6] in a 33 x 22 cm tray and incubated at 32°C for 24 hr.

**Construction of *plsB* mutants**. Preliminary sequence data was obtained from The Institute for Genomic Research through the website at http://www.tigr.org. Two *M. xanthus plsB* homologs were identified using the *E. coli* PlsB protein sequence (P0A7A7) to search the *M. xanthus* genome (available at http://www.tigr.org/tigr-scripts/CMR2/CMRHomePage.spl) and analyzed using the ClustalW (http://align.genome.jp/) and Boxshade (http://bioweb.pasteur.fr/seqanal/interfaces/boxshade.html) programs. In-frame deletion mutants of *plsB1* and *plsB2* were constructed as described previously (Julien *et al.*, 2000). Wild-type *M. xanthus* chromosomal DNA was purified (Easy-DNA kit, Invitrogen) and approximately 750 bp of sequence upstream of *plsB1* was amplified using primers INFRB1P1F and INFRB1P1R, which add *Bam*HI and *Xba*I restriction sites respectively (Table 2-1). Approximately 750 bp of downstream sequence was amplified using primers INFRB1P2F and INFRB1P2R, which add *Xba*I and *Hin*dIII sites respectively. PCR products were separated on 1.0% agarose and the desired fragments were extracted using the UltraClean 15 DNA Purification Kit (Mo Bio Laboratories). Extracted fragments were used in a third PCR reaction with primers INFRB1P1F and INFRB1P2R and the products were separated on 1.0% agarose. A band of approximately 1.5 kb was extracted and cloned into pCR2.1-TOPO (TOPO TA Cloning Kit, Invitrogen) to create plasmid pINFR6. The integrity of the construct was verified by DNA sequencing. Plasmids pBJ113 (Julien *et al.*, 2000) and pINFR6 were digested with *Bam*HI and *Hin*dIII and

**Table 2-1.** Primers used in construction and examination of *plsB* and *plsC* mutants.

| Primer Name | Sequence (5' → 3') |
|---|---|
| INFRB1P1F | GGA TCC GCA CCG TCC ACG TCG CGT TCG |
| INFRB1P1R | CAT CTA GAC ATG GGG CCG AAT TCG TCC TTC AGC |
| INFRB1P2F | ATG TCT AGA TGA GCA GCC CTC CCT GGC CCC |
| INFRB1P2R | AAG CTT GGC GCT GAA CAC CAC GGC GGA G |
| INFRB2P1F | GGA TCC GGT GGT GGG CAT GGT CGA CGT G |
| INFRB2P1R | TCA TCT AGA CAT GCC CTC GTT CAC CAC GCG C |
| INFRB2P2F | GTC TAG ATG AAG ACA CTC GTG ACG GGA GCC |
| INFRB2P2R | AAG CTT CGA GCA CCA CGG GGT CCG GCA GC |
| INB2DIAGF | CAT GTT CGT CGG CCG CAA GGA C |
| INB2DIAGR | CGA GCT GTC GAT GTT GAA GCG C |
| MYXplsC2F | AAG CAA CCA CGA GTC CAA |
| MYXplsC2R | TTG GTG GAG ATG GGC GTG |
| MYXplsC4F | TCA TTG GTC TGT CGT TGG |
| MYXplsC4R | GTC TGG ATG CAG CAG CCC |
| MYXplsC5F | CCG TGC TCG TGT CCA ACC |
| MYXplsC5R | GAG GAC CAC GGG GAT GAC |

gel purified. The ~1.5 kb insert from pINFR6 was ligated with pBJ113. The resultant plasmid (pINFR7) was electroporated in *M. xanthus* DK1622 and transformants were selected on CYE agar plates containing 50 μg $ml^{-1}$ kanamycin. Transformants were then grown in CYE broth in the absence of selection and plated on CYE agar plates supplemented with 1.0% galactose. Galactose-resistant colonies were screened for kanamycin sensitivity and analyzed by PCR reactions with primers INFRB1P1F and INFRB1P2R. PCR fragments of ~1.5 kb were verified as deletions by digestion of the PCR fragments with *Xba*I into approximately equal size fragments. A colony that yielded PCR product with appropriate size and digestion pattern was kept as strain LS2300.

Similarly, the *plsB2* mutant (LS2301) was generated using primers INFRB2P1F and INFRB2P1R in the first PCR reaction, INFRB2P2F and INFRB2P2R in the second reaction, INFRB2P1F and INFRB2P2R in the third reaction and INB2DIAGF and INB2DIAGR in the verification reaction. PCR fragments were cloned, digested and ligated exactly as described above.

**Construction of *plsC* mutants**. Five *M. xanthus plsC* homologs were identified by genome search using the *E. coli* PlsC protein sequence (P26647). They were named *plsC1*, *plsC2*, *plsC3*, *plsC4* and *plsC5*. Mutants were created by amplifying internal fragments of approximately 450 bp and using this to disrupt the target genes by recombinational insertion, resulting in two partial gene copies. These were amplified using primers MYXplsC2F and MYXplsC2R for the *plsC2* gene, MYXplsC4F and MYXplsC4R for *plsC4* and MYXplsC5F and MYXplsC5R for *plsC5*. The PCR products were separated on a 1.0% agarose gel, purified, and cloned into pCR2.1-TOPO to create plasmids pPDC1, pPDC2 and pPDC3 respectively. Each plasmid was electroporated in DK1622 and grown on CYE + 50 μg $ml^{-1}$ kanamycin.

Transformants were examined by Southern hybridization and probed with labeled PCR fragments generated using the same primers.

**Characterization of mutants**. Mutants were examined for motility, fruiting body formation, and sporulation. For motility, the edges of colonies on CYE agar were viewed under 400x magnification on a Leitz Laborlux D phase-contrast microscope. To analyze fruiting body formation and sporulation, 1.5 x $10^9$ cells were plated on TPM agar plates and incubated at 32$^o$C with observation on a Wild Heerbrugg dissecting microscope over 5 days. Fruiting bodies were removed with a sterile razor blade and resuspended in 1.0 ml TPM buffer. The fruiting bodies were then incubated at 55$^o$C for 2 hrs and sonicated at a 60% duty cycle for 2 x 15 sec on an Ultrasonic Processor Sonicator (Heat Systems – Ultrasonics Inc.). Refractile myxospores were quantified using a Petroff – Hauser counting chamber. Spores were diluted and plated on CYE plates to enumerate viable spores.

**Fatty acid methylester (FAME) analysis**. Lyophilized cells of *M. xanthus* were extracted and derivatized according to the whole-cell hydrolysate procedure of the Microbial Identification System (MIDI Inc., Newark, Del) (Hartig *et al.*, 2005). Samples were resolved in hexane containing the FAME 21:0 as an internal standard (59 pmol $\mu L^{-1}$) for analysis by gas chromatography – mass spectrometry (GC-MS) (Geyer *et al.*, 2005).

**Dimethyldisulfide (DMDS) derivatization**. FAMEs were derivatized using a modified procedure of Leonhardt and deVilbiss (Leonhardt and deVilbiss, 1985). Samples for derivatisation with dímethyldisulfide were dissolved in 1.0 ml diethylether/hexane (50:50). Approximately 4.0 mg iodine and 300 µL DMDS were added and the mix incubated at 37°C for 30 min. The reaction was completed by adding sodium thiosulfate (10% solution) dropwise until the mixtures remained colorless. The upper organic phase was transferred, dried over sodium

sulfate, evaporated to dryness and resuspended in 500 µL hexane. An aliquot of 1.0 µl was analyzed with GC-MS using the same temperature program as for FAME analysis. Results showed a nearly complete derivatization. Details to interpretation of mass spectra from DMDS derivatives are outlined elsewhere (Christie, 2004).

**Phosphatidylethanolamine purification**. PE was purified using a modified method of Bligh and Dyer (Bligh and Dyer, 1959). Cells were grown in CYE to a density of 7.5 x $10^8$ cells $ml^{-1}$ (approximately mid-log phase) and pelleted by centrifugation at 12,100 x g for 10 min. To 0.8 g (wet cell weight) of *M. xanthus* cells was added 7.5 ml methanol/chloroform (2:1). The mixture was vigorously shaken for 1 hour. Insoluble material was pelleted by centrifugation at 12,100 x g for 5 min and the supernatant was collected. The pellet was re-extracted with 9.5 ml methanol/chloroform/water (2:1:0.8), centrifuged again, the supernatant collected and combined with the supernatant from the first extraction. Chloroform (5.0 ml) and 5.0 ml of water was added to the combined supernatants and mixed by vortexing. The phases were separated by centrifugation at 3,020 x g for 30 seconds. The chloroform layer was air-dried, resuspended in 0.75 ml methanol/chloroform (2:1) and spotted onto silica gel 60 thin layer chromatography (TLC) plates (EM Science). The plates were developed for 3 hr in 100 ml chloroform/acetone/methanol/acetic acid/water (10:4:2:2:1) and dried. Two-cm horizontal swaths of silica were scraped from the plate, leaving only a small vertical section of silica for staining. Lipid was extracted from the scraped silica with methanol/chloroform (2:1, 3 x 0.5 ml) followed by centrifugation at 15,400 x g to pellet the silica, and the extract was dried. The extract was re-extracted 3 x 0.5 ml methanol/chloroform (2:1), centrifuged twice at 15,400 x g for 5 minutes to remove residual silica, and the final extract was dried for analysis. The

remainder of the plate was then stained with 0.5% ninhydrin (3% acetic acid in 1-butanol) and incubated at 100$^{o}$C for 5 minutes. PE resolved with an $R_f$ value of approximately 0.55.

**Phosphatidylethanolamine analysis**. The polar lipid extracts were analyzed by Liquid Chromatography – Tandem Mass Spectrometry performed on an Applied Biosystems/MDS SCIEX 365 tandem MS system with an electrospray interface (LC-ESI-MS-MS). The LC system (Agilent 1100 LC) used for introduction of the sample into the mass spectrometer consisted of an in-line vacuum degasser, a quaternary solvent pump, an autosampler, a column oven and a diode-array detector (Agilent 1100, Agilent, Palo Alto). The autosampler was equipped with a 100 µl sample loop. Details of phospholipid analyses at this system were described elsewhere (Lytle *et al.*, 2000; White *et al.*, 2002). A Thermo Dash-8 20 x 2.1 mm HPLC column was used for the reversed phase chromatographic separation of phospholipids. A gradient solvent system composed of solvent A (water) and solvent B (methanol/acetonitrile 90:10 + 0.002% piperidine) was used with a flow rate of 100 µl min$^{-1}$. At the beginning of the gradient, the mobile phase was 80% of B for 0.5 min. Solvent B was increased to 100% at 15 min. The mobile phase was then held isocratically for 10 min. Solvent B was decreased within 0.5 min to the starting value and the column equilibrated for 5 min. The column oven was held at 40°C.

The mass spectrometer was operated in the positive ionization mode to uniquely detect the PE molecules and determine their mass (*m/z*) by a neutral-loss scan (NL) for the PE head group (*m/z* 141). The acyl-chain composition within the detected PEs was determined by a product ion scan ($MS^2$) in the negative ionization mode. Overviews of methods for ESI-MS-MS of phospholipids were recently given (Sturt *et al.*, 2004; Taguchi *et al.*, 2005).

With a palmitoyl-oleoyl phosphatidylethanolamine standard (PE-16:0/18:1, Avanti Polar Lipids Inc.) infused into the ESI source, the instrument source parameters (e.g., curtain gas,

nebulizer gas, source heater) were optimized as follows. The source temperature was 450ºC. For positive ionization, the ion transfer voltage (IS) between electrospray needle and vacuum interface was set to 5000 V or in the negative mode to -4400 V,with the skimmer held at ground potential. The declustering potential (DP, voltage between orifice plate and ground), the focussing potential (FP, voltage between skimmer and ring potential), and the collision energy (CE) for collision-induced dissociation (CID) were optimized at 30 V, 290 V, and 30 V in the positive mode and at -40 V, -280 V, and -45 V in the negative mode, respectively. Nitrogen was used as collision gas. The nitrogen curtain gas, and the ion-source gases 1 (nebulizer gas) and 2 (turbo gas at the heater) were set to pressures of approximately 20, 30 and 60 psi (1.4, 2.0, 4.1 bar), respectively. The mass spectrometer was tuned from *m/z* 5 to 2000 amu according to the protocol provided by the manufacturer.

The fragementation of the $[M+H]^+$ ions of PEs is dominated by the *m/z* $[M-141]^+$ ion, which unequivocally characterizes molecules of this lipid class. This decomposition, releasing the phosphatidylethanolamine head group as a neutral molecule [$H_2PO_4CH_2CH_2NH_2$], can be assessed by tandem mass spectrometer as loss of *m/z* 141. The obtained masses uniquely characterized the *m/z* $[M+H]^+$ of PEs.

The relative concentration of PE within a sample was assessed based on the ion currents of the individual phospholipids set in relation to the sum of all detectable PE species in the neutral-loss scan. To exclude molecules with low abundances and with background signals, a cut-off of 15% signal intensity was applied. Absolute concentrations of PE species were calculated based on a calibration curve obtained with a PE 16:0/18:0 standard (Avanti Polar Lipids).

In the negative mode, subsequent collision-induced fragmentation of the proposed PE ion m/z $[M-H]^-$ revealed the acyl chain composition within the individual PE. The position on the glycerol backbone was assigned based on the signal intensities of the abundant carboxylate anion as the *sn*-2 derived anion is usually preferred at a ratio greater than 2 to 1 (Pulfer and Murphy, 2003). The assignment as PEs could be additionally verified based on the diagnostic ion of the PE headgroup at *m/z* 140 $[HPO4CH2CH2NH2\ ]^-$, which was visible at a low abundance.

Fragmentation scans in the negative mode indicated that the samples still contained phosphatidylglycerol (PG) characterized by the diagnostic ions *m/z* 153 $[CH_2C(OH)CH_2HPO_4]^-$and m/z 171 $[HPO_4CH_2CH(OH)CH_2OH]^-$. However, the PG did not compromise either the quantification of PE or analysis of fatty acid composition.

Phospholipids were designated as follows: PL-C1:d1/C2:d2 (e.g. PE-16:0/18:1), where C1 and C2 are the numbers of carbon atoms in the fatty acyl chains on the *sn*-1 and *sn*-2 positions, respectively; d1 and d2 are the numbers of double bonds of the *sn*-1 and *sn*-2 fatty acyl chains, respectively; and PL is the abbreviation for phospholipids class.

**Stimulation assay**. Chemotaxis was quantified using the stimulation assay (Kearns and Shimkets, 1998). This assay measures the period of time between cell reversals (reversal period, which is approximately 7 minutes for unstimulated cells) (Blackhart and Zusman, 1985). Attractants increase the reversal period (Kearns and Shimkets, 1998). The stimulation assay was performed as previously described with minor modifications (Kearns and Shimkets, 1998). PE purified from DK1622, LS2300 or JD300 was solubilized in chloroform to 0.5 mg $ml^{-1}$. A TPM agar plate was dried for 10 min at 37$^o$C. Then 4 μl of PE solution was applied to the surface of the agar plate and the solvent was evaporated by incubation at 37$^o$C for 15 minutes. Five microliters of DK1622 cells diluted to 5 x $10^7$ cells $ml^{-1}$ in MOPS buffer (10 mM MOPS, 8 mM

$MgSO_4$, pH 7.6) was applied to the PE spot and incubated at 32°C for 15 minutes. Cells were then observed at 25°C with a Leitz Laborlux D microscope for 45 min at 640x magnification. Stop-motion digital movies were produced with a microscope-mounted Sony Power HAD 3CCD color video camera and a Macintosh 9500 with Adobe PREMIERE software (Adobe Systems, Mountain View, CA; frame capture rate, 12 frames per min). The reversal period was manually enumerated for 15-20 isolated cells per movie. The mean and standard deviation were calculated from three movies.

## Results

**Analysis of double bond position in unsaturated fatty acids.** Fatty acid methyl esters (FAMEs) were prepared from wild type cells (Hartig *et al.*, 2005), separated by gas chromatography (GC), and analyzed by mass spectrometry (MS) (Figure 2-1A). The most abundant fatty acid was iso15:0 while the second most abundant was 16:1ω5; this result agrees with previous analyses (Kearns *et al.*, 2001b; Ware and Dworkin, 1973). In order to identify the positions of the double bond, unsaturated fatty acids were derivatized with dimethyldisulfide (DMDS), which derivatizes the carbons flanking the double bond and facilitates fragmentation between the derivatized carbons (Figure 2-1B inset). The resulting mass spectrum verifies the position of unsaturation. In the case of the major 16:1 GC peak, the double bond was as the ω5 position (Figure 2-1B). The minor 16:1 species was the ω11 isomer. 15:1 exists as both ω10 and ω4 isomers (data not shown), although the ω4 isomer is more abundant (Figure 2-1A). Finally, an iso17:1 was found. Because it eluted from the GC column earlier than the iso17:0, it appeared to be a branched monounsaturated fatty acid. The fragmentation of the DMDS-derivitized product indicated unsaturation at the ω5 position ($\Delta^{11}$, data not shown).

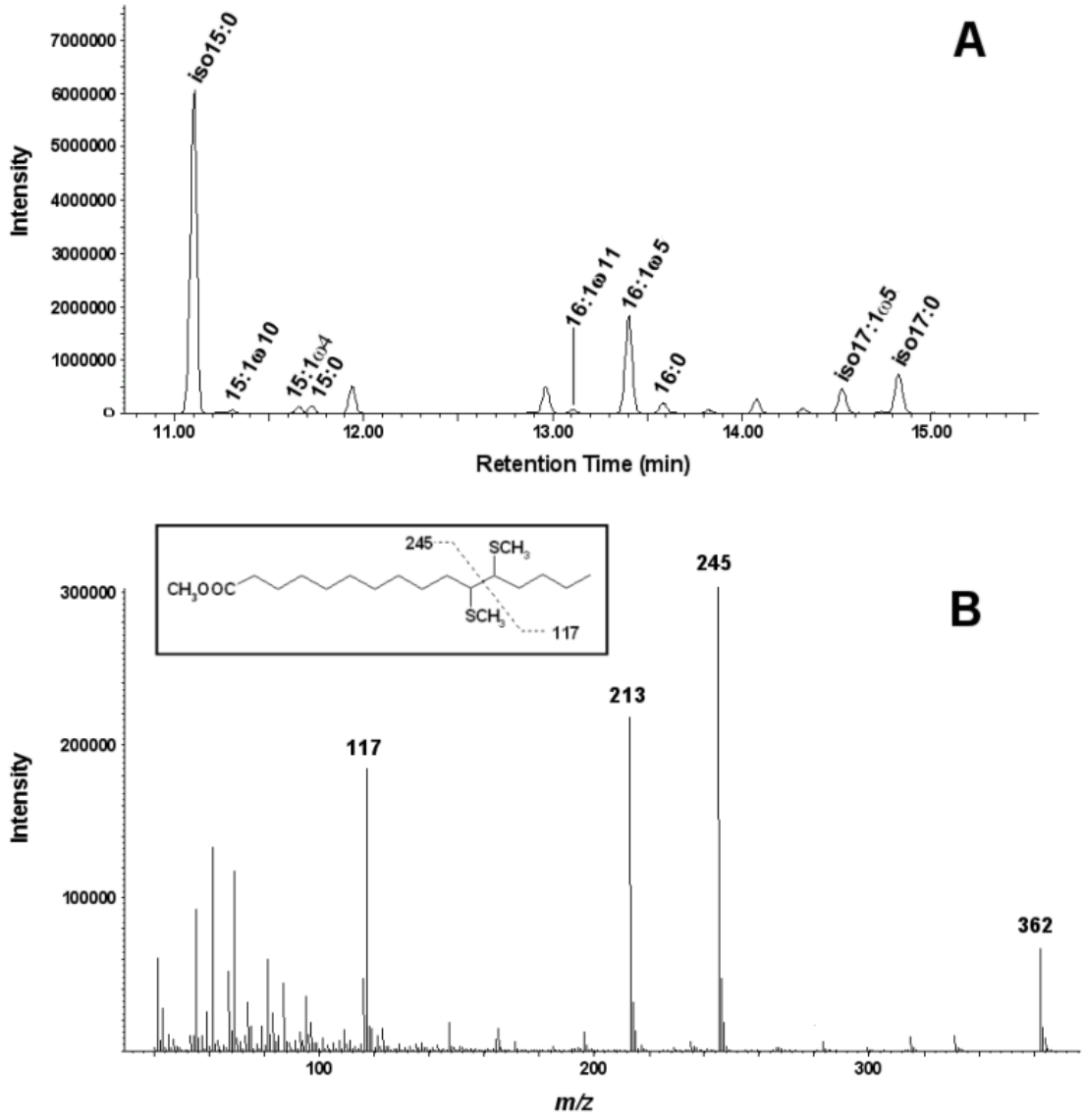


**Figure 2-1**: Analysis of fatty acids from *M. xanthus.* A. Fatty acid methyl esters were prepared from wild type *M. xanthus* DK1622 cells, separated by gas chromatography, and analyzed by mass spectrometry. B. Unsaturated fatty acid methyl esters were derivatized with dimethyldisulfide (DMDS) to determine the point of unsaturation by detecting the size of resultant fragments after derivatization and fragmentation. The mass spectrum of the 16:1ω5 DMDS derivative is depicted. Fragmentation between the ω5 and ω6 carbons would result in *m/z* 245 and 117 fragments respectively (inset). The parent ion (*m/z* 362) and fragment ions are detected in addition to the ion *m/z* 213 resulting from the loss of methanol from the fragment *m/z* 245.

**Analysis of *M. xanthus* vegetative and developmental PE**. PE from vegetative and developmental cells was purified by thin-layer chromatography (TLC) and liquid chromatography (LC). Finally, high-performance liquid chromatography (HPLC)-coupled electrospray ionization tandem mass spectrometry (HPLC-ESI-MS-MS) was used to identify the location and abundance of specific acyl chains in PE. The molecular ions of PE molecules were isolated by their mass (*m/z*, amu) in the negative mode $(M-H)^{\cdot}$, fragmented with $N_2$ causing collision-induced dissociation (CID), and the fragments were analyzed. The fatty-ester bonds at *sn*-1 and *sn*-2 exhibit different stabilities during CID, enabling the positions of fatty acids in PE molecules to be determined by the relative abundance of the fragment ions (Ekroos *et al.*, 2002; Taguchi *et al.*, 2005).

PE from vegetative *M. xanthus* cells contains at least 17 different molecular species; this number rises to at least 19 during development (Table 2-2). The most abundant PE species during vegetative growth is PE-15:0/15:0 (PE with the fatty acid 15:0 at the *sn*-1 and *sn*-2 positions, respectively, 20.3%) followed by PE-16:1/15:0 (12.0%). The lipids PE-16:1/16:1 and PE-17:2/15:0 (combined 12.0%) have the same *m/z* ratio and could not be separated. Because CID is a partial hydrolysis, it is difficult to separately quantify the abundances of different PE species with the same molecular weight. In this example, however, relative abundance of the two species is easy to infer from the CID. The abundance of 15:0 after CID is 30-fold lower than 16:1, indicating that there is much more PE-16:1/16:1 than PE-17:2/15:0. This conclusion is supported by GC-MS which shows that 17:2 is a low abundance fatty acid (data not shown) (Kearns *et al.*, 2001b).

The *sn*-1 position in vegetative PE is occupied by 5 saturated fatty acids and 12 unsaturated fatty acids, while the *sn*-2 position is occupied by 9 saturated fatty acids and 8

**Table 2-2.** Mass Spectrometry – Collision Induced Dissociation analysis of PE in *M. xanthus* strains.

| | PE Species | | Percent of Total PE (wild type and mutants) | | | | | | | |
|---|---|---|---|---|---|---|---|---|---|---|
| Progenitor Ion (*m/z*, amu) | Fragment Ion | | WT Veg. (DK1622) | WT Dev. (DK1622) | *plsB1* (LS2300) | *plsB2* (LS2301) | *esg*[a] (JD300) | *plsC2* (LS2305) | *plsC4* (LS2306) | *plsC5* (LS2307) |
| | *sn*-1 | *sn*-2 | | | | | | | | |
| 646.6 | 14:1<br>16:1 | 15:0<br>13:1 | | 2.5 | | 2.8 | 3.0 | 3.3 | | 3.9 |
| 648.6 | 14:0 | 15:0 | 5.6 | 5.3 | 8.0 | 4.4 | 6.3 | 6.8 | 6.1 | 8.1 |
| 658.6 | 16:1<br>15:1 | 14:1<br>15:1 | | | | | 3.2 | | | |
| 660.6 | 15:1<br>16:1 | 15:0<br>14:0 | 10.2 | 11.0 | 2.9 | 5.8 | 9.6[b] | 14.2 | 10.7 | 7.2 |
| 662.4 | 15:0 | 15:0 | 20.3 | 12.2 | 29.9 | 21.2 | 10.3 | 21.5 | 27.9 | 19.7 |
| 672.3 | 16:1<br>16:2 | 15:1<br>15:0 | 7.1 | | | 4.3 | 6.1 | 4.6 | 5.0 | 6.2 |
| 674.4 | 16:1 | 15:0 | 12.0 | 6.1 | 13.1 | 7.9 | 11.3 | 10.9 | 10.3 | 12.3 |
| 676.6 | 15:0 | 16:0 | | | 4.7 | | 5.0 | | | |
| 684.6 | 16:1 | 16:2 | 7.1 | 6.5 | 3.0 | 4.7 | 9.7 | 4.4 | 4.6 | 4.0 |
| 686.3 | 16:1<br>17:2 | 16:1<br>15:0 | 12.0 | 15.5 | 7.3 | 8.2 | 27.8 | 9.5 | 12.2 | 11.6 |
| 688.5 | 17:1<br>16:0 | 15:0<br>16:1 | 4.1 | 7.0 | 9.3 | 3.6 | 7.8[c] | 6.0 | 6.5 | 6.3 |
| 690.5 | 17:0 | 15:0 | 4.5 | 3.3 | 14.4 | 6.1 | | | | 4.3 |
| 698.4 | 17:2 | 16:1 | 3.4 | 4.5 | | | | 5.7 | 5.3 | 3.9 |
| 700.6 | 17:1 | 16:1 | 6.0 | 9.4 | | 3.5 | | 8.7 | 6.1 | 8.0 |
| 702.3 | 17:0<br>18:1 | 16:1<br>15:0 | 7.5 | 8.6 | | 4.0 | | 4.6 | 5.3 | 4.7 |
| 704.7 | 17:0 | 16:0 | | | | 2.6 | | | | |
| 712.2 | n/d | n/d | | 3.3 | | | | | | |
| 714.4 | n/d | n/d | | 4.9 | | | | | | |
| 716.7 | n/d | n/d | | | | 2.5 | | | | |
| 718.7 | n/d | n/d | | | | 3.5 | | | | |

[a] Strain JD300 (*esg*) was created previously (Toal *et al.*, 1995).
[b] PE-16:1/14:0 is more prevalent than PE-15:1/15:0 in this strain.
[c] PE-17:1/15:0 is undetectable and both PE-16:1/16:0 and PE-16:0/16:1 are detected in this strain.
Phospholipids were extracted from whole cells and purified by thin layer chromatography. The PE fraction was extracted from the silica and separated by liquid chromatography followed by electrospray ionization tandem mass spectrometry, wherein collision with nitrogen gas causes a preferential fragmentation of the *sn*-2 fatty ester linkage. The most abundant fatty acid after CID is the *sn*-2 fatty acid. The abundance of the PE species was determined by signal intensity (cps). In the case that two PE species have the same mass (*m/z*, amu), the more abundant species is listed above the less abundant as determined by the ratio of *sn*-2 fatty acid abundances after CID. PE species below 2% of total were not found consistently and have been omitted.

unsaturated fatty acids. The 16:1 fatty acid that is associated with chemotaxis is found in the *sn*-1 position of 5 PE species. In sum, they account for approximately 38.2% of all PE molecules.

16:1 is also found at the *sn*-2 position, where it accounts for about 28.9% of total. The fatty acid pairings in vegetative PE species did not change during development (Table 2-2), although some species changed in abundance. In vegetative cells, PE-15:0/15:0 was most abundant (20.3%), whereas under developmental conditions PE-16:1/16:1 was most abundant (15.5% including a small amount of PE-17:2/15:0). Four new PE species appear at the midpoint of development and two disappear. Development induces a notable increase in larger PE species, many of which contain 16:1 in the *sn*-2 position. Concordantly, the summed percentage of PE containing 16:1 at the *sn*-2 position rises from 28.9% to 38.0%.

**PE from *M. xanthus plsB1* and *plsB2* mutants**. PlsB initiates PE biosynthesis by transferring a fatty acid from the acyl carrier protein to the *sn*-1 position of glycerol-3-phosphate (Cronan and Rock, 1996). The *plsB* gene is considered one of the minimal set of 256 genes essential in bacteria (Gil *et al.*, 2004). Synthesis of PEs with unsaturated fatty acids at the *sn*-1 position could involve a PlsB that uses unsaturated fatty acyl substrates. While there is typically one *plsB* gene per organism, a tBLASTn search with the *E. coli* PlsB protein sequence identified two significant *M. xanthus* matches. PlsB1 (MXAN3288) showed 29% identity and 49% similarity to *E. coli* PlsB over the full length of the protein (5e-56 expect). As seen in Figure 2-2, PlsB1 contains the conserved amino acids shown to be essential for cell viability in *E. coli* (Heath and Rock, 1998; Lewin *et al.*, 1999). The TIGR annotation of MXAN3288 places 22 additional amino acids at the N terminus of the product, but these may be incorrectly assigned. Our proposed *plsB1* start site has a near-consensus ribosome binding site (RBS), AGGACG, 12 base pairs upstream of the start site, whereas MXAN3288 has no recognizable RBS. Using our

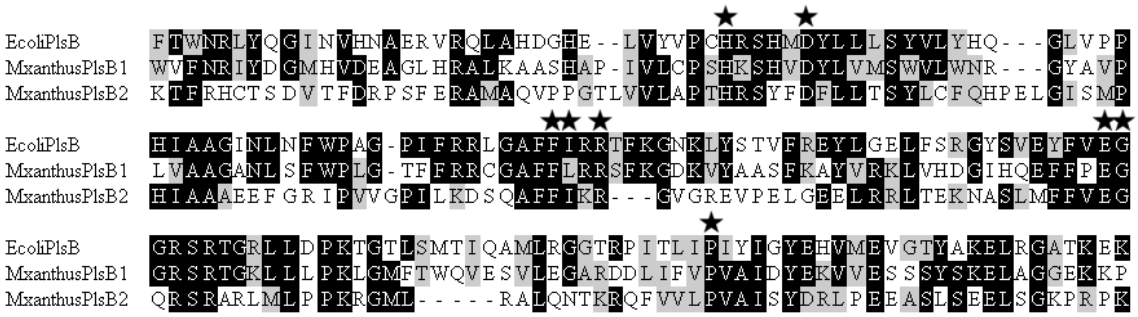


**Figure 2-2.** Alignment of *E. coli* PlsB and *M. xanthus* homologs. The *E. coli* PlsB protein (accession number P0A7A7, amino acids 273-446) was aligned with the *M. xanthus* PlsB1 (MXAN3288; 313-487) and PlsB2 (MXAN1675; 469-635) proteins. Stars indicate conserved amino acids known to be essential for viability in *E. coli* (Heath and Rock, 1998; Lewin *et al.*, 1999).or motility defects, and formed fruiting bodies containing 99% viable spores, comparable to the wild type.

start site, *plsB1* was deleted from the chromosome, leaving only the start codon separated from the stop codon by a six-base-pair *XbaI* site. The resulting mutant, LS2300, exhibited no growth defect. PlsB2 (MXAN1675) showed 33% identity and 48% similarity over the 452 C-terminal amino acids of the *E. coli* PlsB sequence (807 amino acids total).

PlsB2 also contains the conserved amino acids shown to be necessary for *E. coli* viability (Figure 2-2). The N-terminal half of PlsB2 showed some homology to eukaryotic fatty acid reductases (FARs). An alignment of PlsB2 amino acids 1-309 with eukaryotic FARs is shown in Figure 2-3. The NAD(P)H binding motif [I,V, F]-X-[I, L, V]-T-G-X-T-G-F-L-[G, A] conserved among eukaryotic FARs is indicated by the black box (Aarts *et al.*, 1997; Cheng and Russell, 2004; Metz *et al.*, 2000; Moto *et al.*, 2003). The *M. xanthus* sequence has a near-consensus NAD(P)H binding site as well as other conserved blocks of amino acids, suggesting that the N-terminal portion of PlsB2 may function in fatty acid reduction. MXAN1675 has a consensus RBS (AGGAGG) eight base pairs upstream of the predicted start. The portion of the gene containing the PlsB2 active site, corresponding to amino acids 416-868, was deleted to eliminate putative acyltransferase activity. The *plsB2* mutant had no obvious growth, motility or developmental defects (102% viable spores compared to the wild type).

PE was purified from vegetative *plsB1* and *plsB2* cells and analyzed by LC-ESI-MS-MS (Table 2-2). The most significant finding is that each mutant contains unsaturated fatty acids at the *sn*-1 position. While the majority of the fatty acid pairings for individual PE species remain the same, there are some changes in PE composition for these mutants. The *plsB1* mutant lacks many of the large molecular weight PE species present in wild-type, notably the species with *m/z* 698.4, 700.6 and 702.3. Each of these species has 16:1 at the *sn*-2 position. Furthermore, *m/z* 686.3, the principal species with 16:1 at the *sn*-2 position, declines by nearly 40%. For this

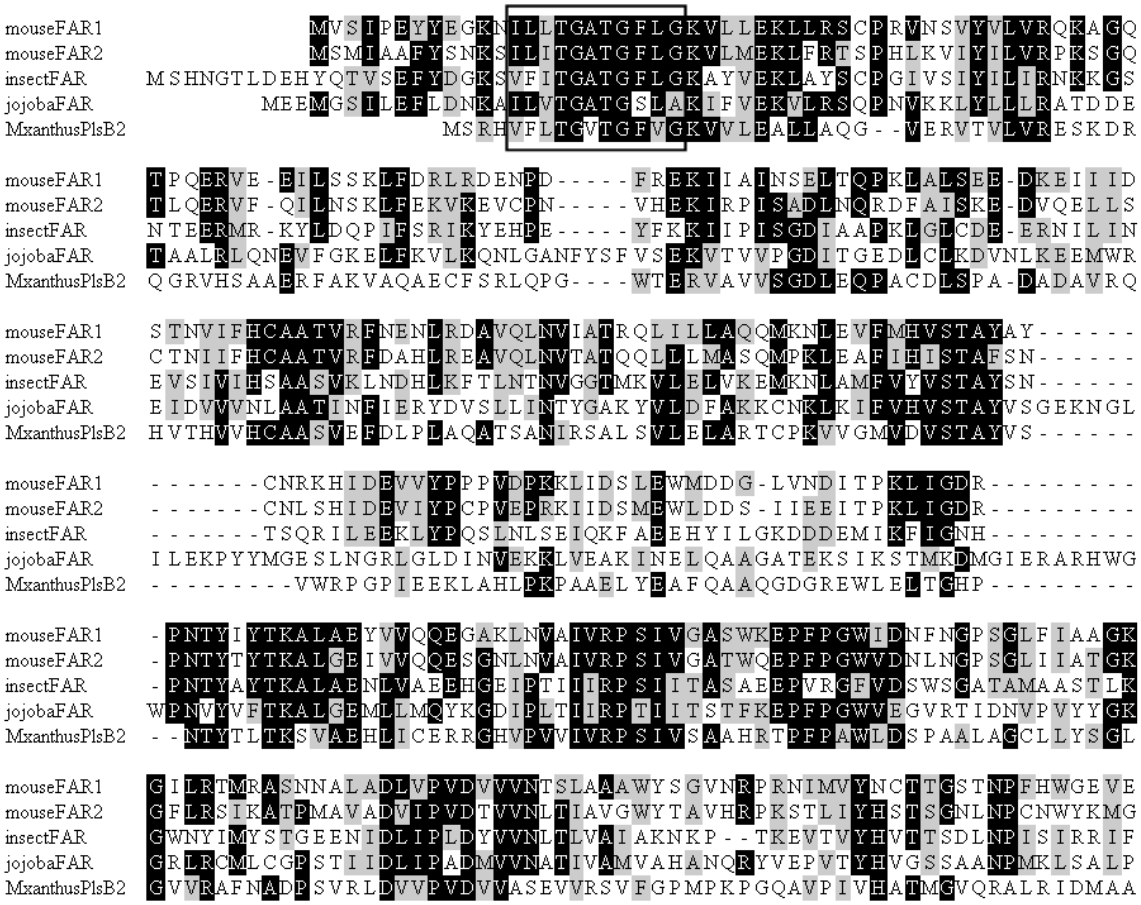


**Figure 2-3.** Alignment of several eukaryotic fatty acid-reductases (FAR) and *M. xanthus*. PlsB2 (amino acids 1-309). Mouse *Mus musculus* FAR 1, BC007178 amino acids 1-319, mouse FAR 2, BC055759 1-319, silkworm *Bombyx mori* FAR, BAC79426, 1-328, jojoba plant *Simmondsia chinensis* FAR, AD38040, 1-353. The boxed portion indicates the NAD(P)H-binding motif [I, V, F]-X-[I, L, V]-T-G-X-T-G-F-L-[G, A] (Aarts *et al.*, 1997; Cheng and Russell, 2004; Metz *et al.*, 2000; Moto *et al.*, 2003).

reason, total unsaturated fatty acids at the *sn*-2 position decline from about 44% to roughly 10% in the *plsB1* mutant. The *plsB2* mutant contains the high molecular weight PE species missing in the *plsB1* mutant in addition to other larger PE species (*m/z* 704.7, 716.7 and 718.7). Despite these changes, the three most abundant PE species are present in quantities similar to those of the wild-type. These results argue that PlsB1 and PlsB2 have overlapping substrate specificities.

The fatty acid composition at the *sn*-2 position appears to be dependent on the *sn*-1 fatty acid, given that a mutation that alters *sn*-1 acyltransferase activity also alters the *sn*-2 fatty acid content. If the *sn*-2 acyltransferase added fatty acids irrespective of which fatty acids occupy the *sn*-1 position, then the *sn*-2 fatty acid content would remain unchanged in this mutant.

**Analysis of PE from an *esg* mutant.** The *esg* mutant (JD300) is deficient in the BCKAD necessary for branched-chain fatty acid synthesis, resulting in PE that is enriched for 16:1 (Toal *et al.*, 1995). As previously reported, this mutant has reduced amounts of branched-chain fatty acids 15:0 and 17:0 (Table 2-2) (Toal *et al.*, 1995). PE-15:0/15:0 in the *esg* mutant decreased nearly two-fold compared to the wild type. Branched-chain fatty acid synthesis is not abolished in this mutant as a bypass mechanism has been recently elucidated (Mahmud *et al.*, 2002). The mass-spectral signal corresponding to PE-16:1/16:1 increased 2.3-fold, constituting 27.8% of the total PE. In the *sn*-1 position, the amount of 16:1 rises from roughly 38.2% in wild type to approximately 71.6% in the *esg* mutant. While this mutant lacks many of the high-molecular-weight PE species found in the wild type due to fact that the 17-carbon branched chain fatty acids are missing, the *sn*-2 16:1 content is similar to that in the wild type, largely due to the increase in PE-16:1/16:1. Fatty-acid pairings are similar in the *esg* mutant and in the wild-type, but the total fatty acid content is changed. This again suggests that the fatty acids added to the *sn*-2 position are dependent on the *sn*-1 acyl chain, and not the overall fatty acyl-ACP pool.

Again, the 16:1 acyl chains can be attributed mainly to the ω5 species, which is by far the most abundant 16:1 isomer in *M. xanthus*.

**Analysis of PE from three *M. xanthus plsC* mutants**. PlsC is an essential enzyme that adds a fatty acid to the *sn*-2 position of 1-acyl-*sn*-glycerol-3-phosphate (Cronan and Rock, 1996). Typically, there are 1-2 *plsC* genes per organism (Cronan and Rock, 1996; Shih *et al.*, 1999). Searching the *M. xanthus* genome with the *E. coli* PlsC sequence (tBLASTn) revealed 5 homologs: *plsC1* (MXAN3330), *plsC2* (MXAN3969), *plsC3* (MXAN5578), *plsC4* (MXAN0955) and *plsC5* (MXAN0147). The related protein products had 28-36% identity and 49-56% similarity to the *E. coli* protein over the entire length of the protein. PlsC enzymes have conserved amino acid blocks similar to PlsB enzymes (Li *et al.*, 2003; Weier *et al.*, 2005), and the *M. xanthus* PlsC homologs contain many of the conserved residues (Figure 2-4). All the homologs had the characteristic small size of PlsC enzymes. The *plsC2*, *plsC4* and *plsC5* genes were each mutated by homologous integration of a plasmid bearing an internal fragment of each gene. This method results in a merodiploid in which both copies of the gene are truncated. PE from each mutant was purified and analyzed by LC-ESI-MS-MS (Table 2-2). Although some changes were observed, such as an increase in PE-15:0/15:0 in the *plsC4* mutant, most values stay within 1.5-fold of each other for comparable PE species. These results suggest that the homologs are either functionally redundant or biologically inactive.

**Chemotactic excitation by PE from different strains.** Previous work demonstrated that *M. xanthus* alters its motility in response to PE with specific fatty acids (Kearns and Shimkets, 1998). Solitary *M. xanthus* cells travel over solid surfaces in one direction for 7 minutes before reversing direction (reversal period) (Blackhart and Zusman, 1985). In the presence of certain PEs, *M. xanthus* cells are stimulated to travel longer distances before

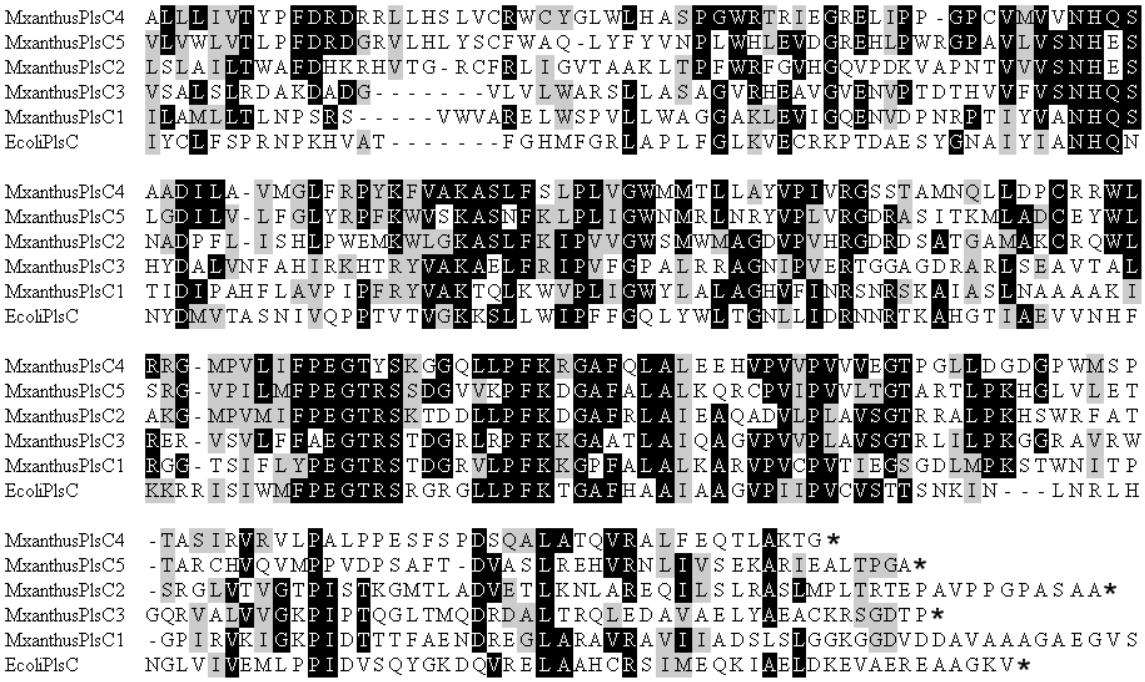


**Figure 2-4.** Alignment of *E. coli* PlsC and *M. xanthus* PlsC homologs. The *E. coli* PlsC protein (P26647, amino acids 22-245) was aligned with the five *M. xanthus* PlsC homologs: PlsC1 (MXAN3330; 22-254), PlsC2 (MXAN3969; 30-263), PlsC3 (MXAN5578; 26-245), PlsC4 (MXAN0955; 45-264) and PlsC5 (MXAN0147; 61-282).

reversing directions. Not all PEs produce this response indicating a molecular specificity related to a particular fatty acid. PE-12:0/12:0 and PE-18:1ω9/18:1ω9 elicit a response, PE-14:0/14:0, PE-16:0/16:0, PE-17:0/17:0 and PE-18:0/18:0 do not (Kearns and Shimkets, 1998). Cells adapt over time and the stimulated reversal period falls back to the unstimulated level. Stimulation and adaptation are hallmarks of chemotaxis (Kearns and Shimkets, 1998).

Neither of the chemoattractants, PE containing 12:0 or PE containing 18:1ω9, are found in *M. xanthus*. PE containing 18:1 is found in many bacteria *M. xanthus* preys on and may be involved in prey recognition. The nature of a native attractant found in the *M. xanthus* membrane was revealed through metabolic engineering and linked to the fatty acid 16:1ω5 (Kearns *et al.*, 2001b). PE-16:1ω5/16:1ω5 was synthesized and found to be about 1000-fold more active than the other two attractants and active at physiological concentrations. The chemical synthesis was performed with identical fatty acids at both positions simply because it was easier and was completed without prior knowledge of the PE composition of the *M. xanthus* membrane. Table 2-2 illustrates the unexpected finding that PE-16:1/16:1 is both present and abundant in *M. xanthus* and there are a wide variety of other species containing 16:1 at the *sn*-1 position. This raises the question of whether the chemotactic response is more sensitive to 16:1ω5 at the *sn*-1 position, or the *sn*-2 position.

The percent PE with 16:1 at a given *sn* position was determined from the data in Table 2-2 by summing the percentages for each PE containing 16:1 at that position. In cases where the PE contained multiple fatty acid pairings, only the most abundant species was considered. The PE with *m/z* 688.5 peak in the *esg* mutant did not contain PE-17:1/15:0 (like the wild type) but instead had a mixture of PE-16:0/16:1 and PE-16:1/16:0, as represented by equal amounts of each fatty acid after CID. For the purpose of this analysis, 3.9% of total PE was assigned to *sn*-1

and 3.9% to *sn*-2 16:1. The 16:1 composition for vegetative wild type, 24-hour-developing wild type, *plsB1* and *esg* cells is reported in Table 2-3 and represent the most varied examples of 16:1 distribution among the strains reported in Table 2-2. *esg* PE had by far the largest amount of *sn*-1 16:1 at 71.6%. The next highest is vegetative wild-type PE at 38.2%, then developmental wild-type PE at 28.1% and finally *plsB1* PE at 23.4%. However, this order is not preserved for the *sn*-2 position. The highest *sn*-2 16:1 composition is developmental wild-type PE at 38.0%, followed by *esg* PE at 31.6%, vegetative wild-type PE at 28.9%, and *plsB1* PE at 7.3%.

The ability of the collective pool of PE from each strain to stimulate chemotaxis was assayed by tracking the movement of wild-type cells by time-lapse video microscopy. The reversal period of cells in the absence of PE was 7.0 ± 1.0 min and provides the baseline for unstimulated cells (Table 2-3). In trial experiments the optimal response was found with 2 μg PE distributed over an area of about 0.16 $mm^2$ and overlaid with about 5 x $10^4$ cells. PE from the *esg* mutant was most active and produced a reversal period of 47.3 ± 17.0 minutes (Table 2-3). *esg* PE has the largest abundance of 16:1 at the *sn*-1 position and more average levels of *sn*-2 16:1. Vegetative and developmental wild-type PE and *plsB1* PE produced comparable reversal periods. PE from the *plsB1* mutant has a similar amount of *sn*-1 16:1 to wild-type cells, but much lower *sn*-2 16:1. Together these results argue that the *sn*-1 position is more important than the *sn*-2 position for stimulating chemotaxis. A linear regression analysis was performed and an excellent correlation with reversal period was observed for *sn*-1 16:1 ($R^2$=0.95), but not *sn*-2 16:1 ($R^2$=0.09).

Although the *sn*-1 position appears to be more important for chemotactic stimulation than *sn*-2, this relationship may be driven by a particular PE species. The most dramatic correlation

**Table 2-3.** PE enriched in *sn*-1 16:1 stimulates chemotaxis.

| PE Type | Reversal Period | *sn*-1 16:1 | *sn*-2 16:1 | PE-16:1/16:1 |
|---|---|---|---|---|
| None | 7.0 ± 1.0 | - | - | - |
| *plsB1* | 16.0 ± 1.9 | 23.4 | 7.3 | 7.3 |
| Dev WT | 17.4 ± 5.2 | 28.1 | 38.0 | 15.5 |
| Veg WT | 18.4 ± 1.1 | 38.2 | 28.9 | 12.0 |
| *esg* | 47.3 ± 17.0 | 71.6 | 31.7 | 27.8 |
| $R^2$ | | 0.95 | 0.09 | 0.88 |

PE was purified from vegetative DK1622 (Veg WT), 24-hour-developing DK1622 (Dev WT), LS2300 (*plsB1*) and JD300 (*esg*) cells. Relative amounts of 16:1 at the *sn*-1 and *sn*-2 positions were calculated from the data in Table 2-2 by summing the percentages of each molecular PE species containing 16:1. Where two molecular species pairings have the same *m/z* only the most abundant pairing was considered. PE from these same strains was used to assess chemotaxis of wild type DK1622 cells using the stimulation assay. In this assay, attractants increase the reversal period from an unstimulated level of 7 minutes depending on the abundance of attractant molecules in the preparation. PE preparations are listed in order of increasing stimulated reversal period. Linear regression was performed between the reversal period stimulated by each sample and the amount of 16:1 at the *sn*-1 position, *sn*-2 position or the species PE-16:1/16:1. Regression analysis was performed using Microsoft Excel.

between reversal period and specific species containing 16:1 was PE-16:1/16:1 ($R^2$=0.88, Table 2-3). PE-16:1ω5/16:1ω5 has been synthesized and is the strongest attractant described for *M. xanthus* (Bonner *et al.*, 2005; Kearns *et al.*, 2001b). Whether other PE species with 16:1 at the *sn*-1 position are chemoattractants and contribute to the observed stimulation is unknown, but it is quite evident that the abundance of 16:1 at the *sn*-1 position is strongly correlated with chemotaxis.

**Abundance of 16:1ω5 in analyzed strains and communities.** The fatty acid 16:1ω5 is rarely found in cultured bacteria and generally represents a small proportion of the total fatty acids (Table 2-4). There are only a few exceptions. For example, 16:1ω5 has been suggested as a biomarker for arbuscular mycorrhizal fungi in soil (Olsson *et al.*, 1995). Elevated proportions of 16:1ω5 and a high ratio of 16:1ω5 to 16:1ω7 (including 16:1ω6) were found in the phospholipid fatty acids (PLFA) of a strain of *Flexibacter flexilis* which contained 51% of its PLFA as 16:1ω5 with a ratio=[16:1ω5]/([16:1ω7]+[16:1ω6]) of 96 (Nichols *et al.*, 1986). This is unusual for the cultured Flavobacterium/Cytophaga. Another unusual strain from this group, *Cytophaga hutchinsonii*, also has a high level of 16:1ω5. Cultured Type I methanotrophs like *Methylomonas* sp. 761 contain high levels of 16:1ω5 (16% of its PLFA as 16:1ω5 and a ratio of 0.94) (Nichols *et al.*, 1985), whereas other cultured methanotrophs do not. In the environmental database compiled by MIDI, Inc. (Newark, DE) 16:1ω5 was found in only 46 of 906 bacterial species. Of these 46, only 3 contained 16:1ω5 above 4% of the total fatty acids released by alkaline saponification: *Bradyrhizobium japonicum* 6.4%, *Mycobacterium marinum* 8.0% and *Empedobacter brevis* 8.6% (data kindly supplied by Gary Jackoway, MIDI Inc., Newark, DE). In these cases, however, the 16:1 fatty acids are mixtures of isomers with different points of unsaturation. The ratio of 16:1ω5 to 16:1ω7 + 16:1ω6 is 3.0 for *B. japonicum*, 1.3 for *M.*

**Table 2-4.** 16:1ω5 and 16:1ω7/16:1ω6 content in cultured bacteria and environment samples.

| Organism | % 16:1ω5 | % 16:1ω7/ω6 | Ratio[a] | Reference |
|---|---|---|---|---|
| *Bacillus firmus* | 3.8 | 0.9 | 4.2 | Jackoway[b] |
| *Bradyrhizobium japonicum GC subgroup B* | 6.4 | 2.1 | 3.0 | Jackoway |
| *Bradyrhizobium japonicum GC subgroup A* | 1.8 | 0.7 | 2.6 | Jackoway |
| *Mycobacterium marinum* | 8.0 | 6.3 | 1.3 | Jackoway |
| *Roseomonas cervicalis* | 3.5 | 2.9 | 1.2 | Jackoway |
| *Hyphomonas neptunium* | 1.3 | 1.8 | 0.7 | Jackoway |
| *Roseomonas genomospecies 5* | 1.2 | 1.8 | 0.6 | Jackoway |
| *Empedobacter brevis* | 8.5 | 21.4 | 0.4 | Jackoway |
| *Streptococcus mitis* | 2.2 | 6.0 | 0.4 | Jackoway |
| *Exiguobacterium acetylicum* | 2.6 | 7.3 | 0.4 | Jackoway |
| *Geobacter metallireducens* | 1.5 | 40.7 | 0.04 | (Lovley *et al.*, 1993) |
| *Caulobacter*-like aerobic dye degrader | 1.4 | 25.7 | 0.05 | (Govindaswami *et al.*, 1993) |
| *Desulfomonile tiedjei* | 2.1 | 23.7 | 0.1 | (Ringelberg *et al.*, 1994) |
| Subsurface Sphingomonas | 0.3 | 2.1 | 0.1 | (Balkwill *et al.*, 1997) |
| *Pseudoalteromonis tunicata* | 0.4 | 47.5 | 0.008 | (Holmstrom *et al.*, 1998) |
| *Syntrophomonas wolfei* (valerate) | 5.7 | 0.2 | 28.5 | (Henson *et al.*, 1988) |
| Soil methanotrophs | 5.3 | 10.3 | 0.5 | (Nichols *et al.*, 1987) |
| Surface soil | 1.7 | 3.5 | 0.5 | (Ringelberg *et al.*, 1989) |
| Propanotrophs | 3.2 | 22.0 | 0.1 | (Ringelberg *et al.*, 1989) |
| Oak rhizosphere | 9.3 | 11.2 | 0.8 | (Ringelberg *et al.*, 1997) |
| *Myxococcus xanthus* | 24.0 | 0.3 | 80.0 | (Ware and Dworkin, 1973) |
| *Myxococcus xanthus* | 16.3 | 0.13 | 125.4 | This study |

[a] Ratio is determined by dividing the percent 16:1ω5 by the percent 16:1ω7 (including 16:1ω6)
[b] Gary Jackoway, (MIDI Inc., Newark, DE) personal communication

*marinum* and 0.4 for *E. brevis*. In a previous study, 16:1ω5c in *M. xanthus* constitutes an even larger percentage of the total fatty acids (24%) than in the previous examples and is in much higher proportion to other 16:1 isomers (a ratio of 80.0, Table 2-4) (Ware and Dworkin, 1973). While, in this study, the relative abundance of 16:1ω5 was smaller (16.3%, Table 2-4), the ratio of isomers still strongly favors the ω5 isomer at 125.4. A high ratio of 16:1ω5 to 16:1ω7 + 16:1ω6 in PLFA can also be found in *Syntrophomonas wolfei/ Desulfovibrio sp.* cocultures growing with valerate instead of butyrate (28.5; (Henson *et al.*, 1988)), however the total 16:1ω5 was comparatively low at 5.7%. 16:1 found in *Stigmatella aurantiaca*, another myxobacterium, is predominantly in the ω5c form and is relatively high in abundance (Dickschat *et al.*, 2005).

The conclusion that *M. xanthus* and *S. aurantiaca* are unusual in having both a high level of 16:1ω5 and a high ratio of 16:1ω5 relative to other 16:1 isomers is strengthened by examining microbial communities. In surface soil and in an oak rhizosphere 16:1ω5 can be detected but is not the most abundant 16:1 isomer (Table 2-4). A similar result is obtained with soils enriched with different carbon sources such as methane and propane.

**Discussion**

*M. xanthus* vegetative PE contains at least 17 different PE species (Table 2-2), rising to 19 during development. Among all the strains examined, 27 different PE species were detected. The number is surprising as most Proteobacteria have on average 5-7 different PE species (Cronan and Rock, 1996; Rahman *et al.*, 2000). Even more unusual is the fact that 12 of the 17 fatty acids found at the *sn*-1 position in *M. xanthus* PE are unsaturated (Table 2-2), which violates the well-established paradigm for Proteobacteria (Cronan and Rock, 1996).

In addition to the diversity observed in PE species, there is a large amount of diversity in the fatty acids themselves, as exemplified by the multiple points of unsaturation found in unsaturated fatty acids. 15:1 fatty acids were represented by ω4 ($\Delta^{11}$) and ω10 ($\Delta^{5}$) isomers, 16:1 by ω5 ($\Delta^{11}$) and ω11 ($\Delta^{5}$) isomers and iso17:1 by ω5 ($\Delta^{11}$). However, the mechanism for generating this diversity is unclear. In the well-characterized *E. coli* fatty acid biosynthetic pathway, unsaturated fatty acids are created by the action of FabA (Cronan and Rock, 1996). FabA isomerizes the *trans*-$\Delta^{2}$ double bond intermediate (which is usually reduced to create a fully saturated acyl chain) to the *cis*-$\Delta^{3}$ double bond, which is preserved in further acyl-chain elongation. Given that only one point of unsaturation is observed in *E. coli*, FabA must have molecular specificity for the intermediate to be isomerized. If *M. xanthus* produces unsaturated fatty acids using a similar pathway, it would require multiple FabA homologs to introduce unsaturations at different positions on different fatty acids.

At least four FabA homologs are found in the *M. xanthus* genome. Additionally, in this model, fatty acids with even numbers of carbons must have unsaturations with odd-numbered ω positions (and the opposite case for fatty acids with odd numbers of carbons). In fact, this pattern is observed. There is, however, a far simpler explanation for the pattern of unsaturations. In the case of 15:1ω4, 16:1ω5 and iso17:1ω5, the point of unsaturation in each fatty acid is conspicuously 11 carbons from the Δ terminus. Similarly, for 15:1ω10 and 16:1ω11, the point of unsaturation is 5 carbons from the Δ terminus. Therefore, the pattern of unsaturations observed could easily be explained by the action of a $\Delta^{11}$ desaturase and a $\Delta^{5}$ desaturase, and in fact desaturases are found in the genome. This model for desaturation is similar to the method used by *Bacillus* (Aguilar *et al.*, 1998) and cyanobacteria (Hongsthong *et al.*, 2004). In *Bacillus* and in cyanobacteria, the acyl-lipid desaturases introduce double bonds at specific positions (usually

relative to the Δ terminus) in fatty acids that have already been esterified to glycerolipids. While the *E. coli* model for biosynthesis of unsaturated fatty acids is viable for *M. xanthus*, the desaturase model is the simplest explanation for the pattern of unsaturations observed. Further testing will be needed to determine exactly what role each model has in contributing to unsaturated fatty acid diversity in this organism.

The chemotactic activity of *M. xanthus* PE is associated with the fatty acid 16:1ω5. This compound is rare in bacteria and in other natural samples. It may be a chemoattractant for the myxobacteria, since *M. xanthus* and *S. aurantiaca* both contain high levels of the ω5 isomer. High levels of 16:1 are also present in other myxobacteria *Nannocystis exedens* and *Sorangium cellulosum*, although the isomer(s) is unknown (Iizuka *et al.*, 2003). Synthetic PE-16:1ω5/16:1ω5 is a potent chemoattractant for *M. xanthus* (Kearns *et al.*, 2001b), and here we show that PE-16:1/16:1 is one of the major PE constituents. However, there are several other PE species containing 16:1 at either *sn* position. *M. xanthus* may respond to PE with 16:1 at the *sn*-1 position, the *sn*-2 position, or a particular 16:1-containing species. In addition, PE may be hydrolyzed by a phospholipase and the free fatty acid detected. Regression analysis with chemotactic stimulation by PE of varying composition shows strong linear relationships with *sn*-1 16:1 and with the species PE-16:1/16:1. However, the alternate hypothesis of position specific cleavage by phospholipase $A_1$ cannot be ruled out. Taken as a whole, the results argue that the wide diversity in PE species by *M. xanthus* is due to the fact that some species play a role in cell-cell signaling. It appears that *M. xanthus* has deployed a rare unsaturated fatty acid (16:1ω5) at an unusual position in PE (*sn*-1) to obtain a species or group-specific signaling molecule.

A key to understanding the evolution of this signaling system is the enzymology leading to the deployment of unsaturated fatty acids at the sn-1 position. One case of unsaturated fatty

acid localization at the *sn*-1 position has been examined previously; phospholipids of *Clostridium butyricum* have both saturated and unsaturated fatty acids at the *sn*-1 position while the *sn*-2 position has only saturated fatty acids (Heath *et al.*, 1997). The *sn*-1 fatty acid bias in *C. butyricum* involves a unique PlsC-like *sn*-1 acyltransferase, PlsD. However, there is no evidence *M. xanthus* uses a similar strategy as PlsB1 and all 5 PlsC homologues found in the *M. xanthus* genome closely resemble their *E. coli* counterparts (Figures 2-2 and 2-4). In addition, *M. xanthus* PE does not have a reversed fatty acid bias like *C. butyricum* (variable saturation at the *sn*-1 position and predominantly saturated at the *sn*-2) but rather an aberrant one (predominantly unsaturated at the *sn*-1 and variable at the *sn*-2). Therefore it appears that *M. xanthus* PE has properties that differ from not only the established lipid paradigm, but also other unusual cases.

*M. xanthus* is unusual in the large number of putative acyltransferase genes present in the genome. We suspected that one of the two *plsB* genes might be the source of the unsaturated fatty acids at the *sn*-1 position. However, deletion of *plsB1* or *plsB2* did not eliminate unsaturated fatty acids at the *sn*-1 position, suggesting that both acyltransferases contribute unsaturated fatty acids. The N-terminal half of PlsB2 is similar to several eukaryotic fatty-acid reductases (FAR). These enzymes reduce fatty acyl-CoA substrates to free fatty alcohols (Kolattukudy, 1970) either for synthesis of waxes, a reaction where a fatty alcohol is esterified to another fatty acid, or ether-linked phospholipids synthesis [for review, see (Nagan and Zoeller, 2001)]. Prokaryotic fatty acid reduction utilizes two enzymes, one to reduce the fatty acyl-CoA to the fatty aldehyde, and a second to reduce the fatty aldehyde to the fatty alcohol (Reiser and Somerville, 1997). Eukaryotic FAR use a single enzyme with a NAD(P)H-binding motif to reduce fatty acyl-CoA to the fatty alcohol in a single enzyme (Kolattukudy, 1970). In both eukaryotic and prokaryotic systems, the reductases are separate enzymes from the

acyltransferases. Therefore, PlsB2 is unique in that the FAR is more similar to eukaryotic reductases, and is uniquely coupled to an acyltransferase domain. It appears unlikely that PlsB2 functions solely in ether-lipid production, though ether lipids are detected in myxobacteria (Caillon *et al.*, 1983; Kleinig, 1972), because the *plsB1* mutation would be lethal. The *plsB1* gene was deleted without complication and while there is a loss of some of the higher molecular weight species, the majority of the species and their abundances remain similar to the wild type (Table 2-2). Therefore, it seems likely that the PlsB2 acyltransferase domain functions in PE biosynthesis.

The *plsB2* gene is located next to a putative alkyl-dihydroxyacetone phosphate synthase gene; the stop codon of the synthase overlaps the start codon of *plsB2* by one base pair suggesting translational coupling. This enzyme catalyzes the exchange of a fatty alcohol for a fatty acid at the *sn*-1 position of 1-acyl-dihydroxyacetone phosphate, creating an intermediate in eukaryotic ether lipid biosynthesis. The proximity of these genes combined with the nature of the FAR domain would suggest that PlsB2 functions in ether lipid biosynthesis. Therefore, it is possible that PlsB2 has a dual role in both PE biosynthesis and ether lipid biosynthesis.

Lipid signaling may be involved in maintaining culture specificity during fruiting body formation in the midst of a complex microbial community. The output from lipid signaling assayed in these experiments is an alteration of motility. The chemotaxis signal passes through the *dif* chemosensory pathway (Bonner *et al.*, 2005; Kearns *et al.*, 2000), which also regulates extracellular matrix production, another component of surface-dwelling organisms that is essential for fruiting body formation (Bellenger *et al.*, 2002; Black and Yang, 2004; Yang *et al.*, 2000). The coupling of matrix production and lipid sensing is unusual and may reflect the fact that extracellular matrix is essential for a response to some lipid attractants.

*M. xanthus* responds chemotactically to another lipid, PE-18:1ω9/18:1ω9. The fatty acid 18:1ω9 was not observed in the cells of *M. xanthus*, but is found in many other proteobacteria, such as *E. coli* (Cronan and Rock, 1996), which *M. xanthus* preys on in the soil (Shimkets *et al.*, 2005; Yamanaka *et al.*, 1987). It is speculated that 18:1 chemotaxis is used for finding prey. Correlatively, neither the conditions nor part of the machinery for the 18:1 response have much in common with the 16:1 response. Whereas 16:1 stimulation requires starvation conditions and production of the extracellular matrix (factors for the developmental cycle), 18:1 can stimulate chemotaxis under nutrient rich conditions and independently of the presence of the extracellular matrix (Kearns *et al.*, 2000). It was also recently shown that the 18:1 signaling pathway is partially independent of the Dif chemosensory pathway used for 16:1 signaling; 18:1 requires the histidine kinase (DifE) and response regulator (DifD) but not the methyl-accepting chemotaxis protein (DifA) or the coupling protein (DifC) to stimulate chemotaxis (Bonner *et al.*, 2005). Therefore it appears that *M. xanthus* has two largely independent lipid sensory systems.

*Pseudomonas aeruginosa* also travels up gradients of PE-18:1ω9/18:1ω9 and PE-12:0/12:0 (Barker *et al.*, 2004; Kearns *et al.*, 2001a). Interestingly, the response to PE-18:1ω9/18:1ω9 is dependent on the activity of a Phospholipase C (PlcB) while the response to PE-12:0/12:0 is not (Barker *et al.*, 2004), indicating that *P. aeruginosa*, like *M. xanthus*, has two lipid-signaling pathways. Indeed, *P. aeruginosa* shares several characteristics in common with *M. xanthus*. They are both soil-dwelling microbes, utilize surface motility, produce an extracellular matrix and display forms of multicellular behavior (biofilm formation in the case of *P. aeruginosa*). Lipids may be ideal signals for surface-translocating organisms; surface motility is prohibitively slow compared to flagellar motility of planktonic cells. Whereas soluble chemical signals could freely diffuse and therefore collapse gradients before surface-motile

organisms have a chance to respond, lipids will establish more stable gradients due to the insoluble nature of the molecules. Other microorganisms may provide a broad variety of unique fatty acids and lipid species (signature lipid biomarkers) and may also utilize lipid based signaling.

**Acknowledgements**

The authors wish to thank Pamela Bonner for her insightful discussions and critical analysis, Roy Welch for supplying annotated versions of the genome, and Gary Jackoway for supplying fatty acid data. Sequencing of *M. xanthus* DK1622 was accomplished with support from the National Science Foundation. This material is based upon work supported by the National Science Foundation under Grant No. 0343874 to L. Shimkets, and Grant DE-FG02-04ER63939, Department of Energy, Office of Science, to D. C. White, as well as support of the UFZ Leipzig-Halle to R.Geyer.

**References**

Aarts, M.G., Hodge, R., Kalantidis, K., Florack, D., Wilson, Z.A., Mulligan, B.J., Stiekema, W.J., Scott, R., and Pereira, A. (1997) The Arabidopsis MALE STERILITY 2 protein shares similarity with reductases in elongation/condensation complexes. *Plant J* **12**: 615-623.

Aguilar, P.S., Cronan, J.E., Jr., and de Mendoza, D. (1998) A *Bacillus subtilis* gene induced by cold shock encodes a membrane phospholipid desaturase. *J Bacteriol* **180**: 2194-2200.

Balkwill, D.L., Drake, G.R., Reeves, R.H., Fredrickson, J.K., White, D.C., Ringelberg, D.B., Chandler, D.P., Romine, M.F., Kennedy, D.W., and Spadoni, C.M. (1997) Taxonomic

study of aromatic-degrading bacteria from deep-terrestrial-subsurface sediments and description of *Sphingomonas aromaticivorans* sp. nov., *Sphingomonas subterranea* sp. nov., and *Sphingomonas stygia* sp. nov. *Int J Syst Bacteriol* **47**: 191-201.

Barker, A.P., Vasil, A.I., Filloux, A., Ball, G., Wilderman, P.J., and Vasil, M.L. (2004) A novel extracellular phospholipase C of *Pseudomonas aeruginosa* is required for phospholipid chemotaxis. *Mol Microbiol* **53**: 1089-1098.

Bellenger, K., Ma, X., Shi, W., and Yang, Z. (2002) A CheW homologue is required for *Myxococcus xanthus* fruiting body development, social gliding motility, and fibril biogenesis. *J Bacteriol* **184**: 5654-5660.

Black, W.P., and Yang, Z. (2004) *Myxococcus xanthus* chemotaxis homologs DifD and DifG negatively regulate fibril polysaccharide production. *J Bacteriol* **186**: 1001-1008.

Blackhart, B.D., and Zusman, D.R. (1985) "Frizzy" genes of *Myxococcus xanthus* are involved in control of frequency of reversal of gliding motility. *Proc Natl Acad Sci U S A* **82**: 8767-8770.

Bligh, E.G., and Dyer, W.J. (1959) A rapid method of total lipid extraction and purification. *Can J Biochem Physiol* **37**: 911-917.

Bonner, P.J., Xu, Q., Black, W.P., Li, Z., Yang, Z., and Shimkets, L.J. (2005) The Dif chemosensory pathway is directly involved in phosphatidylethanolamine sensory transduction in *Myxococcus xanthus*. *Mol Microbiol* **57**: 1499-1508.

Caillon, E., Lubochinsky, B., and Rigomier, D. (1983) Occurrence of dialkyl ether phospholipids in *Stigmatella aurantiaca* DW4. *J Bacteriol* **153**: 1348-1351.

Campos, J.M., Geisselsoder, J., and Zusman, D.R. (1978) Isolation of bacteriophage MX4, a generalized transducing phage for *Myxococcus xanthus*. *J Mol Biol* **119**: 167-178.

Cheng, J.B., and Russell, D.W. (2004) Mammalian wax biosynthesis. I. Identification of two fatty acyl-Coenzyme A reductases with different substrate specificities and tissue distributions. *J Biol Chem* **279**: 37789-37797.

Christie, W. (2004) The Lipid Library, Mass Spectra of Methylesters of Fatty Acids. In *Part 6. Further Derivatizations* URL www.lipidlibrary.co.uk.

Cronan, J.E., and Rock, C.O. (1996) Biosynthesis of Membrane Lipids. In *Escherichia coli and Salmonella*. Neidhardt, F.C., Curtiss, R., Ingram, J.L., Lin, E.C.C., Low, K.B. and Magasanik, B. (eds). Washington D.C.: American Society for Microbiology Press, pp. 612-636.

Dickschat, J.S., Bode, H.B., Kroppenstedt, R.M., Muller, R., and Schulz, S. (2005) Biosynthesis of iso-fatty acids in myxobacteria. *Org Biomol Chem* **3**: 2824-2831.

Downard, J., and Toal, D. (1995) Branched-chain fatty acids: the case for a novel form of cell-cell signalling during Myxococcus xanthus development. *Mol Microbiol* **16**: 171-175.

Ekroos, K., Chernushevich, I.V., Simons, K., and Shevchenko, A. (2002) Quantitative profiling of phospholipids by multiple precursor ion scanning on a hybrid quadrupole time-of-flight mass spectrometer. *Anal Chem* **74**: 941-949.

Fiegna, F., and Velicer, G.J. (2005) Exploitative and hierarchical antagonism in a cooperative bacterium. *PLoS Biol* **3**: e370.

Geyer, R., Peacock, A.D., Miltner, A., Richnow, H.H., White, D.C., Sublette, K.L., and Kastner, M. (2005) In situ assessment of biodegradation potential using biotraps amended with $^{13}$C-labeled benzene or toluene. *Environ Sci Technol* **39**: 4983-4989.

Gil, R., Silva, F.J., Pereto, J., and Moya, A. (2004) Determination of the core of a minimal bacterial gene set. *Microbiol Mol Biol Rev* **68**: 518-537.

Govindaswami, M., Schmidt, T.M., White, D.C., and Loper, J.C. (1993) Phylogenetic analysis of a bacterial aerobic degrader of azo dyes. *J Bacteriol* **175**: 6062-6066.

Hartig, C., Loffhagen, N., and Harms, H. (2005) Formation of trans fatty acids is not involved in growth-linked membrane adaptation of *Pseudomonas putida*. *Appl Environ Microbiol* **71**: 1915-1922.

Heath, R.J., Goldfine, H., and Rock, C.O. (1997) A gene (*plsD*) from *Clostridium butyricum* that functionally substitutes for the *sn*-glycerol-3-phosphate acyltransferase gene (*plsB*) of *Escherichia coli*. *J Bacteriol* **179**: 7257-7263.

Heath, R.J., and Rock, C.O. (1998) A conserved histidine is essential for glycerolipid acyltransferase catalysis. *J Bacteriol* **180**: 1425-1430.

Henson, J.M., McInerney, M.J., Beaty, P.S., Nickels, J., and White, D.C. (1988) Phospholipid fatty acid composition of the syntrophic anaerobic bacterium *Syntrophomonas wolfei*. *Appl Environ Microbiol* **54**: 1570-1574.

Holmstrom, C., James, S., Neilan, B.A., White, D.C., and Kjelleberg, S. (1998) *Pseudoalteromonas tunicata* sp. nov., a bacterium that produces antifouling agents. *International Journal of Systematic Bacteriology* **48**: 1205-1212.

Hongsthong, A., Subudhi, S., Sirijuntarat, M., and Cheevadhanarak, S. (2004) Mutation study of conserved amino acid residues of *Spirulina* $\Delta^6$-acyl-lipid desaturase showing involvement of histidine 313 in the regioselectivity of the enzyme. *Appl Microbiol Biotechnol* **66**: 74-84.

Iizuka, T., Jojima, Y., Fudou, R., Hiraishi, A., Ahn, J.W., and Yamanaka, S. (2003) *Plesiocystis pacifica* gen. nov., sp. nov., a marine myxobacterium that contains dihydrogenated

menaquinone, isolated from the Pacific coasts of Japan. *Int J Syst Evol Microbiol* **53**: 189-195.

Julien, B., Kaiser, A.D., and Garza, A. (2000) Spatial control of cell differentiation in *Myxococcus xanthus*. *Proc Natl Acad Sci U S A* **97**: 9098-9103.

Kaiser, D. (1979) Social gliding is correlated with the presence of pili in *Myxococcus xanthus*. *Proc Natl Acad Sci U S A* **76**: 5952-5956.

Kearns, D.B., and Shimkets, L.J. (1998) Chemotaxis in a gliding bacterium. *Proc Natl Acad Sci U S A* **95**: 11957-11962.

Kearns, D.B., Campbell, B.D., and Shimkets, L.J. (2000) *Myxococcus xanthus* fibril appendages are essential for excitation by a phospholipid attractant. *Proc Natl Acad Sci U S A* **97**: 11505-11510.

Kearns, D.B., Robinson, J., and Shimkets, L.J. (2001a) *Pseudomonas aeruginosa* exhibits directed twitching motility up phosphatidylethanolamine gradients. *J Bacteriol* **183**: 763-767.

Kearns, D.B., Venot, A., Bonner, P.J., Stevens, B., Boons, G.-J., and Shimkets, L.J. (2001b) Identification of a developmental chemoattractant in *Myxococcus xanthus* through metabolic engineering. *Proc Natl Acad Sci U S A* **98**: 13990-13994.

Kleinig, H. (1972) Membranes from *Myxococcus fulvus* (Myxobacterales) containing carotenoid glucosides. I. Isolation and composition. *Biochim Biophys Acta* **274**: 489-498.

Kolattukudy, P.E. (1970) Reduction of fatty acids to alcohols by cell-free preparations of *Euglena gracilis*. *Biochemistry* **9**: 1095-1102.

Leonhardt, B.A., and deVilbiss, E.D. (1985) Separation and double-bond determination on nanogram quantities of aliphatic monounsaturated alcohols, aldehydes and carboxylic acid methyl esters. *Journal of Chromatography* **322**: 484-490.

Lewin, T.M., Wang, P., and Coleman, R.A. (1999) Analysis of amino acid motifs diagnostic for the *sn*-glycerol-3-phosphate acyltransferase reaction. *Biochemistry* **38**: 5764-5771.

Li, D., Yu, L., Wu, H., Shan, Y., Guo, J., Dang, Y., Wei, Y., and Zhao, S. (2003) Cloning and identification of the human LPAAT-zeta gene, a novel member of the lysophosphatidic acid acyltransferase family. *J Hum Genet* **48**: 438-442.

Lovley, D.R., Giovannoni, S.J., White, D.C., Champine, J.E., Phillips, E.J.P., Gorby, Y.A., and Goodwin, S. (1993) Geobacter metallireducens gen. nov. sp. nov., a microorganism capable of coupling the complete oxidation of organic compounds to the reduction of iron and other metals. *Archives of Microbiology* **159**: 336-344.

Lytle, C.A., Gan, Y.D., and White, D.C. (2000) Electrospray ionization/mass spectrometry compatible reversed-phase separation of phospholipids: piperidine as a post column modifier for negative ion detection. *J Microbiol Methods* **41**: 227-234.

Mahmud, T., Bode, H.B., Silakowski, B., Kroppenstedt, R.M., Xu, M., Nordhoff, S., Hofle, G., and Muller, R. (2002) A novel biosynthetic pathway providing precursors for fatty acid biosynthesis and secondary metabolite formation in myxobacteria. *J Biol Chem* **277**: 32768-32774.

Metz, J.G., Pollard, M.R., Anderson, L., Hayes, T.R., and Lassner, M.W. (2000) Purification of a jojoba embryo fatty acyl-coenzyme A reductase and expression of its cDNA in high erucic acid rapeseed. *Plant Physiol* **122**: 635-644.

Moto, K., Yoshiga, T., Yamamoto, M., Takahashi, S., Okano, K., Ando, T., Nakata, T., and Matsumoto, S. (2003) Pheromone gland-specific fatty-acyl reductase of the silkmoth, *Bombyx mori*. *Proc Natl Acad Sci U S A* **100**: 9156-9161.

Nagan, N., and Zoeller, R.A. (2001) Plasmalogens: biosynthesis and functions. *Prog Lipid Res* **40**: 199-229.

Nichols, P., Stulp, B.K., Jones, J.G., and White, D.C. (1986) Comparison of fatty acid content and DNA homology of the filamentous gliding bacteria *Vitreoscilla, Flexibacter, Filibacter*. *Archives of Microbiology* **146**: 1-6.

Nichols, P.D., Smith, G.A., Antworth, C.P., Hanson, R.S., and White, D.C. (1985) Phospholipid and lipopolysaccharide normal and hydroxy fatty acids as potential signatures for methane-oxidizing bacteria. *Fems Microbiology Ecology* **31**: 327-335.

Nichols, P.D., Henson, J.M., Antworth, C.P., Parsons, J., Wilson, J.T., and White, D.C. (1987) Detection of a microbial consortium, including type-II methanotrophs, by use of phospholipid fatty-acids in an aerobic halogenated hydrocarbon-degrading soil column enriched with natural-gas. *Environmental Toxicology and Chemistry* **6**: 89-97.

Olsson, P.A., Baath, E., Jakobsen, I., and Soderstrom, B. (1995) The use of phospholipid and neutral lipid fatty acids to estimate biomass of arbuscular mycorrhizal fungi in soil. *Mycological Research* **99**: 623-629.

Pulfer, M., and Murphy, R.C. (2003) Electrospray mass spectrometry of phospholipids. *Mass Spectrom Rev* **22**: 332-364.

Rahman, M.M., Kolli, V.S., Kahler, C.M., Shih, G., Stephens, D.S., and Carlson, R.W. (2000) The membrane phospholipids of *Neisseria meningitidis* and *Neisseria gonorrhoeae* as

characterized by fast atom bombardment mass spectrometry. *Microbiology* **146**: 1901-1911.

Reiser, S., and Somerville, C. (1997) Isolation of mutants of *Acinetobacter calcoaceticus* deficient in wax ester synthesis and complementation of one mutation with a gene encoding a fatty acyl coenzyme A reductase. *J Bacteriol* **179**: 2969-2975.

Ringelberg, D.B., Davis, J.D., Smith, G.A., Pfiffner, S.M., Nichols, P.D., Nickels, J.S., Henson, J.M., Wilson, J.T., Yates, M., Kampbell, D.H., Read, H.W., Stocksdale, T.T., and White, D.C. (1989) Validation of signature polarlipid fatty acid biomarkers for alkane-utilizing bacteria in soils and subsurface aquifer materials. *Fems Microbiology Ecology* **62**: 39-50.

Ringelberg, D.B., Townsend, G.T., Deweerd, K.A., Suflita, J.M., and White, D.C. (1994) Detection of the anaerobic dechlorinating microorganism *Desulfomonile tiedjei* in environmental matrices by its signature lipopolysaccharide branched-long-chain hydroxy fatty acids. *Fems Microbiology Ecology* **14**: 9-18.

Ringelberg, D.B., Stair, J.O., Almeida, J., Norby, R.J., ONeill, E.G., and White, D.C. (1997) Consequences of rising atmospheric carbon dioxide levels for the belowground microbiota associated with white oak. *Journal of Environmental Quality* **26**: 495-503.

Shih, G.C., Kahler, C.M., Swartley, J.S., Rahman, M.M., Coleman, J., Carlson, R.W., and Stephens, D.S. (1999) Multiple lysophosphatidic acid acyltransferases in *Neisseria meningitidis*. *Mol Microbiol* **32**: 942-952.

Shimkets, L.J., Dworkin, M., and Reichenbach, H. (2005) The Myxobacteria. In *The Prokaryotes*. Dworkin, M. (ed). New York: Springer-Verlag.

Sturt, H.F., Summons, R.E., Smith, K., Elvert, M., and Hinrichs, K.U. (2004) Intact polar membrane lipids in prokaryotes and sediments deciphered by high-performance liquid

chromatography/electrospray ionization multistage mass spectrometry--new biomarkers for biogeochemistry and microbial ecology. *Rapid Commun Mass Spectrom* **18**: 617-628.

Taguchi, R., Houjou, T., Nakanishi, H., Yamazaki, T., Ishida, M., Imagawa, M., and Shimizu, T. (2005) Focused lipidomics by tandem mass spectrometry. *J Chromatogr B Analyt Technol Biomed Life Sci* **823**: 26-36.

Toal, D.R., Clifton, S.W., Roe, B.A., and Downard, J. (1995) The *esg* locus of *Myxococcus xanthus* encodes the E1α and E1β subunits of a branched-chain keto acid dehydrogenase. *Mol Microbiol* **16**: 177-189.

Ware, J.C., and Dworkin, M. (1973) Fatty acids of *Myxococcus xanthus*. *J Bacteriol* **115**: 253-261.

Weier, D., Muller, C., Gaspers, C., and Frentzen, M. (2005) Characterisation of acyltransferases from *Synechocystis* sp. PCC6803. *Biochem Biophys Res Commun* **334**: 1127-1134.

White, D.C., Lytle, C.A., Gan, Y.D., Piceno, Y.M., Wimpee, M.H., Peacock, A.D., and Smith, C.A. (2002) Flash detection/identification of pathogens, bacterial spores and bioterrorism agent biomarkers from clinical and environmental matrices. *J Microbiol Methods* **48**: 139-147.

Yamanaka, S., Kawaguchi, A., and Komagata, K. (1987) Isolation and identification of myxobacteria from soils and plant materials, with special reference to DNA base composition, quinone system, and cellular fatty acid composition, and with a description of a new species, *Myxococcus flavescens*. *J. Gen. Appl. Micriobiol.* **33**: 247-265.

Yang, Z., Ma, X., Tong, L., Kaplan, H.B., Shimkets, L.J., and Shi, W. (2000) *Myxococcus xanthus dif* genes are required for biogenesis of cell surface fibrils essential for social gliding motility. *J Bacteriol* **182**: 5793-5798.

# CHAPTER 3

# PROTEINS ASSOCIATED WITH THE *MYXOCOCCUS XANTHUS* EXTRACELLULAR MATRIX[1]

[1] Curtis, P.D., Atwood, J., Orlando, R. and Shimkets, L.J. To be submitted to *J Bacteriol*.

**Abstract**

Fruiting body formation of *Myxococcus xanthus*, like biofilm formation in many other organisms, requires the production of an extracellular matrix (ECM). While the polysaccharide component has been studied, the protein component has been largely unexplored. Proteins associated with the ECM were solubilized from purified ECM by boiling with sodium dodecylsulfate, and identified by coupled liquid chromatography – tandem mass spectrometry of tryptic fragments. The ECM is enriched in proteins of novel sequence and unknown function; putative functions were assigned for only five of the twenty one proteins. Thirteen putative ECM proteins had lipoprotein secretion signals. The genes for many ECM proteins were disrupted in wild type, *fibA* and *pilA* backgrounds. Disruption of MXAN4860 had no effect in the WT or *fibA* backgrounds, but in the *pilA* background resulted in a 24 hour delay in aggregation and sporulation compared to its parent. The results of this study show that the *M. xanthus* ECM proteome is diverse and novel.

**Introduction**

The transition from planktonic cells to biofilm-associated cells in bacteria involves changes in gene expression (Domka *et al.*, 2007; Stanley *et al.*, 2003; Whiteley *et al.*, 2001), and is mediated at least in part by intercellular communication (Davies *et al.*, 1998). Biofilm formation by prokaryotic organisms begins with the production of an extracellular matrix (ECM) composed of carbohydrate polymers, proteins and sometimes nucleic acids (Branda *et al.*, 2005; Sutherland, 2001; Whitchurch *et al.*, 2002). ECM proteins have not been extensively studied, but could potentially play significant roles in both structural and intercellular signaling functions, similar to the capacities of ECM proteins in mammals. Mammalian cells are connected in tissues

by a proteinaceous ECM. Remodeling of ECM by proteinases is regulated by signaling pathways (Grabellus *et al.*, 2007; Zaragoza *et al.*, 2006) and stimulates wound healing, the inflammatory response and angiogenesis (Li and Pflugfelder, 2005; Lund *et al.*, 1999; Malik and Kakar, 2006). Many pathological conditions arise from incorrectly applied ECM proteinase activity, such as periodontitis, cancer metastasis and cartilage degradation leading to arthritis (Blom *et al.*, 2007; Bodet *et al.*, 2007; Malik and Kakar, 2006; Sternlicht and Werb, 2001; Tjaderhane *et al.*, 2007). By analogy, prokaryotic ECM proteins may play structural and signaling roles to regulate metabolism, motility, cell attachment, immune evasion, and predation.

*Myxococcus xanthus* is a δ-proteobacterium commonly found in soil where it grows as a microbial predator. Under starvation conditions approximately 50,000 cells aggregate into a multicellular fruiting body wherein some cells differentiate into dormant myxospores. Like other prokaryotic biofilm-forming organisms, *M. xanthus* produces an extracellular matrix. During swarming, cell-cell proximity induces ECM formation (Behmlander and Dworkin, 1991), which aids social (S) motility (Li *et al.*, 2003) where cells extend a pilus that attaches onto an ECM substrate and retracts thereby dragging the cell forward (Sun *et al.*, 2000). ECM biogenesis is strongly induced during starvation and is essential for fruiting body formation (Arnold and Shimkets, 1988a, b; Chang and Dworkin, 1996; Lu *et al.*, 2005; Yang *et al.*, 2000). Signals controlling ECM production the PilA protein, the structural protein of Type IV pili (Black *et al.*, 2006; Bonner *et al.*, 2006) and the Dif chemosensory system (Bellenger *et al.*, 2002; Black and Yang, 2004; Bonner *et al.*, 2005; Yang *et al.*, 2000), which is composed of DifA (a methyl-accepting chemotaxis protein homolog), DifC (a CheW coupling protein homolog) and DifE (a CheA histidine kinase homolog). The Dif system is also required for

development. Development in *difACE* mutants can be restored with exogenously supplied *M. xanthus* ECM (Chang and Dworkin, 1994; Yang *et al.*, 2000).

*M. xanthus* ECM is composed of 55% carbohydrate and 45% protein (Behmlander and Dworkin, 1994a). Exopolysaccharide forms the ECM backbone and contains primarily glucose and glucosamine, with galactose, rhamnose and xylose as lesser components (Behmlander and Dworkin, 1994a). Biosynthesis of exopolysaccharide is mediated by the *eps* and *eas* loci (Lu *et al.*, 2005). The ECM proteins are tightly associated with the exopolysaccharide, requiring detergent and boiling to remove them (Behmlander and Dworkin, 1994b). The identity of only a single ECM protein is known, FibA, which is a zinc-metalloprotease of the elastase family (Behmlander and Dworkin, 1994b; Kearns *et al.*, 2002) and the most abundant protein associated with the ECM (Behmlander and Dworkin, 1994b). FibA is required for lipid chemotaxis and, under certain conditions, fruiting body development. During starvation, *M. xanthus* responds chemotactically to membrane phospholipids containing the rare fatty acid 16:1ω5c (Curtis *et al.*, 2006; Kearns *et al.*, 2001). A FibA active site mutant is incapable of chemotaxis towards this molecule (Bonner *et al.*, 2006; Kearns *et al.*, 2002), although the substrate and role of this enzyme in chemotaxis remains unknown. While disruption of *fibA* has no obvious effect on development, disruption of both *fibA* and *pilA* abolishes development. It is unclear whether the loss of development in the *fibA pilA* mutant is due to disruption of lipid chemotaxis or another as yet unknown FibA-mediated process.

PilA monomers form the retractile Type IV pilus (Li *et al.*, 2005). Deletion of the *pilA* gene results in a lack of S motility and a delay in development (Wu and Kaiser, 1996), however these cells still form fruiting bodies using A-motility. The *pilT* mutant forms pili but is unable to retract them and also lacks S motility (Wu *et al.*, 1997). While the *fibA pilA* mutant is unable

to develop (Bonner *et al.*, 2006), a *fibA pilT* mutant develops normally (Bonner *et al.*, 2006). This result suggests that the PilA requirement for development is not due its role in S motility. The only other known function of PilA is control of ECM biogenesis. Strains harboring mutations that disrupt pilus formation, such as *pilA*, *pilB* (encoding the pilus extension motor) and *pilR* (encoding a transcriptional regulator), have reduced levels of ECM (Black *et al.*, 2006). Conversely, strains carrying a disruption in *pilT* (which causes hyperpiliation (Wu *et al.*, 1997)) overproduce ECM (Black *et al.*, 2006). *dif* mutations are epistatic on *pil* mutations, showing that pilus signaling functions upstream of the Dif system in ECM biogenesis. These results argue that PilA or the structural pilus serves as a sensor for signal transduction leading to ECM biogenesis. The specific signal sensed and method of signal transduction into the Dif system remains unknown. Taken together, these results suggest that development has a partially branched signaling pathway upstream of DifACE where PilA (or the pilus) services one branch and FibA the other (Bonner *et al.*, 2006).

Proteomic analysis was used to identify matrix-associated proteins and examine their possible roles in development within the scope of the PilA/FibA branched signaling pathway for development. A number of diverse proteins are associated with the matrix, but only one protein could be added to the branched pathway.

## Experimental Procedures

**Strains and growth conditions**. *M. xanthus* strains (see Table 3-1) were grown at 32$^{o}$C in CYE [1.0% Bacto Casitone, 0.5% Difco yeast extract, 10 mM 3-[*N*-morpholino]propanesulfonic acid (MOPS), pH 7.6 and 0.1% $MgSO_4$] broth with vigorous shaking (Campos *et al.*, 1978). Cultures were grown on plates containing CYE with 1.5% Difco

**Table 3-1.** Strains Used In This Study.

| Strain | Genotype or Description | Source or Reference[1] |
|---|---|---|
| DK1622 | wild type | (Kaiser, 1979) |
| DK10410 | Δ*pilA* | (Wu *et al.*, 1997) |
| LS2429 | Δ*fibA* | Lawrence Shimkets |
| LS2333 | MXAN4860 $Km^r$ | DK1622 x pPDC9 → $Km^r$ |
| LS2337 | MXAN4860 Δ*pilA* $Km^r$ | DK10410 x LS2333 → $Km^r$ |
| LS2341 | MXAN4860 Δ*fibA* $Km^r$ | LS2429 x LS2333 → $Km^r$ |
| LS2344 | MXAN2791 $Km^r$ | DK1622 x pPDC18 → $Km^r$ |
| LS2345 | MXAN5684 $Km^r$ | DK1622 x pPDC19 → $Km^r$ |
| LS2347 | MXAN2791 Δ*pilA* $Km^r$ | DK10410 x LS2344 → $Km^r$ |
| LS2348 | MXAN5684 Δ*pilA* $Km^r$ | DK10410 x LS2345 → $Km^r$ |
| LS2355 | MXAN0075 Δ*pilA* $Km^r$ | DK10410 x pPDC26 → $Km^r$ |
| LS2356 | MXAN7023 $Km^r$ | DK1622 x pPDC40 → $Km^r$ |
| LS2357 | MXAN5686 $Km^r$ | DK1622 x pPDC39 → $Km^r$ |
| LS2358 | MXAN6985 $Km^r$ | DK1622 x pPDC30 → $Km^r$ |
| LS2360 | MXAN5391 $Km^r$ | DK1622 x pPDC24 → $Km^r$ |
| LS2361 | MXAN2375 $Km^r$ | DK1622 x pPDC36 → $Km^r$ |
| LS2362 | MXAN2710 $Km^r$ | DK1622 x pPDC42 → $Km^r$ |
| LS2363 | MXAN0793 $Km^r$ | DK1622 x pPDC38 → $Km^r$ |
| LS2364 | MXAN1493 $Km^r$ | DK1622 x pPDC41 → $Km^r$ |
| LS2365 | MXAN1424 $Km^r$ | DK1622 x pPDC27 → $Km^r$ |
| LS2366 | MXAN4915 $Km^r$ | DK1622 x pPDC43 → $Km^r$ |
| LS2367 | MXAN0075 $Km^r$ | DK1622 x pPDC26 → $Km^r$ |
| LS2369 | MXAN6985 Δ*pilA* $Km^r$ | DK10410 x LS2358 → $Km^r$ |
| LS2370 | MXAN5686 Δ*pilA* $Km^r$ | DK10410 x LS2357 → $Km^r$ |
| LS2371 | MXAN7023 Δ*pilA* $Km^r$ | DK10410 x LS2356 → $Km^r$ |
| LS2372 | MXAN2375 Δ*pilA* $Km^r$ | DK10410 x LS2361 → $Km^r$ |
| LS2373 | MXAN1493 Δ*pilA* $Km^r$ | DK10410 x LS2364 → $Km^r$ |
| LS2374 | MXAN5391 Δ*pilA* $Km^r$ | DK10410 x LS2360 → $Km^r$ |
| LS2375 | MXAN2710 Δ*pilA* $Km^r$ | DK10410 x LS2362 → $Km^r$ |
| LS2376 | MXAN0793 Δ*pilA* $Km^r$ | DK10410 x LS2363 → $Km^r$ |
| LS2377 | MXAN1424 Δ*pilA* $Km^r$ | DK10410 x LS2365 → $Km^r$ |
| LS2378 | MXAN4915 Δ*pilA* $Km^r$ | DK10410 x LS2366 → $Km^r$ |
| LS2381 | MXAN5686 Δ*fibA* $Km^r$ | LS2429 x LS2357 → $Km^r$ |
| LS2382 | MXAN2710 Δ*fibA* $Km^r$ | LS2429 x LS2362 → $Km^r$ |
| LS2383 | MXAN2375 Δ*fibA* $Km^r$ | LS2429 x LS2361 → $Km^r$ |
| LS2384 | MXAN1424 Δ*fibA* $Km^r$ | LS2429 x LS2365 → $Km^r$ |
| LS2385 | MXAN1493 Δ*fibA* $Km^r$ | LS2429 x LS2364 → $Km^r$ |
| LS2386 | MXAN5684 Δ*fibA* $Km^r$ | LS2429 x LS2345 → $Km^r$ |
| LS2387 | MXAN0075 Δ*fibA* $Km^r$ | LS2429 x LS2367 → $Km^r$ |
| LS2388 | MXAN0793 Δ*fibA* $Km^r$ | LS2429 x LS2363 → $Km^r$ |
| LS2389 | MXAN7023 Δ*fibA* $Km^r$ | LS2429 x pPDC40 → $Km^r$ |
| LS2390 | MXAN5391 Δ*fibA* $Km^r$ | LS2429 x LS2360 → $Km^r$ |

| | | |
|---|---|---|
| LS2391 | MXAN6985 Δ*fibA* $Km^r$ | LS2429 x LS2358 → $Km^r$ |
| LS2392 | MXAN2791 Δ*fibA* $Km^r$ | LS2429 x pPDC18 → $Km^r$ |
| LS2393 | MXAN4915 Δ*fibA* $Kan^r$ | LS2429 x pPDC43 → $Km^r$ |

[1] The first strain listed in the column is the recipient and the second strain is the source of DNA use to modify the recipient

agar. For selective grown, kanamycin was added to a final concentration of 100 μg $ml^{-1}$ (CYE Km).

**Isolation of Extracellular Matrix Material**. ECM was extracted and purified from 24 hour developing cells using 0.5% sodium dodecylsulfate (Behmlander and Dworkin, 1994b; Kearns *et al.*, 2000). Solubilization of ECM-associated proteins was developed in this study. Attempts to solubilize ECM proteins with 9.5 M urea, 2% 3-[(3-cholamidopropyl)dimethylammonio]propanesulfonic acid (CHAPS), 2% ethylene glycol octyl phenyl ether (Triton X-100), 350 mM NaCl, boiling for extended periods of time, and many combinations thereof failed, as did digestion of isolated ECM material with trypsin (data not shown). Boiling with a high concentration of SDS and a reducing agent solubilized at least some of the proteins. A protease inhibitor cocktail was necessary to prevent digestion of proteins by proteases found in the sample.

To induce development, 7.5 ml of 5 x $10^9$ cells $ml^{-1}$ were plated on TPM agar [10 mM Tris (hydroxymethyl) aminomethane HCl, 8 mM $MgSO_4$, 1 mM $KHPO_4$-$KH_2PO_4$, 1.5% Difco agar, pH 7.6] in a 33 x 22 cm tray and incubated at 32°C for 24 hr. Fruiting bodies were harvested by scraping with a razor blade into a clean glass beaker. ECM material was collected using a modification of the method described by Behmlander and Dworkin (Behmlander and Dworkin, 1994b). Five ml of TNE buffer [10 mM Tris [pH 7.5], 100 mM NaCl, 5 mM EDTA (Behmlander and Dworkin, 1991)] was added to the cell suspension and stirred for 10 minutes at room temperature. Five ml of TNE containing 1.0% sodium dodecylsulfate (SDS) was then added and stirred for 30 minutes. The solution was centrifuged at 12,000 x g for 10 minutes at 4°C and the supernatant discarded. The pellet was resuspended in 5.0 ml TNE containing0.5% SDS and stirred for 1 hour at room temperature. The suspension was centrifuged at 12,000 x g at

4°C for 10 minutes and the supernatant discarded. The pellet was washed once with 5.0 ml TNE, twice with 5.0 ml 10 mM MOPS, and twice with 5.0 ml Cohesion Buffer (10 mM MOPS pH 6.8, 1 mM $CaCl_2$, 1 mM $MgCl_2$). Finally the pellet was resuspended in 1.0 ml of Cohesion Buffer containing 5x Complete EDTA-free protease inhibitor cocktail (Roche) and stored at 4°C. A variation of this procedure using 0.1% SDS in the two initial wash steps (Behmlander and Dworkin, 1994b) resulted in ECM containing a wider variety of proteins, but was extensively contaminated with membrane proteins.

**Extraction of Matrix-Associated Proteins**. Proteins were solubilized from the ECM by boiling in SDS. Solubilized proteins were separated from the insoluble ECM material by SDS-PAGE long enough for the proteins to enter the resolving gel but not separate into distinct bands. The SDS was removed from the gel by washing, allowing tryptic digestion of proteins within the gel. Liquid Chromatography – Tandem Mass Spectrometry (LC-MS/MS) was used in the identification of tryptic fragments of ECM proteins.

Two ml of purified ECM material containing 127 μg $ml^{-1}$ protein was pelleted by centrifuging at 12,000 x g for 10 minutes at room temperature. The pellet was resuspended in 400 μl Cohesion Buffer containing 3% SDS. Dithiothreitol was added to a final concentration of 100 mM and protease inhibitor to 2.5x concentration. The suspension was boiled for 30 minutes and non-solubilized material pelleted by centrifugation at 12,000 x g for 10 minutes. The supernatant was collected and centrifuged at 62,000 x g for 30 minutes at 4°C. The supernatant was collected and concentrated using a Microcon YM-3 centrifugation filter (3,000 MW cut off) for 1.5 hours, resulting in 5-fold concentration of protein (approximately 80 μl volume). To this 40 μl of sample buffer (52.5 mM Tris-HCl, pH 6.8, 2% SDS, 25% glycerol, 0.01% Bromophenol Blue, 100 mM DTT) was added and boiled for 15 minutes. The solution was then loaded on to a

12% SDS polyacrylamide gel. The gel was run at 50 mA current until the proteins migrated through the stacking gel and began to enter the resolving gel. Protein detection was performed using Silver Stain Plus (Bio Rad).

The portion of the gel containing protein (approximately 1.0 x 1.5 cm) was excised, cut into smaller fragments, destained with 200 μl 15 mM potassium ferricyanide, 50 mM sodium thiosulfate, and washed three times with 200 μl water. The gel pieces were dehydrated by washing three times with 200 μl of 20 mM ammonium bicarbonate containing 50% (v/v) acetonitrile for 15 minutes each, followed by one 15 minute wash with 200 μl acetonitrile. The gel slices were dried under vacuum and rehydrated with 100 μl of 10 mM DTT in 40 mM ammonium bicarbonate at 55$^{o}$C for 1 hour, at which point the solution was exchanged for 100 μl of 55 mM iodoacetamide, 40 mM ammonium bicarbonate and incubated 45 minutes at room temperature. The gel pieces were washed three times with 200 μl of 20 mM ammonium bicarbonate in 50% (v/v) acetonitrile and once with 100% acetonitrile for 15 minutes then dried under vacuum. The gel pieces were rehydrated with 100 μl of 10 ng $\mu l^{-1}$ proteomics grade trypsin (Sigma) in 40 mM ammonium bicarbonate and incubated on ice for 45 minutes, then with 100 μl of 40 mM ammonium bicarbonate and incubated at 37$^{o}$C overnight. Solutions from the trypsin digestion were pooled. The gel slices were washed with 150 μl of 2.5% trifluoroacetic acid in 50% acetonitrile three times for 10 minutes each. The washes were combined with the solutions from the previous step and taken to dryness under vacuum.

**Proteomic Identification of ECM Proteins**. The peptide samples obtained from proteolytic digestion were analyzed on an Agilent 1100 capillary LC (Palo Alto, CA) interfaced directly to a LTQ linear ion trap mass spectrometer (Thermo Electron, San Jose, CA). Mobile phase A and B were $H_2O$/0.1% formic acid and acetonitrile/0.1% formic acid, respectively. The

peptide samples were loaded for 30 min onto a PicoFrit 8 cm x 50 µm column (New Objective, Woburn, MA) packed with 5 µm diameter $C_{18}$ beads using positive $N_2$ pressure. The peptides were then desalted for 10 min with 0.1% formic acid using positive $N_2$ pressure. Peptides were eluted from the column into the mass spectrometer during a 90 min linear gradient from 5-60% B at a flow rate of 200 $\eta$l $min^{-1}$. The instrument was set to acquire MS/MS spectra on the 9 most abundant precursor ions from each MS scan with a repeat count of 3 and repeat duration of 15 sec. Dynamic exclusion was enabled for 20 sec. Raw tandem mass spectra were converted into mzXML format and then into peak list using ReAdW followed by mzMXL2Other (Pedrioli *et al.*, 2004). The peak lists were then searched using Mascot 1.9 (Matrix Science, Boston, MA).

**Database searching and protein identification.** Two sequence databases were constructed. The first database (normal) consisted of annotated proteins from *M. xanthus* genes (as annotated by The Institute for Genome Research, provided by Dr. Roy Welch) and a decoy database (random) was then constructed by reversing the sequences in the normal database. Database searches were performed against the normal and random databases using the following parameters: full tryptic enzymatic cleavage with 3 possible missed cleavages, peptide tolerance of 500 parts-per-million, fragment ion tolerance of 0.6 Da, and a variable modification due to carboxyamidomethylation (+57 Da). Following the database searches, the identified peptides were grouped into proteins and statistically validated using PROVALT (Weatherly *et al.*, 2005). Only proteins meeting with a protein false discovery rate of less than 1% were considered to be a statistically significant identification. Protein sequences were analyzed using LipoP (Seydel *et al.*, 1999), pfam (http://pfam.janelia.org/hmmsearch.shtml) and Prosite (http://us.expasy.org/tools/scanprosite/).

**Mutagenesis of Genes Encoding ECM Proteins**. Genes for fourteen putative ECM proteins were disrupted by Campbell mutagenesis, which constitutes recombinational insertion of a plasmid containing an internal fragment of each gene. The internal fragments were generated by PCR using the primers listed in Table 3-2 for each target gene. PCR products were separated on 1.0% agarose, excised, extracted using the Gel Extraction kit (Qiagen) and cloned into pCR2.1-TOPO (Invitrogen). The identity of each insert was verified by DNA sequencing. Each plasmid was electroporated in *M. xanthus* DK1622 with selection on CYE Km. Genomic DNA was purified from each transformant using the Easy DNA extraction kit (Invitrogen). To verify the mutations, primers were used to amplify genomic DNA from sites outside of the internal fragment (see Table 3-2, diagnostic primers). Plasmid integration causes a mobility shift of the WT amplicon such that positive transformants had PCR products the size of the wild-type allele plus the size of the plasmid (vector size = 3.9 kb).

In order to transfer the mutations to the *pilA* and *fibA* strains, approximately 3.75 μg of genomic DNA from each mutant strain was electroporated into strains DK10410 and LS2429 (Kashefi and Hartzell, 1995; Vlamakis *et al.*, 2004), except for strains LS2355, LS2389, LS2392 and LS2393 where plasmids were used directly for disruption. Selection and screening were performed as before.

**Development Assay**. Cells from exponentially growing cultures were pelleted by centrifugation and resuspended to cell densities of $5 \times 10^8$, $2.5 \times 10^9$, $5 \times 10^9$ and $7.5 \times 10^9$ cells $ml^{-1}$ in CYE broth. 10 μl of each cell suspension were spotted in duplicate on TPM agar plates and incubated at 32°C for 5 days. The cell spots were viewed using a Wild Heerbrugg dissecting microscope and images were captured every 24 hours with a Spot Insight 2 camera using the Spot Software v4.5 (Diagnostic Instruments Inc.).

**Table 3-2.** Primers Involved In Mutagenesis[1].

| Gene | | Internal Fragment Primers | Diagnostic Primers |
|---|---|---|---|
| MXAN0075 | F | GGT TGG ATT TGG AGA CGA AGG | GGA CGG GCA GTT CAT CGT GGC G |
| | R | GTC GTC CAC CGT TTC AAT GGG | CAG GTT GTG CTG GAG CAG TGA GCC |
| MXAN0793 | F | GGT CCG ACA TCA GTG AGC CCG G | GGG TGC TCG GCG CTT CAT CCT CG |
| | R | GCC GCG GGC ATG ACG AAG AAG G | CGA TGA CGG GAC TCG CGG AGC CC |
| MXAN1424 | F | GCA ACC CGC CGA GGA CCT TCG | GGG CTC TAC CTT CGA GGT TTT GG |
| | R | CGT CAT CAC CCC GAC GTG CG | CGT GGC GGT AGC CGA AGT CC |
| MXAN1493 | F | CCT CAT TCT CTG GAC CCT GCT G | GGA ATC AGC GCT GAA CGA GCG |
| | R | GCG CGA AGA GGA AGG GTG AGC | CCT CGA AGG TGC TGG TCT TCC |
| MXAN2375 | F | GCG TCC TAT CTG TTG CGT CCC G | CCT CTT CGT CTC GCT GTT CGC C |
| | R | CTG GGC CAT GAG GCG GAA CAC C | CCG CGG TGT TCG AAC ATC GC |
| MXAN2710 | F | GGT ACG CCG GTG TCC TTC ACG C | GTG GGT GGC CTT CGC GAG CCT G |
| | R | GCC GTT GGT GTC CAC GTA GCG C | GGT TGT ACC AGG GGT CGG AGA CG |
| MXAN2791 | F | GAG CTG CAG TCC TCG CGG TGA CCG | CAA GGG CCG GGA CGC GTC TCG |
| | R | CCG TAG GTG GCC GTG CCG GTG CC | CCC GGG ATG TGG ATG GCG CC |
| MXAN4860 | F | GGT CTC ATG GCT GGT TGC GGT GAC | GGG CGG CGT TCC AAA CAA GAG G |
| | R | GGG CAG GTT AGC AGG ACA GAA CGC | GCG GGG CTC GAT GAC TCA CC |
| MXAN4915 | F | GGT CTG ATT TTC GGC TCG CTC CTG | CTG CGT GGA GGT CAC GGC C |
| | R | CGA GAA CCG GTT GAG GGG GCC | GAG CAC ACC GCC AAA GCG GGA GC |
| MXAN5391 | F | GAC ACC CAC CTT CGC GAA CAA CG | GGC GAC ATG GGC GAG CCA TGG |
| | R | CGC GGT GGA GAT GCG GAT GCC C | CGA GAA GCC CGC TGG CGA TTC GC |
| MXAN5684 | F | GCT TCG CTG TCC GCC TGC ACG GG | CGA ATG GAA CTA GGA GTG ACC C |
| | R | GGG CCC TTG GCG GTG TTC GGG TCG | CTG CTT CTC GTC CGT CCA TTC G |
| MXAN5686 | F | GTG GGG CCC TTG CGA TGG TGG | GGC ATG GGG TTT TGA ATA GTC GG |
| | R | CCC AGC TGC GGC GAG ATG CCG | GCT GGG CAA TCA TGT CAA AAC CTC C |
| MXAN6985 | F | CAT ACA CGC GAA ACT CAA CGA CC | GGT GGA CTC CGT ATC GAC GG |
| | R | CCC CGT GAC GAT GTC GGT CC | GCG TAG CTC TGC GTG AAG CCC |
| MXAN7023 | F | GCT GGA GAG CTA CAA GCA GTA CG | CCC TGG CTG TGA GGC CCT GGA GC |
| | R | GGT CGC GGA TGT CGA ACT TGT GG | CGG GTG GAT GTA CGT GGA GAA GCC |

[1] Internal fragment primers were used to generate PCR products homologous to an internal portion of each gene. PCR products were ligated into pCR2.1-TOPO and electroporated into *M. xanthus*. Diagnostic PCR primers were designed to amplify from outside the internal fragment primers. Successful recombinants increase the WT amplicon by the length of the plasmid as examined by agarose gel electrophoresis.

**Spore Assay**. Cells from exponentially growing cultures were resuspended in CYE broth at a density of 5 x $10^9$ cells $ml^{-1}$ and 10 μl spots were plated on TPM agar. After incubation at 32°C for 5 days fruiting bodies were collected with a sterile razor blade and resuspended in 0.5 ml TPM buffer. The fruiting bodies were then sonicated at a 60% duty cycle for 10 seconds on an Ultrasonic Processor Sonicator (Heat Systems – Ultrasonics Inc.) and incubated at 55°C for 2 hrs. Refractile myxospores were quantified using a Petroff – Hauser counting chamber. Spores were diluted and plated on CYE or CYE Km to enumerate viable spores. A time course of spore production was examined for select strains every 24 hours for 5 days.

## Results

Little is known about the structure and function of ECM proteins in any bacterium. The purpose of this study was to identify the ECM proteins by mass spectrometry and ascertain their function by mutant analysis. The ECM was purified following solubilization of cells with 0.5% SDS. Proteins were liberated from the insoluble ECM by boiling in 3% SDS and 100 mM dithiothreitol, and separated from the insoluble matrix by SDS PAGE. Proteolytic fragments were released by trypsin digestion and identified using LC-MS/MS and the *M. xanthus* genome sequence (Goldman *et al.*, 2006).

**Identification of ECM Proteins**. A total of 41 proteins were identified with 99% confidence. Putative ECM proteins were selected from the list based on the presence of a Sec-dependent secretion signal using the LipoP program (Juncker *et al.*, 2003), the absence of transmembrane helices, and the lack of conserved membrane domain structures. These criteria reduced the number to 21 putative ECM proteins (Table 3-3). Eighteen of the twenty-one putative ECM proteins were also found in another ECM sample prepared with 0.1% SDS instead

**Table 3-3.** Putative ECM proteins in *M. xanthus*.

| Gene | Peptides[1] | Size (kDa) | Lipoprotein[2] | Identity |
|---|---|---|---|---|
| MXAN6106 | 16 | 79.82 | + | FibA |
| MXAN2183 | 12 | 46.45 | +/- | Conserved hypothetical |
| MXAN5391 | 11 | 47.26 | +/- | Hypothetical |
| MXAN4860 | 9 | 30.88 | + | Hypothetical |
| MXAN5684 | 7 | 22.60 | + | Conserved hypothetical Curli protein |
| MXAN2710 | 6 | 56.89 | + | Conserved hypothetical |
| MXAN6985 | 4 | 52.78 | + | Hypothetical |
| MXAN0793 | 4 | 57.95 | + | Hypothetical |
| MXAN1493 | 4 | 28.88 | - | Hypothetical |
| MXAN3885 | 3 | 18.44 | - | Spore coat protein U |
| MXAN5685 | 3 | 30.77 | - | Hypothetical |
| MXAN6720 | 2 | 11.44 | + | Hypothetical |
| MXAN5686 | 2 | 19.81 | - | Hypothetical |
| MXAN2791 | 1 | 27.52 | + | Protease B |
| MXAN1424 | 1 | 29.91 | - | Hypothetical |
| MXAN4915 | 1 | 36.41 | - | Hypothetical |
| MXAN7023 | 1 | 78.34 | +(+2E) | Conserved hypothetical (COG4880) |
| MXAN0075 | 1 | 124.17 | - | Amidohydrolase domain protein |
| MXAN2375 | 1 | 47.97 | - | Amidohydrolase |
| MXAN0235 | 1 | 15.72 | + | Hypothetical |
| MXAN1657 | 1 | 12.22 | + | Hypothetical |

[1] Number of peptides matched from each protein by LC-MS/MS.
[2] Plus symbols (+) indicate a predicted lipoprotein secretion signal using the LipoP program (Juncker *et al.*, 2003). Minus symbols (-) indicate a predicted Sec-dependent secretion signal. The +/- for MXAN2183 and MXAN5391 indicates that the program predicted both a lipoprotein secretion signal and a non-lipoprotein signal with equal probability. The +(+2E) for MXAN7023 indicates that the residue following the acylated cysteine (+1) is an aspartate residue. In *E. coli*, aspartate at the +2 position directs proteins to the periplasmic face of the inner membrane (Seydel *et al.*, 1999), though this has not been demonstrated in *M. xanthus*.

of 0.5% SDS (data not shown). The sample prepared with 0.1% SDS contained a higher proportion of non-ECM proteins and for that reason it was less specific in extracting ECM proteins. FibA has been shown to be associated with the ECM using immunogold labeling (Behmlander and Dworkin, 1991), and identification of FibA in the present study (Table 3-3) suggests that the ECM isolation technique enriches for ECM proteins.

Of the 21 putative ECM proteins, 13 are predicted to have lipoprotein secretion signals (Table 3-3), though MXAN2183 and MXAN5391 are predicted to have both lipoprotein and normal secretion signals with equal probability. Only 5 of the putative ECM proteins have predicted functions. MXAN6106 is the zinc metalloprotease FibA, the most abundant and only known ECM protein (Behmlander and Dworkin, 1994b; Kearns *et al.*, 2002). MXAN3885 is spore coat protein U, a protein known to be secreted during development and assembled on spores (Gollop *et al.*, 1991). MXAN2791 is a zinc metalloprotease known as Protease B that has been identified in two studies examining milk-clotting ability by *E. coli* containing *M. xanthus* genomic DNA libraries (Poza *et al.*, 2004; Quillet *et al.*, 1997). A C-terminal portion of MXAN0075 and the entire length of MXAN2375 share homology to amidohydrolase family, subgroup 1 (pfam01979). The rest of the putative ECM proteins are derived from either hypothetical or conserved hypothetical genes, suggesting that the *M. xanthus* ECM is enriched for proteins with novel functions.

Other proteins identified in this fraction that are unlikely to be associated with the ECM are listed in Table 3-4. The presence of PilQ suggests that ECM protein enrichment also contains material from cell poles. PilQ forms the outer membrane pore for polarly-localized pili. The membranes at *M. xanthus* cell poles appear to be difficult to separate (Simunovic *et al.*, 2003) and it is possible that 0.5% SDS was unable to completely solublize these polar

**Table 3-4.** Predicted non-ECM proteins identified by proteomic analysis of partially purified ECM.

| Gene | Peptides[1] | Size (kDa) | Identity |
|---|---|---|---|
| Outer Membrane[2] | | | |
| MXAN5572 | 13 | 96.36 | PilQ |
| MXAN5855 | 9 | 52.56 | Probable outer membrane porin |
| MXAN7203 | 7 | 26.54 | Conserved hypothetical membrane protein |
| MXAN2514 | 4 | 94.11 | XcpQ |
| MXAN3106 | 4 | 51.89 | CpaC homolog |
| MXAN7407 | 3 | 21.64 | Hypothetical outer membrane protein |
| MXAN1450 | 2 | 122.47 | OAR |
| Inner Membrane[2] | | | |
| MXAN5402 | 13 | 52.84 | Cytochrome C |
| MXAN3729 | 7 | 109.47 | Pyrrolo quinoline quinine-containing dehydrogenase |
| Intracellular[3] | | | |
| MXAN6601 | 21 | 80.86 | Prolyl endopeptidase |
| MXAN4808 | 15 | 56.12 | DUF87 protein of unknown function |
| MXAN4494 | 12 | 83.96 | Conserved hypothetical: phage tail sheath protein |
| MXAN4807 | 11 | 18.00 | DUF770 protein of unknown function |
| MXAN5407 | 9 | 45.48 | Choloylglycine hydrolase |
| MXAN2815 | 4 | 36.49 | Glyceraldehyde-3-phosphate dehydrogenase |
| MXAN6090 | 4 | 34.81 | DUF481 protein of unknown function |
| MXAN5012 | 3 | 85.62 | Tyrosine decarboxylase |
| MXAN5582 | 3 | 37.72 | Hypothetical |
| MXAN4495 | 2 | 16.42 | Conserved hypothetical: phage tail region protein |
| MXAN1394 | 2 | 36.38 | Zinc-dependent hydrolase of the β-lactamase fold |

[1] Number of peptides matched from each protein by LC-MS/MS.
[2] Membrane proteins were assigned based on the presence of a Sec-dependent secretion signal and the cellular location of the closest homologs.
[3] Intracellular proteins were assigned based on the absence of a Sec-dependent secretion signal as determined by LipoP analysis.

complexes, which led to the isolation of some membrane and intracellular proteins. Additionally, the LC-MS/MS technique is very sensitive, which may have resulted in the unintended identification of highly abundant intracellular proteins.

**Mutagenesis of putative ECM genes**. Each gene encoding a putative ECM protein was disrupted by Campbell insertion of a plasmid containing an internal fragment of the gene. Not all genes were disrupted: MXAN3885, MXAN6720, MXAN0235 and MXAN1657 are less than 600 bp in length and too small to disrupt using this method (Table 3-3). Repeated attempts to disrupt MXAN2183 were unsuccessful, suggesting that it or the small hypothetical gene located downstream in an operon may be essential. MXAN5686, MXAN5685 and MXAN5684, the first three genes in a six gene operon, were all detected in the ECM proteome. Disruption of MXAN5686 is expected to create a polar mutation on the rest of the operon. MXAN5684 was also disrupted.

Genes encoding ECM proteins were disrupted in the wild type (DK1622) and screened for fruiting body defects after spotting 5 x $10^6$ cells for 72 hours (Figure 3-1). All mutants develop at a similar rate and have a similar fruiting body distribution relative to DK1622. Previous work provided genetic evidence that FibA and PilA are components of partially redundant pathways for fruiting body morphogenesis (Bonner *et al.*, 2006). While *fibA* and *pilA* mutants form fruiting bodies (Figure 3-1), the double mutant neither aggregates nor sporulates (Bonner *et al.*, 2006). Therefore each ECM mutation was placed into *pilA* (DK10410) and *fibA* (LS2429) backgrounds to determine whether they function in a particular branch of the pathway. The fruiting bodies of the *pilA* mutant are more numerous and closely packed, possibly due to the loss of S motility (Figure 3-1). With the exception of MXAN4860, strains containing each mutation in combination with *pilA* develop comparably to the *pilA* parent strain. Strains

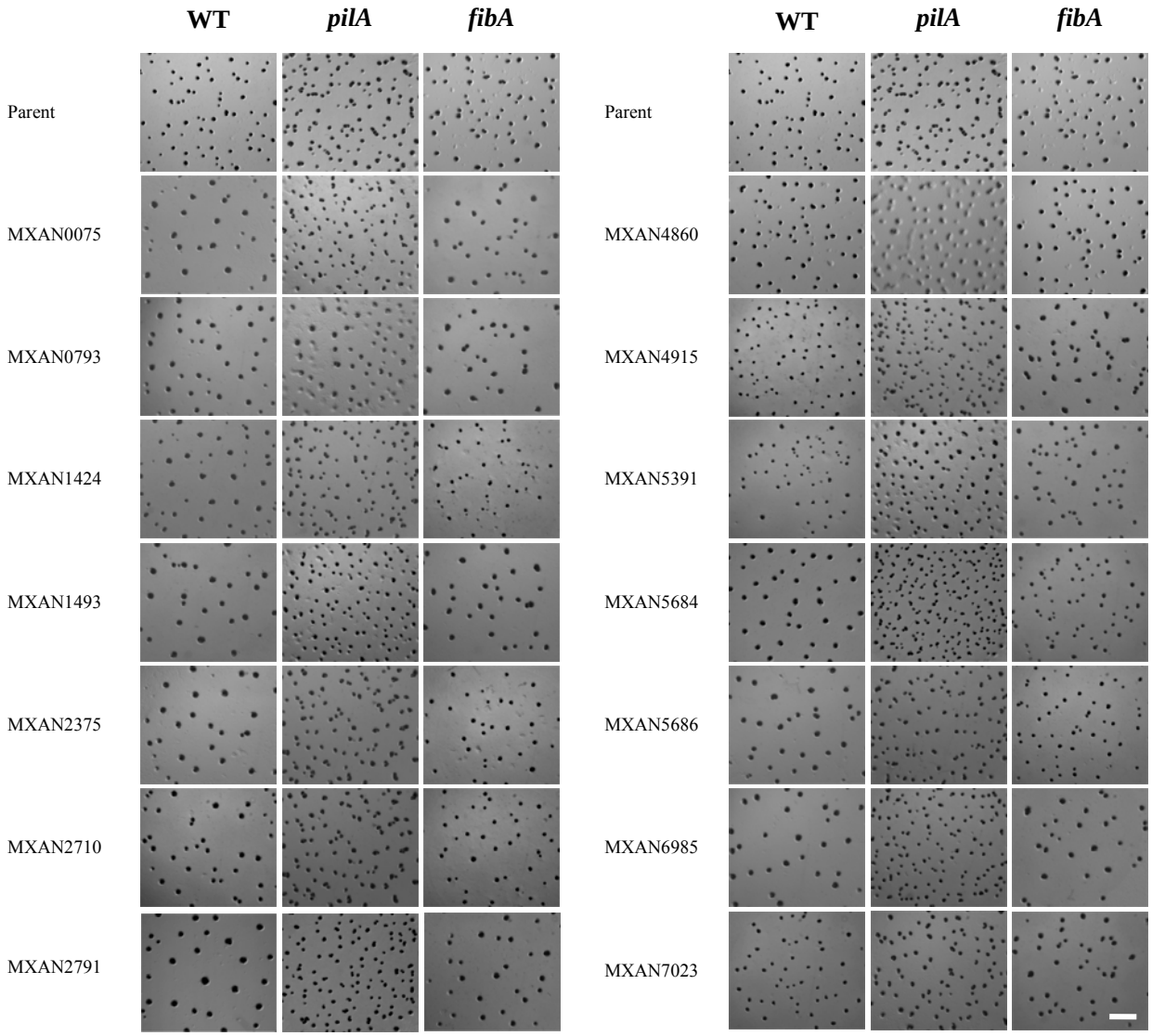


**Figure 3-1.** Fruiting body formation of ECM mutants compared with wild type, *pilA* and *fibA* strains. 5 x $10^6$ cells were spotted in 10 μl on TPM agar and photographed following 72 hours of incubation. Genes listed on the left indicate the putative ECM gene disrupted, while each column indicates the genetic background. Parent indicates the parental strain; WT (wild type, DK1622), *pilA* (Δ*pilA*, DK10410) and *fibA* (Δ*fibA*, LS2429). Bar = 1 mm.

containing each mutation in combination with *fibA* demonstrate the same timing and distribution of development as the wild type.

All strains were assessed for spore production and viability (Figure 3-2). In order to obtain enough spores to facilitate enumeration, spore assays were performed using 10-fold more cells than the fruiting body assays shown in Figure 3-1. The majority of the mutants produced spores within 1.5-fold of that produced by the parent strain and approximately 40-75% viable spores. However, disruption of MXAN7023 in the WT background caused a nearly two-fold increase in spore production, and a more modest increase in viable spores. Similarly, the MXAN4915 *fibA* mutant produced nearly two-fold more spores than the *fibA* parent, but viable spore production was similar to that of the parent strain. Disruption of MXAN2710 in the *pilA* background caused no defect in total spore production, but a nearly 10-fold decrease in spore viability.

**MXAN4860**. MXAN4860 was identified by 9 peptides in the C-terminal half, covering 27% of the total protein (Fig. 3-3A, shaded boxes), suggesting that this region is more trypsin sensitive than the cysteine-rich, N-terminal domain (Figure 3-3A, white bars). Neither the whole protein nor the individual domains have known homologs. While mutation of MXAN4860 alone results in no discernable phenotype (Figure 3-3B), it causes a lengthy delay in fruiting body formation in combination with *pilA*. The *pilA* parent undergoes aggregation between 24 and 48 hours, and sporulation begins at approximately 48 hours. The MXAN4860 *pilA* strain begins to aggregate at approximately the same time as the *pilA* parent, but development arrests at 48 hours when the cells are in large, translucent mounds. This arrest lasts approximately 24 hours until sporulation begins within the large mounds at approximately 72 hours. Sporulation is completed by 96 hours. The same disruption in the *pilT* background results in no developmental

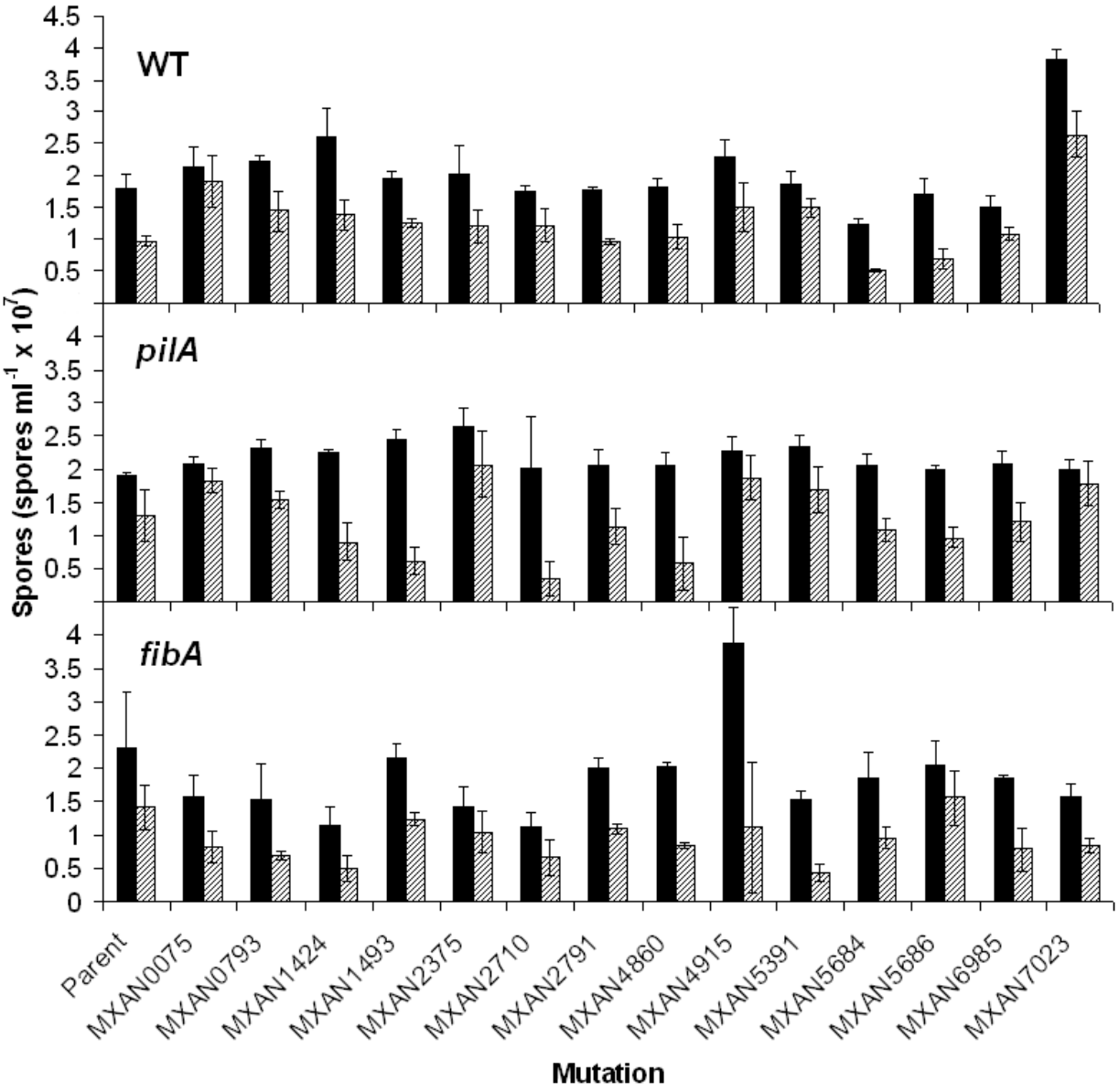


**Figure 3-2.** Spore production and viability of ECM mutants. Total spores from 5 x $10^7$ cells incubated for 5 days were enumerated microscopically (solid bars). Viable spores were determined by plating spores on CYE agar (hashed bars). Error bars indicate the standard deviation (n=3). Top left of each panel displays the genetic background containing each mutation; WT (wild type, DK1622), *pilA* (Δ*pilA*, DK10410) and *fibA* (Δ*fibA*, LS2429).

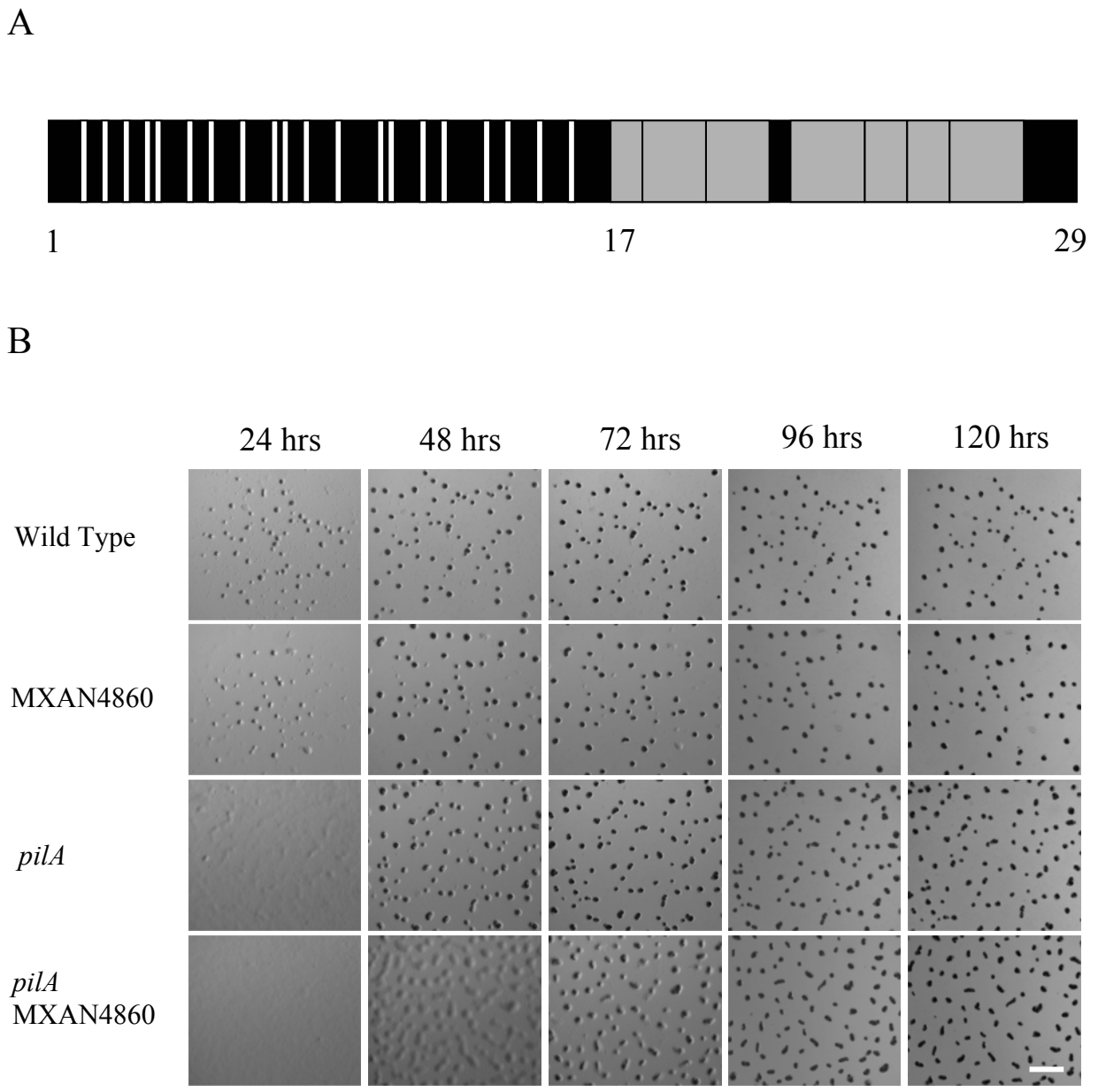


**Figure 3-3.** Primary structure analysis of MXAN4860 and developmental timing of MXAN4860 disruptions in WT and *pilA* strains. A. Schematic of the MXAN4860 protein product. Vertical white bars indicate positions of 20 cysteine residues found in the N-terminal portion of the protein. Gray boxes indicate the tryptic peptides detected by mass spectrometry. B. Developmental time course of fruiting body morphogenesis. 5 x $10^6$ cells were spotted in 10 µl on TPM agar and photographed every 24 hours. Strains with the MXAN4860 mutation develops normally unless coupled with a *pilA* mutation, in which case there is an approximately 24 hour delay in development between the 48 and 72 hour time points. Bar = 1 mm.

defect (data not shown), indicating that the defect is dependent on the absence of the pilus, similar to defects observed with strains harboring *fibA* disruptions. The phenotype of the MXAN4860 *fibA* double mutant is comparable to the *fibA* parent. These results are consistent with MXAN4860 functioning in the FibA branch of the proposed model for development.

Spore yields for all MXAN4860 mutants as well as parent strains were measured every 24 hours for 5 days (Figure 3-4). The MXAN4860 and MXAN4860 *fibA* mutants had similar timing and spore yield to their WT and *fibA* parents. Sporulation in the *pilA* strain is delayed 24 hours compared to WT, however by 72 hours spore production has reached WT levels. At 72 hours the MXAN4860 *pilA* mutant shows 46% sporulation compared to its parent. By 96 hours the MXAN4860 *pilA* mutant produces the same amount of spores as the *pilA* strain. The sporulation levels indicate an approximately 18 hour delay in sporulation, corroborating the observed delay in fruiting body morphogenesis.

**Discussion**

While proteins may be significant components of the ECM there have been few attempts to identify and characterize these proteins. Examples of identified ECM proteins include TasA and FibA. TasA is a structural component of *Bacillus subtilis* biofilms (Branda *et al.*, 2006). TasA and exopolysaccharide (EPS) are required for robust pellicle formation. Scanning electron microscopy revealed that pellicle-associated cells are covered with a thick matrix material, which is greatly reduced in a *tasA* mutant. *B. subtilis eps* mutants produce even less matrix material, and *tasA eps* double mutants do not make any matrix. *M. xanthus* strains carrying an active-site mutation in *fibA* make normal levels of ECM material but are unable to respond to the chemotactic lipid PE-16:1ω5c/16:1ω5c (Bonner *et al.*, 2006; Kearns *et al.*, 2002).

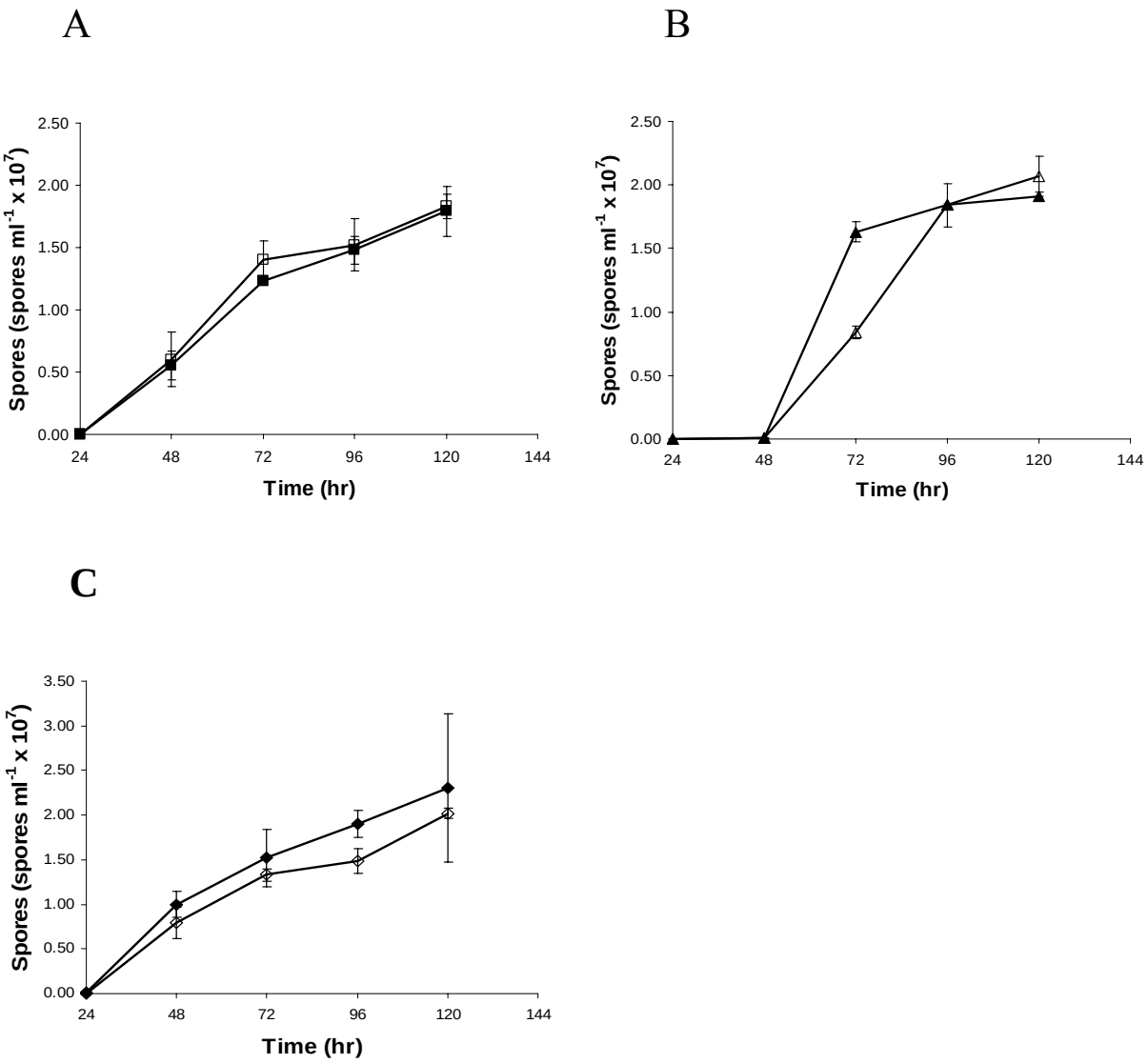


**Figure 3-4.** Sporulation time courses of MXAN4860 mutants compared to wild type, *pilA* and *fibA* strains. 5 x $10^7$ cells of each strain were plated on TPM and harvested at 24 hour intervals. Spores were quantified using a Petroff-Hauser counting chamber. A. wildtype (DK1622, closed square) and MXAN4860 (open square). B. *pilA* (DK10410, closed triangle) and MXAN4860 *pilA* (open triangle). C. *fibA* (LS2429, closed diamond) and MXAN4860 *fibA* (open diamond). Error bars indicate the standard deviation.

Though *M. xanthus* ECM proteins may be involved in many functions, of particular interest are the timing and spatial coordination of development. A broad-scale proteomic analysis identified 20 putative ECM proteins in addition to FibA. Many of the putative ECM proteins identified are hypothetical. Phenol extraction of 0.5% SDS-isolated ECM only removed 57% of the protein content (data not shown). It is possible that some protein is covalently associated with the insoluble ECM material.

Initially, matrix-assisted laser desorption ionization – time of flight mass spectrometry (MALDI-TOF MS) was utilized for protein identification. However poor protein coverage led to ambiguous identification. The LC-MS/MS technique negates the need for greater peptide coverage because a single peptide can identify a protein with 99% confidence. The lack of peptide coverage may be due to the abundance of extracellular proteases. ECM proteins are constantly exposed to these proteases, and may have evolved protease resistance, leading to inadequate digestion by trypsin. A specific example is MXAN4860. All the peptides detected by LC-MS/MS were derived from the C-terminal portion of MXAN4860 (Figure 3-3A), suggesting that the cysteine-rich N-terminal domain is trypsin resistant. The lack of peptide coverage with other proteins suggests that protease resistance may be important for protein stability and function in the extracellular milieu.

Proteomic analysis of FibA may offer new insight into its function. FibA contains a lipoprotein secretion signal, a propeptide domain to prevent catalytic function until needed, the catalytic domain, and two C-terminal PPC repeat domains of unknown function (Figure 3-5) (Bonner *et al.*, 2006). The epitope for the FibA antibody Mab2105 is proposed to be in the last C-terminal repeat, within the final 107 amino acids of the protein (Bonner *et al.*, 2006). Western blots using this antibody against proteins liberated from the ECM reveal bands of different sizes,

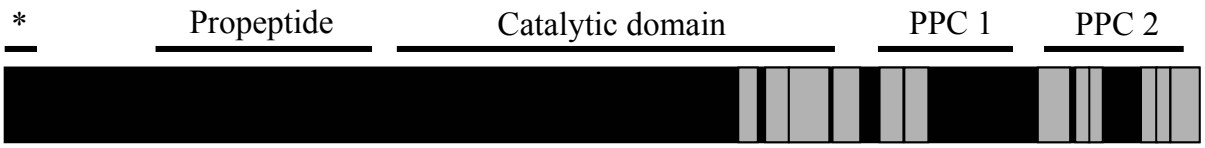


**Figure 3-5.** Primary structure analysis of FibA. Horizontal lines indicate the lipoprotein secretion signal (*, amino acids 1-20), propeptide domain (amino acids 93-228), catalytic domain (amino acids 244-517), PPC domain 1 (amino acids 542-626) and PPC domain 2 (647-734) (Bonner *et al.*, 2006). Gray boxes indicate peptides detected by mass spectrometry.

indicating that FibA is proteolytically processed into several pieces (Behmlander and Dworkin, 1994b; Bonner *et al.*, 2006). Most peptide fragments detected by LC-MS/MS are from the C-terminal repeats and C-terminal side of the catalytic domain (Figure 3-5). This result corroborates the Western results showing that the PPC repeats are found associated with the ECM. C-terminal repeats in eukaryotic matrix metalloproteinases confer substrate specificity by anchoring the enzyme next to the substrate [for a review see (Overall, 2002)], and by analogy FibA repeats may dictate the protease target(s) for the chemotactic signaling pathway. The repeats in *M. xanthus* may be involved in protein-protein interaction or protein scaffolding within the ECM. Alternatively, the repeats may anchor FibA to the matrix and proteolytic processing releases the catalytic domain to diffuse away.

*fibA* and *fibA pilT* mutants develop, but the *fibA pilA* mutant does not. Similarly, MXAN4860, MXAN4860 *fibA* and MXAN4860 *pilT* mutants develop while the MXAN4860 *pilA* mutant displays a delay in development compared to *pilA*. This pattern of phenotypes is consistent with MXAN4860 functioning in the FibA branch of the proposed developmental pathway. If the MXAN4860-FibA branch were linear, disruption of MXAN4860 in the *pilA* background would be expected to abolish development like a *fibA* disruption. Instead only a partial defect was observed, suggesting that multiple pathways integrate into or out of FibA, including an MXAN4860-mediated pathway affecting developmental timing. Therefore, FibA may act as a signal transduction protein and an integration point for an ECM signaling network instead of functioning in a single linear pathway. FibA signaling may involve a protease cascade, proteolytic activation of downstream elements as a signaling mechanism, or mediate protein-protein interaction through its C-terminal repeats.

Alternatively, FibA may not function as a signal transduction protein, but instead aid in signal transduction of other pathways by proteolytically activating, or allowing protein interaction through its released C-terminal repeats, extracellular signaling proteins. In humans, membrane-associated matrix metalloproteinase-1 (MMP-1) proteolytically activates extracellular matrix metalloproteinase-2 (gelatinase A) and is regulated by a prostaglandin-cAMP pathway (Shankavaram *et al.*, 2001). By analogy, an unknown regulatory pathway (prostaglandin-cAMP) may induce FibA (MMP-1) to proteolytically activate other extracellular signaling proteins (gelatinase A). In this case, FibA does not transduce signals in developmental or lipid chemotaxis pathways, but activates components of those pathways for signaling.

The function of the MXAN4860 protein is unclear. The unusual N-terminal domain may offer an insight. MXAN4860 shares some characteristics with Wnt proteins, a large family of eukaryotic proteins controlling development in organisms from nematodes to mammals (Wodarz and Nusse, 1998). Wnt proteins are approximately 350-390 amino acids in length and have 22 conserved cysteines. They are secreted, bind tightly with glycosaminoglycans in the extracellular matrix, and are difficult to extract from matrix fractions (Bradley and Brown, 1990; Reichsman *et al.*, 1996). Interaction between Wnt and a cell surface receptor (such as Fz and LRP5/6) transduces an extracellular signal into intracellular responses (Cong *et al.*, 2004), including the planar cell polarity pathway regulating tissue polarity, cell migration and cytoskeleton arrangement. Another eukaryotic protein involved in some of the same pathways as Wnt is Norrin. Norrin, like Wnt, is a secreted signaling protein (approximately 130 amino acids in length with 11 conserved cysteines), interacting with specific Fz and LRP receptors (Berger *et al.*, 1992). Though Norrin is cysteine rich like Wnt, they are unrelated, suggesting that cysteine-richness may have a conserved function in intercellular signaling in unrelated proteins. It is

intriguing to think that MXAN4860 may have similar functions in *M. xanthus* to Wnt and Norrin. Interestingly, some Wnts are acylated, and it has been shown in at least one case that acylation is necessary for signaling (Kurayoshi *et al.*, 2007). MXAN4860 is predicted to have a lipoprotein secretion signal and, therefore, may also be acylated.

Thirteen of twenty-one putative ECM proteins (62%) have predicted lipoprotein secretion signals. The structural function of acylation is to anchor proteins to either the outer membrane or the outer face of the inner membrane. While membrane-targeting of these proteins would seem to preclude secretion to the ECM, this is not observed with FibA. FibA associated with the inner membrane likely in the acylated pro-form (Simunovic *et al.*, 2003), but is also associated with the ECM (Behmlander and Dworkin, 1991). It is possible that targeting of ECM proteins to the inner membrane may be a method of keeping ECM proteins inactive until they are secreted. Alternatively, membrane targeting may segregate ECM proteins from other constitutively secreted proteins, preventing them from being exported until exopolysaccharide has been produced.

None of the genes encoding putative ECM proteins disrupted is essential for cell attachment, adventurous or social motility, or fruiting body formation and sporulation (outside of MXAN4860 and MXAN2710). Some of these processes have been shown to be dependent on the ECM (Arnold and Shimkets, 1988a, b; Li *et al.*, 2003; Lu *et al.*, 2005; Yang *et al.*, 2000), which would suggest that the polysaccharide component of the matrix performs the bulk of ECM functions. However, functional redundancy has been well established in this organism. In the case of development, both *fibA* and *pilA* deletions cause little to no loss of development until they were combined. The lack of phenotype for many of the mutants suggests that if the proteins identified here are involved in these processes, they are functionally redundant. Additionally,

this study did not identify proteins covalently linked to EPS. Identification and characterization of covalently-linked ECM proteins may not only reveal new signaling and structural capacities of the ECM, but also increase the understanding of previously identified ECM-mediated functions.

**Acknowledgements**

The authors wish to thank Dr. Jon Amster and Dr. Dennis Phillips for their advice, expertise and general help with proteomics, and Dr. Roy Welch for supplying annotated versions of the genome. This material is based upon work supported by the National Science Foundation under Grant No. 0343874 to L. Shimkets.

**References**

Arnold, J.W., and Shimkets, L.J. (1988a) Inhibition of cell-cell interactions in *Myxococcus xanthus* by Congo red. *J Bacteriol* **170**: 5765-5770.

Arnold, J.W., and Shimkets, L.J. (1988b) Cell surface properties correlated with cohesion in *Myxococcus xanthus*. *J Bacteriol* **170**: 5771-5777.

Behmlander, R.M., and Dworkin, M. (1991) Extracellular fibrils and contact-mediated cell interactions in *Myxococcus xanthus*. *J Bacteriol* **173**: 7810-7820.

Behmlander, R.M., and Dworkin, M. (1994a) Biochemical and structural analyses of the extracellular matrix fibrils of *Myxococcus xanthus*. *J Bacteriol* **176**: 6295-6303.

Behmlander, R.M., and Dworkin, M. (1994b) Integral proteins of the extracellular matrix fibrils of *Myxococcus xanthus*. *J Bacteriol* **176**: 6304-6311.

Bellenger, K., Ma, X., Shi, W., and Yang, Z. (2002) A CheW homologue is required for *Myxococcus xanthus* fruiting body development, social gliding motility, and fibril biogenesis. *J Bacteriol* **184**: 5654-5660.

Berger, W., van de Pol, D., Warburg, M., Gal, A., Bleeker-Wagemakers, L., de Silva, H., Meindl, A., Meitinger, T., Cremers, F., and Ropers, H.H. (1992) Mutations in the candidate gene for Norrie disease. *Hum Mol Genet* **1**: 461-465.

Black, W.P., and Yang, Z. (2004) *Myxococcus xanthus* chemotaxis homologs DifD and DifG negatively regulate fibril polysaccharide production. *J Bacteriol* **186**: 1001-1008.

Black, W.P., Xu, Q., and Yang, Z. (2006) Type IV pili function upstream of the Dif chemotaxis pathway in *Myxococcus xanthus* EPS regulation. *Mol Microbiol* **61**: 447-456.

Blom, A.B., van Lent, P.L., Libregts, S., Holthuysen, A.E., van der Kraan, P.M., van Rooijen, N., and van den Berg, W.B. (2007) Crucial role of macrophages in matrix metalloproteinase-mediated cartilage destruction during experimental osteoarthritis: involvement of matrix metalloproteinase 3. *Arthritis Rheum* **56**: 147-157.

Bodet, C., Chandad, F., and Grenier, D. (2007) Inhibition of host extracellular matrix destructive enzyme production and activity by a high-molecular-weight cranberry fraction. *J Periodontal Res* **42**: 159-168.

Bonner, P.J., Xu, Q., Black, W.P., Li, Z., Yang, Z., and Shimkets, L.J. (2005) The Dif chemosensory pathway is directly involved in phosphatidylethanolamine sensory transduction in *Myxococcus xanthus*. *Mol Microbiol* **57**: 1499-1508.

Bonner, P.J., Black, W.P., Yang, Z., and Shimkets, L.J. (2006) FibA and PilA act cooperatively during fruiting body formation of *Myxococcus xanthus*. *Mol Microbiol* **61**: 1283-1293.

Bradley, R.S., and Brown, A.M. (1990) The proto-oncogene int-1 encodes a secreted protein associated with the extracellular matrix. *Embo J* **9**: 1569-1575.

Branda, S.S., Vik, S., Friedman, L., and Kolter, R. (2005) Biofilms: the matrix revisited. *Trends Microbiol* **13**: 20-26.

Branda, S.S., Chu, F., Kearns, D.B., Losick, R., and Kolter, R. (2006) A major protein component of the *Bacillus subtilis* biofilm matrix. *Mol Microbiol* **59**: 1229-1238.

Campos, J.M., Geisselsoder, J., and Zusman, D.R. (1978) Isolation of bacteriophage MX4, a generalized transducing phage for *Myxococcus xanthus*. *J Mol Biol* **119**: 167-178.

Chang, B.Y., and Dworkin, M. (1994) Isolated fibrils rescue cohesion and development in the Dsp mutant of *Myxococcus xanthus*. *J Bacteriol* **176**: 7190-7196.

Chang, B.Y., and Dworkin, M. (1996) Mutants of *Myxococcus xanthus dsp* defective in fibril binding. *J Bacteriol* **178**: 697-700.

Cong, F., Schweizer, L., and Varmus, H. (2004) Wnt signals across the plasma membrane to activate the beta-catenin pathway by forming oligomers containing its receptors, Frizzled and LRP. *Development* **131**: 5103-5115.

Curtis, P.D., Geyer, R., White, D.C., and Shimkets, L.J. (2006) Novel lipids in *Myxococcus xanthus* and their role in chemotaxis. *Environ Microbiol* **8**: 1935-1949.

Davies, D.G., Parsek, M.R., Pearson, J.P., Iglewski, B.H., Costerton, J.W., and Greenberg, E.P. (1998) The involvement of cell-to-cell signals in the development of a bacterial biofilm. *Science* **280**: 295-298.

Domka, J., Lee, J., Bansal, T., and Wood, T.K. (2007) Temporal gene-expression in *Escherichia coli* K-12 biofilms. *Environ Microbiol* **9**: 332-346.

Goldman, B.S., Nierman, W.C., Kaiser, D., Slater, S.C., Durkin, A.S., Eisen, J.A., Ronning, C.M., Barbazuk, W.B., Blanchard, M., Field, C., Halling, C., Hinkle, G., Iartchuk, O., Kim, H.S., Mackenzie, C., Madupu, R., Miller, N., Shvartsbeyn, A., Sullivan, S.A., Vaudin, M., Wiegand, R., and Kaplan, H.B. (2006) Evolution of sensory complexity recorded in a myxobacterial genome. *Proc Natl Acad Sci U S A* **103**: 15200-15205.

Gollop, R., Inouye, M., and Inouye, S. (1991) Protein U, a late-developmental spore coat protein of *Myxococcus xanthus*, is a secretory protein. *J Bacteriol* **173**: 3597-3600.

Grabellus, F., Worm, K., and Schmid, K.W. (2007) Induction of the matrix metalloproteinase-2 activation system in arteries by tensile stress. Involvement of the p38 MAP-kinase pathway. *Pathol Res Pract* **203**: 135-143.

Juncker, A.S., Willenbrock, H., Von Heijne, G., Brunak, S., Nielsen, H., and Krogh, A. (2003) Prediction of lipoprotein signal peptides in Gram-negative bacteria. *Protein Sci* **12**: 1652-1662.

Kaiser, D. (1979) Social gliding is correlated with the presence of pili in *Myxococcus xanthus*. *Proc Natl Acad Sci U S A* **76**: 5952-5956.

Kashefi, K., and Hartzell, P.L. (1995) Genetic suppression and phenotypic masking of a *Myxococcus xanthus frzF*- defect. *Mol Microbiol* **15**: 483-494.

Kearns, D.B., Campbell, B.D., and Shimkets, L.J. (2000) *Myxococcus xanthus* fibril appendages are essential for excitation by a phospholipid attractant. *Proc Natl Acad Sci U S A* **97**: 11505-11510.

Kearns, D.B., Venot, A., Bonner, P.J., Stevens, B., Boons, G.-J., and Shimkets, L.J. (2001) Identification of a developmental chemoattractant in *Myxococcus xanthus* through metabolic engineering. *Proc Natl Acad Sci U S A* **98**: 13990-13994.

Kearns, D.B., Bonner, P.J., Smith, D.R., and Shimkets, L.J. (2002) An extracellular matrix-associated zinc metalloprotease is required for dilauroyl phosphatidylethanolamine chemotactic excitation in *Myxococcus xanthus*. *J Bacteriol* **184**: 1678-1684.

Kurayoshi, M., Yamamoto, H., Izumi, S., and Kikuchi, A. (2007) Post-translational palmitoylation and glycosylation of Wnt-5a are necessary for its signalling. *Biochem J* **402**: 515-523.

Li, D.Q., and Pflugfelder, S.C. (2005) Matrix metalloproteinases in corneal inflammation. *Ocul Surf* **3**: S198-202.

Li, Y., Sun, H., Ma, X., Lu, A., Lux, R., Zusman, D., and Shi, W. (2003) Extracellular polysaccharides mediate pilus retraction during social motility of *Myxococcus xanthus*. *Proc Natl Acad Sci U S A* **100**: 5443-5448.

Li, Y., Lux, R., Pelling, A.E., Gimzewski, J.K., and Shi, W. (2005) Analysis of type IV pilus and its associated motility in *Myxococcus xanthus* using an antibody reactive with native pilin and pili. *Microbiology* **151**: 353-360.

Lu, A., Cho, K., Black, W.P., Duan, X.Y., Lux, R., Yang, Z., Kaplan, H.B., Zusman, D.R., and Shi, W. (2005) Exopolysaccharide biosynthesis genes required for social motility in *Myxococcus xanthus*. *Mol Microbiol* **55**: 206-220.

Lund, L.R., Romer, J., Bugge, T.H., Nielsen, B.S., Frandsen, T.L., Degen, J.L., Stephens, R.W., and Dano, K. (1999) Functional overlap between two classes of matrix-degrading proteases in wound healing. *Embo J* **18**: 4645-4656.

Malik, M.T., and Kakar, S.S. (2006) Regulation of angiogenesis and invasion by human Pituitary tumor transforming gene (PTTG) through increased expression and secretion of matrix metalloproteinase-2 (MMP-2). *Mol Cancer* **5**: 61.

Overall, C.M. (2002) Molecular determinants of metalloproteinase substrate specificity: matrix metalloproteinase substrate binding domains, modules, and exosites. *Mol Biotechnol* **22**: 51-86.

Pedrioli, P.G., Eng, J.K., Hubley, R., Vogelzang, M., Deutsch, E.W., Raught, B., Pratt, B., Nilsson, E., Angeletti, R.H., Apweiler, R., Cheung, K., Costello, C.E., Hermjakob, H., Huang, S., Julian, R.K., Kapp, E., McComb, M.E., Oliver, S.G., Omenn, G., Paton, N.W., Simpson, R., Smith, R., Taylor, C.F., Zhu, W., and Aebersold, R. (2004) A common open representation of mass spectrometry data and its application to proteomics research. *Nat Biotechnol* **22**: 1459-1466.

Poza, M., Prieto-Alcedo, M., Sieiro, C., and Villa, T.G. (2004) Cloning and expression of clt genes encoding milk-clotting proteases from *Myxococcus xanthus* 422. *Appl Environ Microbiol* **70**: 6337-6341.

Quillet, L., Bensmail, L., Barray, S., and Guespin-Michel, J. (1997) Cloning and sequencing of two genes, *prtA* and *prtB*, from *Myxococcus xanthus*, encoding PrtA and PrtB proteases, both of which are required for the protease activity. *Gene* **198**: 135-140.

Reichsman, F., Smith, L., and Cumberledge, S. (1996) Glycosaminoglycans can modulate extracellular localization of the wingless protein and promote signal transduction. *J Cell Biol* **135**: 819-827.

Seydel, A., Gounon, P., and Pugsley, A.P. (1999) Testing the '+2 rule' for lipoprotein sorting in the *Escherichia coli* cell envelope with a new genetic selection. *Mol Microbiol* **34**: 810-821.

Shankavaram, U.T., Lai, W.C., Netzel-Arnett, S., Mangan, P.R., Ardans, J.A., Caterina, N., Stetler-Stevenson, W.G., Birkedal-Hansen, H., and Wahl, L.M. (2001) Monocyte

membrane type 1-matrix metalloproteinase. Prostaglandin-dependent regulation and role in metalloproteinase-2 activation. *J Biol Chem* **276**: 19027-19032.

Simunovic, V., Gherardini, F.C., and Shimkets, L.J. (2003) Membrane localization of motility, signaling, and polyketide synthetase proteins in *Myxococcus xanthus*. *J Bacteriol* **185**: 5066-5075.

Stanley, N.R., Britton, R.A., Grossman, A.D., and Lazazzera, B.A. (2003) Identification of catabolite repression as a physiological regulator of biofilm formation by *Bacillus subtilis* by use of DNA microarrays. *J Bacteriol* **185**: 1951-1957.

Sternlicht, M.D., and Werb, Z. (2001) How matrix metalloproteinases regulate cell behavior. *Annu Rev Cell Dev Biol* **17**: 463-516.

Sun, H., Zusman, D.R., and Shi, W. (2000) Type IV pilus of *Myxococcus xanthus* is a motility apparatus controlled by the *frz* chemosensory system. *Curr Biol* **10**: 1143-1146.

Sutherland, I.W. (2001) The biofilm matrix--an immobilized but dynamic microbial environment. *Trends Microbiol* **9**: 222-227.

Tjaderhane, L., Hotakainen, T., Kinnunen, S., Ahonen, M., and Salo, T. (2007) The effect of chemical inhibition of matrix metalloproteinases on the size of experimentally induced apical periodontitis. *Int Endod J*.

Vlamakis, H.C., Kirby, J.R., and Zusman, D.R. (2004) The Che4 pathway of *Myxococcus xanthus* regulates type IV pilus-mediated motility. *Mol Microbiol* **52**: 1799-1811.

Weatherly, D.B., Atwood, J.A., Minning, T.A., Cavola, C., Tarleton, R.L., and Orlando, R. (2005) A heuristic method for assigning a false-discovery rate for protein identifications from mascot database search results. *Molecular & Cellular Proteomics* **4**: 762-772.

Whitchurch, C.B., Tolker-Nielsen, T., Ragas, P.C., and Mattick, J.S. (2002) Extracellular DNA required for bacterial biofilm formation. *Science* **295**: 1487.

Whiteley, M., Bangera, M.G., Bumgarner, R.E., Parsek, M.R., Teitzel, G.M., Lory, S., and Greenberg, E.P. (2001) Gene expression in *Pseudomonas aeruginosa* biofilms. *Nature* **413**: 860-864.

Wodarz, A., and Nusse, R. (1998) Mechanisms of Wnt signaling in development. *Annu Rev Cell Dev Biol* **14**: 59-88.

Wu, S.S., and Kaiser, D. (1996) Markerless deletions of pil genes in *Myxococcus xanthus* generated by counterselection with the *Bacillus subtilis sacB* gene. *J Bacteriol* **178**: 5817-5821.

Wu, S.S., Wu, J., and Kaiser, D. (1997) The *Myxococcus xanthus pilT* locus is required for social gliding motility although pili are still produced. *Mol Microbiol* **23**: 109-121.

Yang, Z., Ma, X., Tong, L., Kaplan, H.B., Shimkets, L.J., and Shi, W. (2000) *Myxococcus xanthus dif* genes are required for biogenesis of cell surface fibrils essential for social gliding motility. *J Bacteriol* **182**: 5793-5798.

Zaragoza, R., Gimeno, A., Miralles, V.J., Garcia-Trevijano, E.R., Carmena, R., Garcia, C., Mata, M., Puertes, I.R., Torres, L., and Vina, J.R. (2006) Retinoids induce MMP-9 expression through RARα during mammary gland remodeling. *Am J Physiol Endocrinol Metab*.

# CHAPTER 4

# CONCLUSION

The developmental program of *Myxococcus xanthus* resembles biofilm formation of other prokaryotic organisms in several facets. In the simplest way, both are mechanisms by which cells come together in large numbers associated with a surface. Both processes require the production of an extracellular matrix (Arnold and Shimkets, 1988a; Branda *et al.*, 2005; Chang and Dworkin, 1996; Lu *et al.*, 2005; Sutherland, 2001; Yang *et al.*, 2000), both make use of intercellular communication (Davies *et al.*, 1998; Kuspa *et al.*, 1992a, b), and both alter gene expression in biofilms (Domka *et al.*, 2007; Kroos *et al.*, 1986; Stanley *et al.*, 2003; Whiteley *et al.*, 2001). Development of *M. xanthus* also resembles aspects of cellular development in eukaryotic organisms. Both of these processes begin with a uniform cell population and end with differentiated cell lines (Anderson *et al.*, 2001; O'Connor and Zusman, 1991c). In *M. xanthus* cells in fruiting bodies can either become myxospores (White, 1993) or undergo programmed cell death (Wireman and Dworkin, 1975, 1977), another aspect resembling eukaryotic development. Cells outside the fruiting body (known as peripheral rods) have altered gene expression compared to cells in the fruiting bodies (O'Connor and Zusman, 1991a, b, c). Both *M. xanthus* and eukaryotic development make use signaling cascades (Ueki and Inouye, 2006; Wang and Tournier, 2006). Therefore, *M. xanthus* development is an intriguing area not just to study the specifics of this amazing process, but as a starting point to unravel the underlying mechanisms of how cellular life transitions from solitary to communal existence.

Principal of interest are mechanisms of intercellular signaling as these may exert the greatest control over temporal and spatial events within the community. *M. xanthus* offers a suite of signaling pathways during development. Though this organism lacks traditional quorum sensing mechanisms characterized in other bacteria, it does employ a novel form of cell density-sensing based upon mixtures of amino acids and small peptides (known as A signaling) (Kuspa

*et al.*, 1992a, b). The main developmental timer is known as C signal and is correlated with expression of the short chain alcohol dehydrogenase CsgA (Li *et al.*, 1992; Rhie and Shimkets, 1989). *M. xanthus* uses multiple two-component regulatory systems (Higgs *et al.*, 2005) and serine/threonine kinase cascades throughout development (Ueki and Inouye, 2006). Of interest to this study are three unusual signaling pathways for lipid chemotaxis, extracellular matrix-dependent developmental signaling and pilus-dependent developmental signaling.

**Lipid chemotaxis as a self-recognition marker**

*M. xanthus* has no demonstrable chemotaxis towards soluble substrates such as sugars, amino acids and other common chemotactic molecules (Dworkin and Eide, 1983). The lack of chemotaxis towards these substrates likely stems from the limited rate of motility. As a surface motile organism, *M. xanthus* moves at a rate of 1 μm $min^{-1}$, about the same rate as diffusion of soluble chemicals, so chemical gradients collapse before a cell can respond. However, *M. xanthus* preferentially moves up gradients of phospholipids derived from its own membrane, which was correlated with an increase of reversal period (a longer period of time between reversals) (Kearns and Shimkets, 1998). Prolonged exposure to these lipids leads to the reversal period returning to basal levels, demonstrating adaptation to the chemotactic signal (Bonner *et al.*, 2005). This response only occurs during starvation (Kearns and Shimkets, 1998). Through metabolic engineering it was found that the chemotactic activity was linked the specific fatty acid 16:1ω5c in membrane phosphatidylethanolamine (PE) (Kearns *et al.*, 2001). Chemotaxis towards lipids containing this fatty acid require the catalytic activity of the ECM-associated zinc metalloprotease FibA (an active site mutant of FibA does not respond (Bonner *et al.*, 2006)), though it is unclear exactly how FibA functions in the signaling pathway (Kearns *et al.*, 2002).

Also required for the response is the Dif chemotaxis sensory system, though it is unknown how the lipid signal enters the Dif system (Bonner *et al.*, 2005).

The fatty acid 16:1ω5c is found in only a handful of organisms, often at low levels. However, the myxobacteria are particularly enriched in this fatty acid (Dickschat *et al.*, 2005; Iizuka *et al.*, 2003; Kearns *et al.*, 2001; Toal *et al.*, 1995), and in *M. xanthus* it is the second most abundant fatty acid. This result suggests that the 16:1ω5c chemotactic response may be tied to the phylogeny of the organism. 16:1ω5c is also primarily located at the *sn*-1 position in *M. xanthus*, which contradicts the established dogma for Gram-negative organisms wherein the *sn*-1 position contains solely saturated fatty acids. Here again, the *M. xanthus* distinguishes itself from other bacteria, though it is unknown if all myxobacteria have this unusual fatty acid bias. In relation to chemotaxis, the results presented in this study indicate that 16:1ω5c at the *sn*-1 position has a greater ability to induce chemotactic excitation than 16:1ω5c found at the *sn*-2 position, thereby implicating the rare position bias of this rare fatty acid in the unusual chemotaxis of this organism (Curtis *et al.*, 2006).

While myxobacteria are often referred to as social bacteria, a more appropriate term may be that they are “cliquish”, as myxobacteria prefer to associate with the same species. Swarms of different myxobacterial species compete to the point of territorial dominance (Qualls and White, 1982; Smith and Dworkin, 1994). Species exclusion also occurs during development (Fiegna and Velicer, 2005), where different species mixed together form distinct, same-species fruiting bodies (Smith and Dworkin, 1994). Maintaining species purity in the most diverse bacterial environment on earth (the soil) is an impressive feat, and therefore must employ similarly impressive mechanisms to maintain it. It is possible that a rare fatty acid at an unusual position in PE serves as a self-recognition mechanism during development. It seems unlikely that this

response functions in species-specific self recognition as 16:1ω5c is found in several other myxobacteria at significant quantities. This could mean that myxobacteria have multiple means of maintaining species purity.

Although it is tantalizing to assign a developmental function to lipid chemotaxis because the behavior is starvation dependent, there is little evidence to support this hypothesis. Disruption of *fibA* (thereby abolishing lipid chemotaxis) does not impact development (Bonner *et al.*, 2006; Kearns *et al.*, 2002). Additionally, severely decreasing 16:1ω5c abundance in the membrane by disrupting a particular *fabH* biosynthetic gene also has no impact on development (Bode *et al.*, 2006). While excitation is correlated with prevalence of 16:1ω5c, evidence indicates that unsaturations may be introduced into *M. xanthus* fatty acids by membrane desaturases instead of during biosynthesis. It is possible the actual stimulus for lipid chemotaxis is a $\Delta^{11}$ double bond on the *sn*-1 fatty acid and it only correlates to 16:1ω5c specifically because it is the most abundant unsaturated fatty acid. Nevertheless, it has been difficult to assign a developmental function to lipid chemotaxis. An alternate function may not be developmental, but predatorial.

Myxobacteria are predators in nature, lysing other soil bacteria with lytic enzymes such as lipases and proteases to digest prey bacteria. The effectiveness of this lifestyle is strongly influenced by cell density (Rosenberg *et al.*, 1977). A single cell releasing lytic enzymes in an environment may find the enzymes too dilute to significantly damage a prey bacterial cell. However, a swarm of myxobacterial cells will have a much greater impact on prey cell lysis due to the higher lytic enzyme concentration. Hence the necessity for myxobacterial strains to travel in swarms. It is thought (Dworkin, 1972) that fruiting body formation is a mechanism to keep myxospores together until conditions become favorable for germination. The spores germinate

together and form a swarm much faster than if the myxospores were dispersed, underscoring the importance of the communal myxobacterial lifestyle. It is possible that the lipid chemotaxis response is a mechanism to maintain swarming behavior.

Assuming that lipid chemotaxis has developmental relevance, the excitation response could begin in the middle of a swarm where the cell density is highest and nutrients are exhausted. Given the high cell density, the chemotactic signal is already in high abundance and adaptation begins in approximately 30-45 minutes (Bonner *et al.*, 2005), saturating the response and allowing only a very narrow window of activity. This situation is contradictory to the nature of chemotaxis, which is to direct a cell from a location of low signal abundance to high signal abundance, or in the case of a chemotactic signal serving as a self-recognition marker, a location of low self abundance to high self abundance. Instead of development, consider a different situation where mxyobacterial cells encounter starvation. Lone cells traveling away from a swarm that are unsuccessful in locating a food source must either return to the swarm for nutrients or development, or starve. In essence, each lone cell must move from a location of low self abundance to high self abundance. Lipid chemotaxis toward a self-recognition marker could accomplish this purpose assuming there is a gradient or trail. Therefore, it is plausible that lipid chemotaxis as self recognition would function in maintaining swarm integrity.

Conversely, lipid chemotaxis may enhance swarm dispersal. Consider the previous situation where cells in the center of a swarm starve and activate lipid chemotaxis. Increasing the reversal period may cause the cells to race out of the swarm, potentially towards better metabolic conditions. However, complete swarm dispersal would inhibit fruiting body formation; therefore the adaptation response would ensure that cells do not travel too far from the swarm. In this case, if the cell continues to starve but is still in a location of high self-signal,

the reversal period returns to normal and fruiting body formation can begin. Presumably the high self-signal means there is a large population of similarly starving cells. The swarm integrity and swarm dispersal hypotheses are not mutually exclusive and may operate in coordination to maintain swarm stability in the face of environmental pressures, particularly in the soil where nutrient conditions can change rapidly. Testing *fibA* and other lipid chemotaxis-deficient mutants in predation assays and development assays under nutrient conditions closely resembling the soil, possibly in competition with strains capable of lipid chemotaxis, may reveal a novel function of this amazing pathway.

**ECM-mediated signaling networks**

The last two signaling pathways considered in this study are linked in purpose, though not in mechanism. While a *fibA* mutant undergoes development as well as wild type, a *fibA pilA* mutant does not develop (Bonner *et al.*, 2006). *pilA* encodes the PilA monomer that forms the Type IV pilus (Li *et al.*, 2005; Wu and Kaiser, 1996). *pilA* mutants have no pili (Wu and Kaiser, 1996), reduced social (S) motility, reduced ECM production (Black *et al.*, 2006), and an approximately 24 hour delay in development compared to wild type ((Bonner *et al.*, 2006), this study), but do eventually form fruiting bodies and sporulate nearly as well as wild type. The fact that the *fibA* and *pilA* mutants develop but the *fibA pilA* mutant does not indicates that development has a branched pathway where FibA functions in one branch and PilA functions in the other (Bonner *et al.*, 2006) (Figure 4-1). PilT is the retractile motor for the Type IV pilus; *pilT* mutants have pili, but are unable to retract them and therefore have reduced swarming motility (Wu *et al.*, 1997). These mutants also have normal-to-slightly overproduced ECM levels and develop the same as wild type (Black *et al.*, 2006). A *fibA pilT* develops normally

(Bonner *et al.*, 2006), suggesting that the absence of development in the *fibA pilA* mutant is due to lack of PilA or pili and not deficiency in S motility. Signaling through both branches integrates at or before the Dif chemotaxis sensory system (Bonner *et al.*, 2005). The Dif system is composed of DifA (a methyl-accepting chemotaxis protein (MCP) homolog), DifC (a CheW coupling protein homolog) and DifE (a CheA histidine kinase homolog) (Lancero *et al.*, 2002). Disruptions in genes encoding these proteins lead to reduced ECM production and no development (Arnold and Shimkets, 1988b; Chang and Dworkin, 1996).

The nature of the developmental signals that pass through each branch is unclear. It is enticing to assume that the self-recognition lipid services the FibA-mediated branch. Lipid chemotaxis not only is dependent on the catalytic activity of FibA (Bonner *et al.*, 2006), but also requires the Dif chemotaxis system (Bonner *et al.*, 2005). *dif* mutants are unable to respond to the lipid stimulus. Though these mutants have reduced ECM production which may explain the lack of response (Black *et al.*, 2006), a mutation in *difD* (which encodes the cognate CheY-like response regulator homolog) results in normal levels of ECM but an inability to respond (Black *et al.*, 2006; Bonner *et al.*, 2005), suggesting the chemotaxis signal does pass through the Dif system. Despite the evidence that lipid chemotaxis requires the Dif system, there is no evidence to indicate that lipid chemotaxis is the FibA developmental signal.

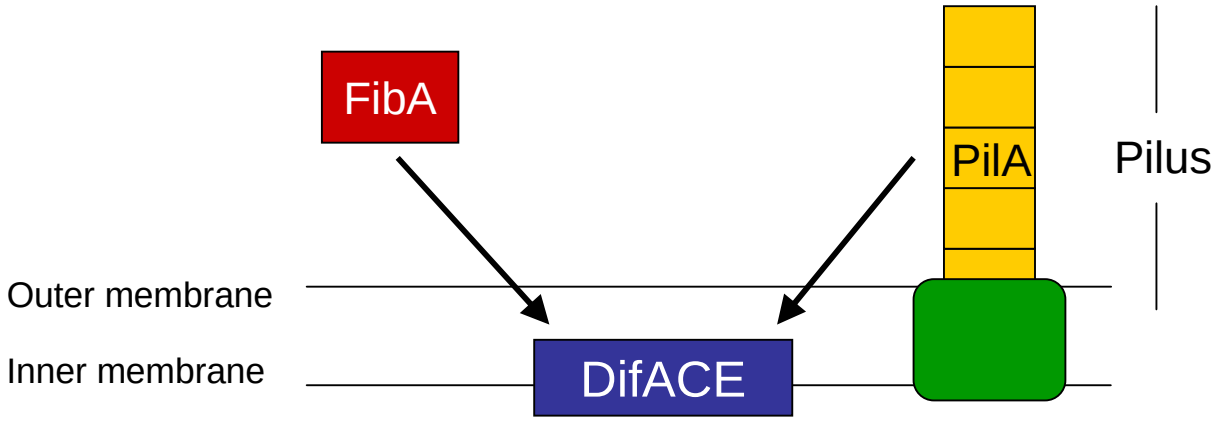


**Figure 4-1.** A model for the partially branched developmental pathway. Two extracellular signaling pathways integrate at the DifACE complex to control development. One pathway is mediated by the ECM-associated zinc metalloprotease FibA. The other pathway is mediated by the Type IV pilus monomer PilA or the extended pilus filament.

An MXAN4860 *pilA* mutant has a 24 hour delay in development compared to its *pilA* parent, but this defect is not seen in the WT, *fibA* or *pilT* backgrounds. This pattern of phenotypes is consistent with MXAN4860 functioning in the FibA branch of development. The fact that the MXAN4860 mutant displays only a delay in development and not a complete abolishment suggests that there are multiple factors affecting development on the FibA branch. If MXAN4860 functions in a single pathway with FibA then the MXAN4860 *pilA* mutant should display the same phenotype as the *fibA pilA* mutant. It is possible that multiple inputs integrate into FibA, or FibA signal transduction has multiple outputs, including an MXAN4860-mediated developmental timing signal. Individual pathways upstream or downstream of FibA control different aspects of development such that in total they allow development in the absence of PilA, and removal of FibA (the integration point) abolishes the concerted action of the pathways (Figure 4-2).

Alternatively, given the nature of FibA as a protease, another plausible explanation is that FibA doesn't function within a particular pathway but instead processes or matures other ECM proteins, activating them for their specific pathways (Figure 4-3). In this case, there would be no actual FibA branch, but a MXAN4860 partial branch among many other branches that, in total, allow development in the absence of PilA, all of which are dependent on FibA processing for activity. Now that many putative ECM proteins have been identified, analyzing them in terms of protein processing, especially in WT and *fibA* strains would be an exciting course of action.

**Lipoprotein secretion**

Type II secretion is the major method by which proteins are exported out of *M. xanthus* cells. Type II secretion is a two step process. In the first step, proteins are translocated to the

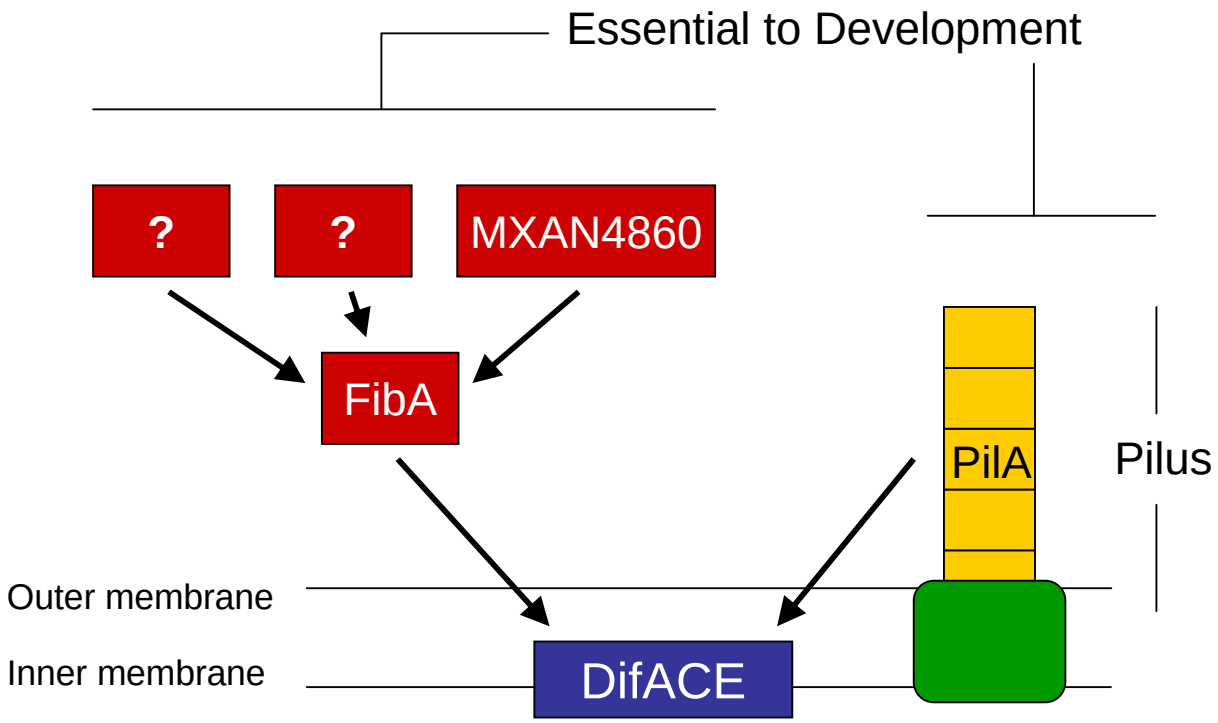


**Figure 4-2.** ECM-signaling model wherein FibA integrates multiple extracellular signals. The partial developmental defect of the MXAN4860 *pilA* mutant necessitates other signaling pathways (question marks) that work in concert with MXAN4860 to control development in the absence of PilA. FibA serves as the integration point for multiple signals because the *fibA pilA* mutant is completely unable to develop.

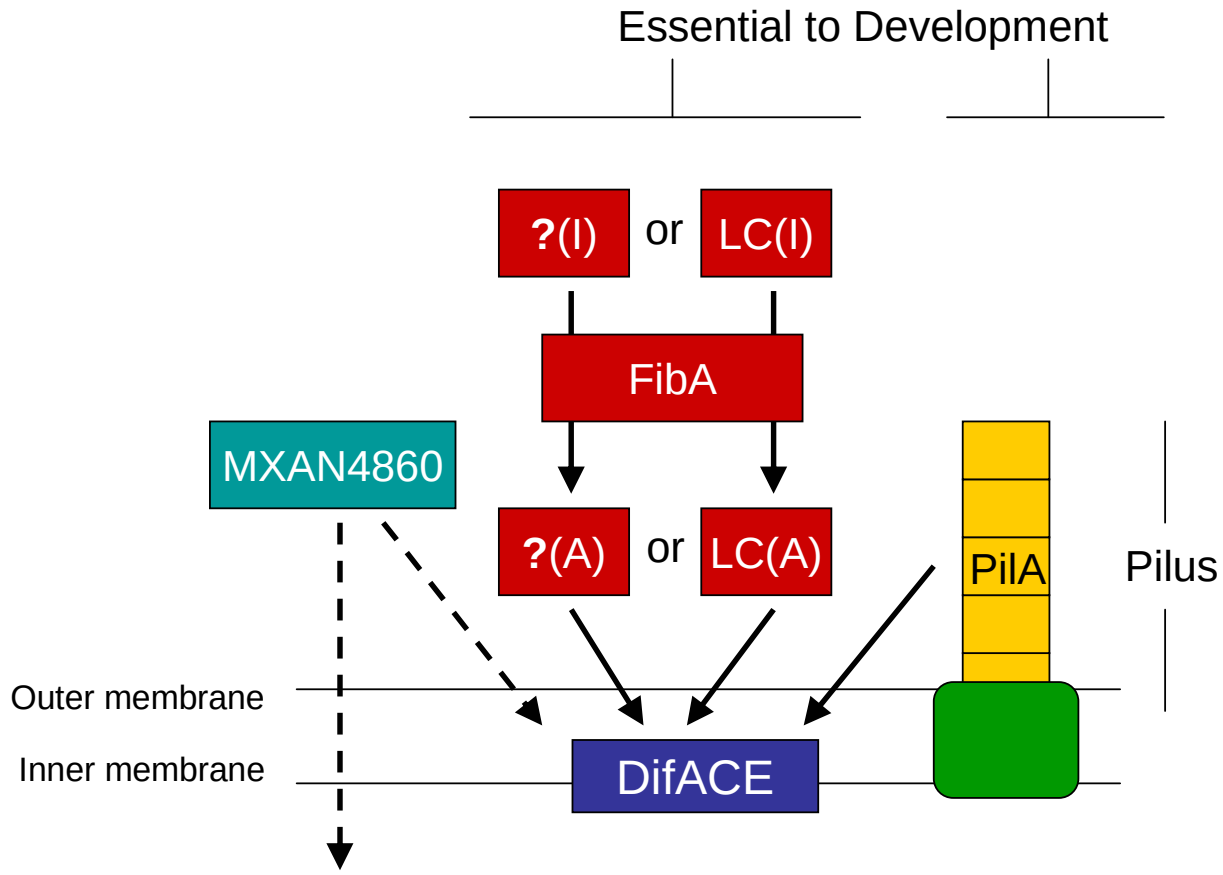


**Figure 4-3.** ECM-signaling model wherein FibA processes extracellular signaling proteins. Instead of FibA functioning within an ECM-associated developmental pathway, FibA proteolytic activity may be necessary to process and activate multiple ECM proteins, including components of an essential ECM developmental pathway. The essential developmental pathway may involve lipid chemotaxis (LC) or an as-yet-undiscovered ECM signaling pathway (?) necessary for development in the absence of PilA. The (I) designation indicates an inactive form of the protein(s), while the (A) designation indicates proteins converted to an active form by FibA proteolytic cleavage. The essential ECM developmental pathway must activate the Dif system as *dif* mutants are unable to develop, suggesting that Dif is the integration point of the PilA and ECM developmental branches. MXAN4860-mediated developmental timing functions in the absence of PilA, but it is unclear whether it utilizes the Dif system and/or is dependent on FibA processing.

periplasm by the Sec pathway (Manting and Driessen, 2000). The Sec mechanism recognizes the N-terminal secretion signal and once the proteins are translocated across the inner membrane the Sec-signal is cleaved off. Proteins in the periplasm are recognized by the Type II secretion machinery and translocated across the outer membrane into the extracellular medium (Filloux, 2004). In the case of lipoprotein signals, the Sec-signal is cleaved off and the cysteine immediately following the cleavage site is acylated, anchoring the protein to a membrane (Wu, 1996).

One unusual aspect of FibA and many of the newly identified putative ECM proteins is the presence of a lipoprotein secretion signal. The *M. xanthus* proteome is particularly enriched in proteins predicted to have lipoprotein secretion signals, including about 1500 of the approximate 7500 predicted proteins (~21%, unpublished). Of the putative ECM-associated proteins identified in this study, 13 of the 21 (62%) are predicted to have lipoprotein secretion signals. The fact that many of these putative ECM proteins have lipoproteins signals is contradictory. The main purpose of acylation following signal peptide cleavage is to anchor a protein to one of the membranes (Wu, 1996). This would seemingly preclude protein export to the extracellular medium, but immunogold labeling has shown that FibA is associated with the ECM (Behmlander and Dworkin, 1991). FibA is also associated with the inner membrane (Simunovic *et al.*, 2003). The key to this conundrum may lie in the different forms of FibA.

The FibA protein contains the lipoprotein secretion signal, a pro-domain often found with proteases that prevents catalytic activity until which time the activity is needed and pro-domain is removed, the catalytic domain, and two PPC domains (Bonner *et al.*, 2006; Kearns *et al.*, 2002). PPC domains are repeated domains of unknown function in bacteria, though in

eukaryotes they are thought to determine target protein specificity (Overall, 2002). In Western blots using αFibA antibody against purified ECM, FibA is found processed into many different forms, though it is unclear where the processing sites are located (Bonner *et al.*, 2006; Kearns *et al.*, 2002). FibA active site mutants become processed as well, suggesting another protease is involved (Bonner *et al.*, 2006). However, the same antibody used in Western blots against the inner membrane fraction shows FibA only in one form (Simunovic *et al.*, 2003), most likely the protein missing the signal peptide. It is possible that targeting of the protein to the membrane via the fatty acid holds it in an inactive state until such time as it is secreted and processed.

FibA production (unpublished) and ECM polysaccharide biosynthesis are only partially regulated transcriptionally (Lu *et al.*, 2005); much of the regulation appears to be post-translational, suggesting that ECM biogenesis is held at a level of readiness to respond to the two types of stimulatory factors: starvation and cell-cell proximity. In the case of starvation, ECM biogenesis begins almost immediately after nutrient depletion (Lu *et al.*, 2005). It is plausible that membrane anchoring of ECM proteins holds them in a state of readiness for secretion at a moment's notice, suggesting an important role for membrane anchoring. This hypothesis provides a rich area of future study in the role of Type II secretion and lipoprotein secretion signals in ECM proteins.

One possibility is that Type II secretion may not be involved in exporting ECM proteins, and the proteins are secreted by another fashion, possibly cell lysis or blebbing. Lipids are components of some biofilms (Pirog *et al.*, 2004) and acylation of ECM proteins may provide a method of anchoring them to the ECM. The method of ECM isolation using SDS lysis performed in this study would not preserve lipid components of the ECM. Disrupting genes encoding Type II secretion proteins and tracking the fate of ECM proteins may reveal if Type II

secretion is necessary for ECM protein export. FibA is an obvious target given that is has a putative lipoprotein secretion signal, an antibody and previous research on targeting and characterization. However, genetically disrupting Type II secretion may prove fatal to the organism. An alternate methodology would be to alter secretion signals of FibA and tracking what affect that has on export. The secretion signal of FibA can be replaced with that of a non-lipoprotein signal. Additionally, adding a C-terminal membrane anchor could permanently attach FibA to the membrane. These three constructs could not only reveal how Type II secretion functions in ECM protein export, but also how the lipoprotein signal itself functions in this process.

**Concluding thoughts.**

The extracellular matrix of *M. xanthus* is a rich area for study, particularly for signaling. It houses at least part of the self-recognition chemotaxis pathway, FibA-mediated factors for development and a pool of proteins of unknown function. By studying the matrix space and components in greater detail, it may be possible to reveal new methods of intercellular communication that help drive a population of cells into an actual community.

**References**

Anderson, D.J., Gage, F.H., and Weissman, I.L. (2001) Can stem cells cross lineage boundaries? *Nat Med* **7**: 393-395.

Arnold, J.W., and Shimkets, L.J. (1988a) Inhibition of cell-cell interactions in *Myxococcus xanthus* by Congo red. *J Bacteriol* **170**: 5765-5770.

Arnold, J.W., and Shimkets, L.J. (1988b) Cell surface properties correlated with cohesion in *Myxococcus xanthus*. *J Bacteriol* **170**: 5771-5777.

Behmlander, R.M., and Dworkin, M. (1991) Extracellular fibrils and contact-mediated cell interactions in *Myxococcus xanthus*. *J Bacteriol* **173**: 7810-7820.

Black, W.P., Xu, Q., and Yang, Z. (2006) Type IV pili function upstream of the Dif chemotaxis pathway in *Myxococcus xanthus* EPS regulation. *Mol Microbiol* **61**: 447-456.

Bode, H.B., Ring, M.W., Kaiser, D., David, A.C., Kroppenstedt, R.M., and Schwar, G. (2006) Straight-chain fatty acids are dispensable in the myxobacterium *Myxococcus xanthus* for vegetative growth and fruiting body formation. *J Bacteriol* **188**: 5632-5634.

Bonner, P.J., Xu, Q., Black, W.P., Li, Z., Yang, Z., and Shimkets, L.J. (2005) The Dif chemosensory pathway is directly involved in phosphatidylethanolamine sensory transduction in *Myxococcus xanthus*. *Mol Microbiol* **57**: 1499-1508.

Bonner, P.J., Black, W.P., Yang, Z., and Shimkets, L.J. (2006) FibA and PilA act cooperatively during fruiting body formation of *Myxococcus xanthus*. *Mol Microbiol* **61**: 1283-1293.

Branda, S.S., Vik, S., Friedman, L., and Kolter, R. (2005) Biofilms: the matrix revisited. *Trends Microbiol* **13**: 20-26.

Chang, B.Y., and Dworkin, M. (1996) Mutants of *Myxococcus xanthus dsp* defective in fibril binding. *J Bacteriol* **178**: 697-700.

Curtis, P.D., Geyer, R., White, D.C., and Shimkets, L.J. (2006) Novel lipids in *Myxococcus xanthus* and their role in chemotaxis. *Environ Microbiol* **8**: 1935-1949.

Davies, D.G., Parsek, M.R., Pearson, J.P., Iglewski, B.H., Costerton, J.W., and Greenberg, E.P. (1998) The involvement of cell-to-cell signals in the development of a bacterial biofilm. *Science* **280**: 295-298.

Dickschat, J.S., Bode, H.B., Kroppenstedt, R.M., Muller, R., and Schulz, S. (2005) Biosynthesis of iso-fatty acids in myxobacteria. *Org Biomol Chem* **3**: 2824-2831.

Domka, J., Lee, J., Bansal, T., and Wood, T.K. (2007) Temporal gene-expression in *Escherichia coli* K-12 biofilms. *Environ Microbiol* **9**: 332-346.

Dworkin, M. (1972) The myxobacteria: new directions in studies of procaryotic development. *Crit. Rev. Microbiol.* **2**: 435-452.

Dworkin, M., and Eide, D. (1983) *Myxococcus xanthus* does not respond chemotactically to moderate concentration gradients. *J Bacteriol* **154**: 437-442.

Fiegna, F., and Velicer, G.J. (2005) Exploitative and hierarchical antagonism in a cooperative bacterium. *PLoS Biol* **3**: e370.

Filloux, A. (2004) The underlying mechanisms of type II protein secretion. *Biochim Biophys Acta* **1694**: 163-179.

Higgs, P.I., Cho, K., Whitworth, D.E., Evans, L.S., and Zusman, D.R. (2005) Four unusual two-component signal transduction homologs, RedC to RedF, are necessary for timely development in *Myxococcus xanthus*. *J Bacteriol* **187**: 8191-8195.

Iizuka, T., Jojima, Y., Fudou, R., Hiraishi, A., Ahn, J.W., and Yamanaka, S. (2003) *Plesiocystis pacifica* gen. nov., sp. nov., a marine myxobacterium that contains dihydrogenated menaquinone, isolated from the Pacific coasts of Japan. *Int J Syst Evol Microbiol* **53**: 189-195.

Kearns, D.B., and Shimkets, L.J. (1998) Chemotaxis in a gliding bacterium. *Proc Natl Acad Sci U S A* **95**: 11957-11962.

Kearns, D.B., Venot, A., Bonner, P.J., Stevens, B., Boons, G.-J., and Shimkets, L.J. (2001) Identification of a developmental chemoattractant in *Myxococcus xanthus* through metabolic engineering. *Proc Natl Acad Sci U S A* **98**: 13990-13994.

Kearns, D.B., Bonner, P.J., Smith, D.R., and Shimkets, L.J. (2002) An extracellular matrix-associated zinc metalloprotease is required for dilauroyl phosphatidylethanolamine chemotactic excitation in *Myxococcus xanthus*. *J Bacteriol* **184**: 1678-1684.

Kroos, L., Kuspa, A., and Kaiser, D. (1986) A global analysis of developmentally regulated genes in *Myxococcus xanthus*. *Dev Biol* **117**: 252-266.

Kuspa, A., Plamann, L., and Kaiser, D. (1992a) A-signalling and the cell density requirement for *Myxococcus xanthus* development. *J Bacteriol* **174**: 7360-7369.

Kuspa, A., Plamann, L., and Kaiser, D. (1992b) Identification of heat-stable A-factor from *Myxococcus xanthus*. *J Bacteriol* **174**: 3319-3326.

Lancero, H., Brofft, J.E., Downard, J., Birren, B.W., Nusbaum, C., Naylor, J., Shi, W., and Shimkets, L.J. (2002) Mapping of *Myxococcus xanthus* social motility *dsp* mutations to the *dif* genes. *J Bacteriol* **184**: 1462-1465.

Li, S., Lee, B.U., and Shimkets, L.J. (1992) *csgA* expression entrains *Myxococcus xanthus* development. *Genes Dev* **6**: 401-410.

Li, Y., Lux, R., Pelling, A.E., Gimzewski, J.K., and Shi, W. (2005) Analysis of type IV pilus and its associated motility in *Myxococcus xanthus* using an antibody reactive with native pilin and pili. *Microbiology* **151**: 353-360.

Lu, A., Cho, K., Black, W.P., Duan, X.Y., Lux, R., Yang, Z., Kaplan, H.B., Zusman, D.R., and Shi, W. (2005) Exopolysaccharide biosynthesis genes required for social motility in *Myxococcus xanthus*. *Mol Microbiol* **55**: 206-220.

Manting, E.H., and Driessen, A.J. (2000) *Escherichia coli* translocase: the unravelling of a molecular machine. *Mol Microbiol* **37**: 226-238.

O'Connor, K.A., and Zusman, D.R. (1991a) Behavior of peripheral rods and their role in the life cycle of *Myxococcus xanthus*. *J Bacteriol* **173**: 3342-3355.

O'Connor, K.A., and Zusman, D.R. (1991b) Analysis of *Myxococcus xanthus* cell types by two-dimensional polyacrylamide gel electrophoresis. *J Bacteriol* **173**: 3334-3341.

O'Connor, K.A., and Zusman, D.R. (1991c) Development in *Myxococcus xanthus* involves differentiation into two cell types, peripheral rods and spores. *J Bacteriol* **173**: 3318-3333.

Overall, C.M. (2002) Molecular determinants of metalloproteinase substrate specificity: matrix metalloproteinase substrate binding domains, modules, and exosites. *Mol Biotechnol* **22**: 51-86.

Pirog, T.P., Kovalenko, M.A., Kuz'minskaia Iu, V., and Votselko, S.K. (2004) [Physicochemical properties of the microbial exopolysaccharide ethapolan synthesized on a mixture of growth substrates]. *Mikrobiologiia* **73**: 19-24.

Qualls, G.T., and White, D. (1982) Developmental cell cohesion in *Stigmatella aurantiaca*. *Archives of Microbiology* **131**: 334-337.

Rhie, H.G., and Shimkets, L.J. (1989) Developmental bypass suppression of *Myxococcus xanthus csgA* mutations. *J Bacteriol* **171**: 3268-3276.

Rosenberg, E., Keller, K.H., and Dworkin, M. (1977) Cell density-dependent growth of *Myxococcus xanthus* on casein. *J Bacteriol* **129**: 770-777.

Simunovic, V., Gherardini, F.C., and Shimkets, L.J. (2003) Membrane localization of motility, signaling, and polyketide synthetase proteins in *Myxococcus xanthus*. *J Bacteriol* **185**: 5066-5075.

Smith, D.R., and Dworkin, M. (1994) Territorial interactions between two *Myxococcus* Species. *J Bacteriol* **176**: 1201-1205.

Stanley, N.R., Britton, R.A., Grossman, A.D., and Lazazzera, B.A. (2003) Identification of catabolite repression as a physiological regulator of biofilm formation by *Bacillus subtilis* by use of DNA microarrays. *J Bacteriol* **185**: 1951-1957.

Sutherland, I.W. (2001) The biofilm matrix--an immobilized but dynamic microbial environment. *Trends Microbiol* **9**: 222-227.

Toal, D.R., Clifton, S.W., Roe, B.A., and Downard, J. (1995) The *esg* locus of *Myxococcus xanthus* encodes the E1α and E1β subunits of a branched-chain keto acid dehydrogenase. *Mol Microbiol* **16**: 177-189.

Ueki, T., and Inouye, S. (2006) A novel regulation on developmental gene expression of fruiting body formation in myxobacteria. *Appl Microbiol Biotechnol* **72**: 21-29.

Wang, X., and Tournier, C. (2006) Regulation of cellular functions by the ERK5 signalling pathway. *Cell Signal* **18**: 753-760.

White, D. (1993) Myxospore and fruiting body morphogenesis. In *Myxobacteria II*. Dworkin, M. and Kaiser, D. (eds). Washington, D.C.: American Society for Microbiology, pp. 307-332.

Whiteley, M., Bangera, M.G., Bumgarner, R.E., Parsek, M.R., Teitzel, G.M., Lory, S., and Greenberg, E.P. (2001) Gene expression in *Pseudomonas aeruginosa* biofilms. *Nature* **413**: 860-864.

Wireman, J.W., and Dworkin, M. (1975) Morphogenesis and developmental interactions in myxobacteria. *Science* **189**: 516-523.

Wireman, J.W., and Dworkin, M. (1977) Developmentally induced autolysis during fruiting body formation by *Myxococcus xanthus*. *J Bacteriol* **129**: 798-802.

Wu, H.C. (1996) Biosynthesis of lipoproteins. In *In Escherichia coli and Salmonella: Cellular and Molecular Biology*. Vol. 1. Neidhardt, F.C. (ed). Washington D.C.: American Society for Microbiology Press, pp. 1005-1014.

Wu, S.S., and Kaiser, D. (1996) Markerless deletions of *pil* genes in *Myxococcus xanthus* generated by counterselection with the *Bacillus subtilis sacB* gene. *J Bacteriol* **178**: 5817-5821.

Wu, S.S., Wu, J., and Kaiser, D. (1997) The *Myxococcus xanthus pilT* locus is required for social gliding motility although pili are still produced. *Mol Microbiol* **23**: 109-121.

Yang, Z., Ma, X., Tong, L., Kaplan, H.B., Shimkets, L.J., and Shi, W. (2000) *Myxococcus xanthus dif* genes are required for biogenesis of cell surface fibrils essential for social gliding motility. *J Bacteriol* **182**: 5793-5798.

# APPENDIX A

# SPATIAL ORGANIZATION OF *MYXOCOCCUS XANTHUS* DURING FRUITING BODY FORMATION

*Myxococcus xanthus* is a soil-dwelling δ-proteobacterium that preys on other bacteria for carbon and energy. To facilitate predation, *M. xanthus* travels in swarms to increase the local concentration of secreted lytic enzymes (Rosenberg *et al.*, 1977). When swarms become starved, approximately 50,000 cells direct their movement into in a large, multicellular fruiting body, wherein cells differentiate into metabolically dormant myxospores. Fruiting body development requires the coordination of both temporal and spatial processes within a population of cells. Much of the research in the field is devoted to signaling mechanisms governing temporal coordination of development [for review see (Dworkin, 1996; Shimkets, 1999)]. However, little is known about how *M. xanthus* cells spatially create a fruiting body, prompting famed myxobacteriologist Martin Dworkin to write, "Morphogenesis, in its literal sense, is the aspect of development that has most eluded the efforts of developmental biologists. Understanding of the one-dimensional nature of the genomic program has not led to an understanding of three-dimensional macroscopic structure. This is ironic in the sense that it is the three-dimensional structure of the myxobacterial fruiting body that initially captured the interest of most myxobacteriologists" (Dworkin, 1996).

Fruiting body structures can vary from the simple mounds of *M. xanthus* and *M. fulvus*, to the complex tree-like structures of *Stigmatella aurantiaca* and *Chondromyces crocatus* (pictures of which can be seen in (Dworkin, 1996)). Experiments examining aspects of fruiting body morphogenesis have used tracking of fluorescently labeled cells to follow their movement in the fruiting body. Many studies focused on the lowest layer of cells in contact with the substrate. Data from these studies were used to generate mathematical models of motile behavior. One study suggests that developing rods in outer, high-density regions of fruiting bodies move with sufficient force to displace spores and spore precursors to an inner domain, thereby localizing

spores in the core of the structure (Sager and Kaiser, 1993). In other studies, it was modeled that streams of *M. xanthus* cells collide with one another, forming "traffic jams" that create the nucleus for aggregation centers, and continued streaming around the aggregation centers leads to a three dimensional mound structure (Sozinova *et al.*, 2005, 2006). One study found that cells entering an aggregation center suffered a reduction in velocity, and mathematical modeling showed that the velocity reduction was sufficient to retain cells in an aggregation center, essentially capturing cells to fill a fruiting body (Sliusarenko *et al.*, 2007). These studies help explain how cells accumulate in aggregation centers, yet none adequately explain how cells transition from two dimensional alignment along the agar surface into the more complicated fruiting body structures.

Unlike previous studies that focused on events at the base of the fruiting body, this study examined fruiting body formation from the top using microcinematography. Strains of *M. xanthus* were grown in CYE broth [1.0% Bacto Casitone, 0.5% Difco yeast extract, 10 mM 3-[*N*-morpholino]propanesulfonic acid (MOPS), pH 7.6 and 0.1% $MgSO_4$ (Campos *et al.*, 1978)] at 32$^{o}$C. Cells were harvested by centrifugation at 12,000 x g for 5 minutes and resuspended to a density of 5 x $10^8$ cells $ml^{-1}$ in CYE broth. An airspace-containing microscope chamber was prepared (protocol provided by Roy Welch). A sterile 0.5-mm-thick silicone rubber gasket (Grace Biolabs, Bend, Oreg.) was placed on top of a flame-sterilized 25 x 25 mm glass microscope coverslip, creating a small well. The well was filled with 0.4 ml molten TPM agarose [10 mM Tris (hydroxymethyl) aminomethane HCl, 8 mM $MgSO_4$, 1 mM $KHPO_4$-$KH_2PO_4$, 1.0% low melting agarose (Bio Rad), pH 7.6] and a flame-sterilized glass microscope slide was placed on top to create a flat agar surface. Once the agarose had cooled, the slide was removed and 0.5 μl of cell culture was spotted on the surface and allowed to dry. A second

gasket was placed on top of a sterilized microscope slide. The two gaskets were joined and gently pressed to seal the chamber. The cell spot was viewed on a Leitz Laborlux D phase contrast microscope under 160X magnification. Chamber temperature was maintained at 32$^{o}$C using a Biostage 600 stage warmer (20/20 Technology, Inc.). Photographs were taken every 5 minutes for 48 hours with a Spot Insight 2 camera using the Spot Software v4.5 (Diagnostic Instruments Inc.), and movies were compiled from the images using Quicktime Pro software (Apple). Each strain in the study was analyzed in triplicate.

The behavior of wild-type *M. xanthus* (DK1622, (Kaiser, 1979)) cells can be divided into three distinct phases (Figure A-1). In the first phase, an initial wave of motile activity leads to the formation of smooth and relatively-stable cell mattes. Cells haphazardly stacked during the drying process (Figure A-1A) rearrange themselves into swarms, wherein cells are longitudinally aligned (Figure A-1B). After approximately 6-8 hours the second phase begins dramatically with a burst of motile activity, leading to the formation of many small cell towers (microaggregation centers), only a few cell layers thick, that shift, merge and split from one another (Figure A-1C). Shortly after the burst of activity, macroaggregation centers are observed (Figure A-1D) that begin to fill with cells dispersing from the small towers. The macroaggregation centers build into fruiting bodies by a process of "tiering" (Figure A-1E, Figure A-2). Cells emerge from a consistent spot somewhere near the center of a layer of cells and expand over the layer in an even matte, forming a top layer. Cells then emerge from the same consistent spot in the top layer (now the new bottom layer), again spreading in an even matte. At the same time as new layers are formed, the bottom layers continue to expand so that the entire structure resembles a circular steppe pyramid. In WT fruiting bodies, the tiering can only be observed for a short period of time before the mass becomes covered by a cap composed

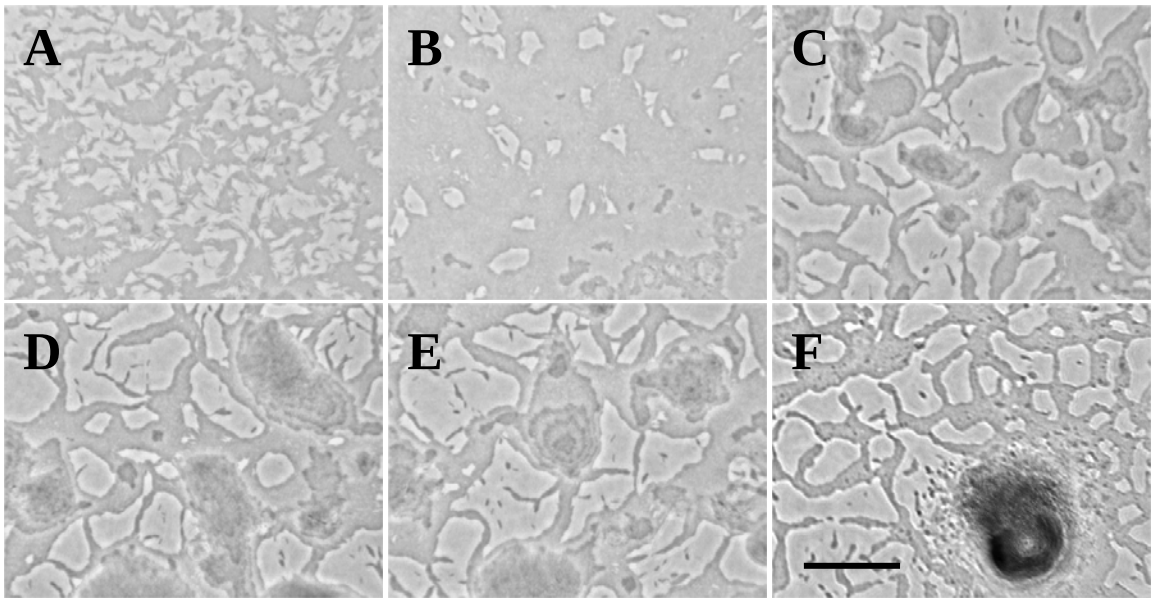


**Figure A-1.** Stages of fruiting body formation in wild type *M. xanthus*. A. Initial disorganization of cells after spotting on agarose surface (0 minutes). B. Rearrangement of cells into mattes (250 minutes). C. Microaggregation centers are towers of cells only a few cell layers thick (570 minutes). D. Macroaggregation centers are larger towers of cells composed of several cell layers (690 minutes). E. Macroaggregation center displaying tiering of the cell layers, tiering is seen briefly in WT fruiting bodies (620 minutes). F. Finished fruiting body. The dark color indicates sporulation has occurred (48 hours). Bar = 0.1 mm.

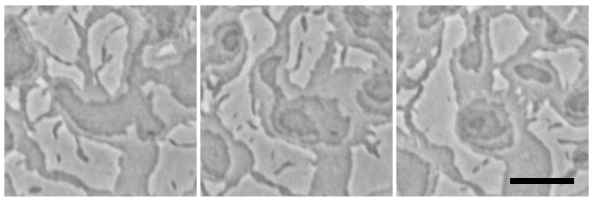

**Figure A-2.** Formation of an aggregation center by tiering. Cells erupt from the center of a cell matte and spread in an even layer (or tier). As that layer expands, another tier forms on top of it originating at the same position as the previous tier. Two tier formations are shown. Minutes 515-525 of the same field shown, 5 minutes between each frame, left to right. Bar = 0.05 mm.

of ECM material (Behmlander and Dworkin, 1991, 1994; Lu *et al.*, 2005). This second phase lasts approximately 8 hours. The last phase consists of fruiting body maturation. The fruiting bodies darken (an indication of sporulation) and cells outside the fruiting body begin to disappear (Figure A-1F).

The tiering of cell layers indicates that the fruiting body is constructed layer by layer from the bottom up. It is possible that a tube exists within the aggregate perpendicular to the agar surface so that cells travel up the tube and emerge from a consistent point from the top. Aggregates that abort development use the reverse process and disassemble a fruiting body from the top down. These observations not only suggest a central tube mechanism for building the tiers, but also that the tube is maintained within the tier for at least a portion of fruiting body formation.

To determine if the pattern formation observed in wild-type *M. xanthus* is seen in other fruiting body-capable strains, a Δ*pilA* (Wu *et al.*, 1997) strain was analyzed. PilA forms the Type IV pilus filament. Pili in *M. xanthus* are used for social (S) motility (Li *et al.*, 2005; Lu *et al.*, 2005), where the pilus extends, attaches onto an adjacent cell, likely the extracellular matrix (ECM) (Li *et al.*, 2003), and retracts to pull the cell forward. The ECM is a polysaccharide and protein material secreted during starvation (Behmlander and Dworkin, 1991; Lu *et al.*, 2005). *pilA* mutants form no pili and cannot use S motility, but are motile using adventurous (A) motility. A motility is the movement of individual cells in a non-cell-contact dependent fashion; the exact mechanism of A motility is unknown. *pilA* mutants produce little ECM (Black *et al.*, 2006), but are able to form fruiting bodies and sporulate as well as WT (Bonner *et al.*, 2006).

Though the loss of S motility results in a longer fruiting body formation process, the same phases observed in WT development are seen in development of the *pilA* strain (Figure A-

3). Initial activity to arrange cells into relatively stable mattes (Figure A-3AB) is followed by the burst of activity and microaggregation/macroaggregation center formation (Figure A-3C). The burst of activity is subdued compared to WT, likely stemming from the reduced motility rate, but the activity is observed approximately 7-8 hours after plating, same as WT. The cap structures observed in WT development are absent at this stage (possibly due to lack of ECM), allowing an unobstructed view of tiering (Figure A-4). The central tube is not a rigid structure because its position can migrate slightly from layer to layer (Figure A-4). Occasionally a second origin point is observed within the same layer (Figure A-3D), though this is uncommon. Eventually a cap structure is formed and the third phase (sporulation) begins (Figure A-3E).

The *pilA* mutant lacks pili, S motility, and ECM, so *pilA* cells interact with one another in fundamentally different ways than WT cells. Yet the same phases and patterns observed in WT development are seen in the *pilA* mutant, implying that the underlying mechanism of fruiting body formation is conserved.

Also tested was a *fibA* mutant strain. FibA is an ECM associated zinc-metalloprotease implicated in lipid chemotaxis (Kearns *et al.*, 2002). *fibA pilA* mutants do not develop, indicating that FibA mediates a developmental process that compliments PilA (Bonner *et al.*, 2006). Pattern formation in the *fibA* mutant closely resembles that of wild type *M. xanthus* (data not shown), indicating that the FibA-mediated development uses the same tiering mechanism.

As stated above, many of the published models for spatial organization during fruiting body formation do not explain the more complex fruiting bodies formed by other myxobacteria. Observations from this study may suggest new avenues of research to address the gaps in previous models. The tiering observed in this study may offer an explanation for stalk formation in complex fruiting bodies. *M. xanthus* does not produce a stalk. Yet, one can see how

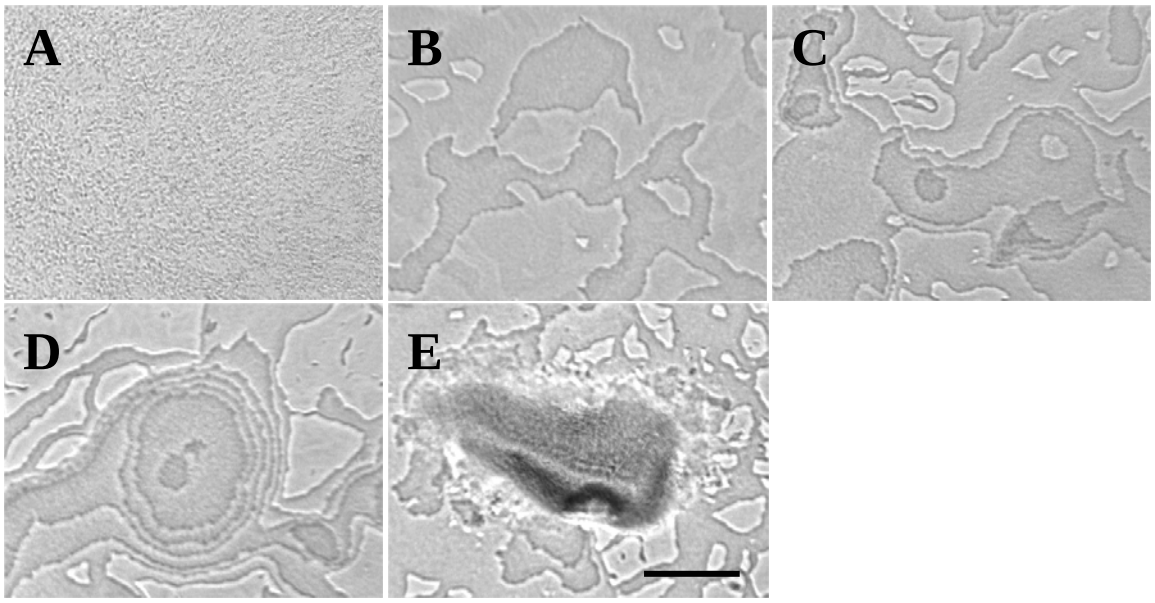


**Figure A-3.** Stages of fruiting body formation in the *pilA* mutant. A. Initial disorganization of cells after spotting on agarose surface (0 minutes). B. Rearrangement of cells into mattes (425 minutes). C. Microaggregation center formation is less robust in the *pilA* mutant than WT, with fewer centers formed and only 3-4 cell layers thick (550 minutes). D. *pilA* macroaggregation centers persist longer uncapped, clearly displaying the tiers. Shown here is a macroaggregation center with two origins for new tiers, not often observed (725 minutes). F. Finished fruiting body. *pilA* mutant fruiting bodies are often less compact and spheroid compared to WT fruiting bodies (48 hours). Bar = 0.1 mm.

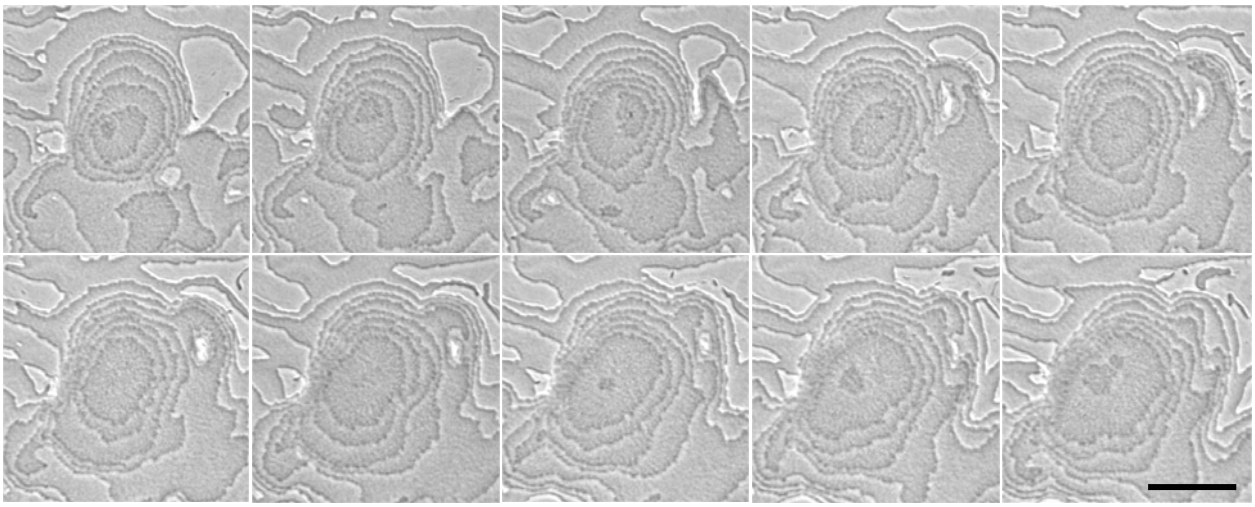

**Figure A-4.** Tier formation during *pilA* fruiting body development. The lack of a cap structure allows clear viewing of tiers. The tier origin point migrates slightly suggesting it is not a rigid structure. Two tier formations in the same fruiting body are shown (minutes 620-710, 10 minutes between frames). Bar = 0.1 mm.

extrapolating the tiering process for a longer period of time would allow for longer and longer fruiting body extensions away from the surface strata, thereby producing a stalk. Microcinematographic observation of other myxobacterial strains that produce prominently stalked fruiting bodies may illuminate this hypothesis.

While tiering can explain the vertical ascension of fruiting bodies, it does not explain spheroid mound formation or sporangiole (spore filled sac) formation observed at the tips of branched fruiting bodies. This behavior may be explained by the fruiting body cap. The cap appears to be a large cover over the entire fruiting body, as if a blanket has been thrown over the structure, and may be the high-density region mentioned previously. The smooth appearance of the cap and the high-density nature postulated indicates that the cap is composed of ECM. The cap may act as a mesh over the aggregation center such that as cells enter the structure from the bottom and move up through the tube they fill up the mesh. An analogy would be a balloon on an air spigot. As air (cells) passes through the spigot (central tube), the balloon (cap structure) inflates. Sporangioles may be balloons fixed to upper points on stalks. In this regard, the timing of ECM biogenesis would govern the timing of mound formation, as early ECM production would lead to early cap formation and shorter stalks. By delaying ECM biogenesis it may be possible to induce stalk formation in *M. xanthus*.

**References**

Behmlander, R.M., and Dworkin, M. (1991) Extracellular fibrils and contact-mediated cell interactions in *Myxococcus xanthus*. *J Bacteriol* **173**: 7810-7820.

Behmlander, R.M., and Dworkin, M. (1994) Biochemical and structural analyses of the extracellular matrix fibrils of *Myxococcus xanthus*. *J Bacteriol* **176**: 6295-6303.

Black, W.P., Xu, Q., and Yang, Z. (2006) Type IV pili function upstream of the Dif chemotaxis pathway in *Myxococcus xanthus* EPS regulation. *Mol Microbiol* **61**: 447-456.

Bonner, P.J., Black, W.P., Yang, Z., and Shimkets, L.J. (2006) FibA and PilA act cooperatively during fruiting body formation of *Myxococcus xanthus*. *Mol Microbiol* **61**: 1283-1293.

Campos, J.M., Geisselsoder, J., and Zusman, D.R. (1978) Isolation of bacteriophage MX4, a generalized transducing phage for *Myxococcus xanthus*. *J Mol Biol* **119**: 167-178.

Dworkin, M. (1996) Recent advances in the social and developmental biology of the myxobacteria. *Microbiol Rev* **60**: 70-102.

Kaiser, D. (1979) Social gliding is correlated with the presence of pili in *Myxococcus xanthus*. *Proc Natl Acad Sci U S A* **76**: 5952-5956.

Kearns, D.B., Bonner, P.J., Smith, D.R., and Shimkets, L.J. (2002) An extracellular matrix-associated zinc metalloprotease is required for dilauroyl phosphatidylethanolamine chemotactic excitation in *Myxococcus xanthus*. *J Bacteriol* **184**: 1678-1684.

Li, Y., Sun, H., Ma, X., Lu, A., Lux, R., Zusman, D., and Shi, W. (2003) Extracellular polysaccharides mediate pilus retraction during social motility of *Myxococcus xanthus*. *Proc Natl Acad Sci U S A* **100**: 5443-5448.

Li, Y., Lux, R., Pelling, A.E., Gimzewski, J.K., and Shi, W. (2005) Analysis of type IV pilus and its associated motility in *Myxococcus xanthus* using an antibody reactive with native pilin and pili. *Microbiology* **151**: 353-360.

Lu, A., Cho, K., Black, W.P., Duan, X.Y., Lux, R., Yang, Z., Kaplan, H.B., Zusman, D.R., and Shi, W. (2005) Exopolysaccharide biosynthesis genes required for social motility in *Myxococcus xanthus*. *Mol Microbiol* **55**: 206-220.

Rosenberg, E., Keller, K.H., and Dworkin, M. (1977) Cell density-dependent growth of *Myxococcus xanthus* on casein. *J Bacteriol* **129**: 770-777.

Sager, B., and Kaiser, D. (1993) Spatial restriction of cellular differentiation. *Genes Dev* **7**: 1645-1653.

Shimkets, L.J. (1999) Intercellular signaling during fruiting-body development of *Myxococcus xanthus*. *Annu Rev Microbiol* **53**: 525-549.

Sliusarenko, O., Zusman, D.R., and Oster, G. (2007) Aggregation during fruiting body formation in *Myxococcus xanthus* is driven by reducing cell movement. *J Bacteriol* **189**: 611-619.

Sozinova, O., Jiang, Y., Kaiser, D., and Alber, M. (2005) A three-dimensional model of myxobacterial aggregation by contact-mediated interactions. *Proc Natl Acad Sci U S A* **102**: 11308-11312.

Sozinova, O., Jiang, Y., Kaiser, D., and Alber, M. (2006) A three-dimensional model of myxobacterial fruiting-body formation. *Proc Natl Acad Sci U S A* **103**: 17255-17259.

Wu, S.S., Wu, J., and Kaiser, D. (1997) The *Myxococcus xanthus pilT* locus is required for social gliding motility although pili are still produced. *Mol Microbiol* **23**: 109-121.

# APPENDIX B

## LIPASES IN *MYXOCOCCUS XANTHUS*

As a bacterial predator, *Myxococcus xanthus* obtains carbon and energy from its prey. Most of these molecules are locked into the prey cytoplasm but can be liberated with lipases, enzymes that hydrolyze the ester bonds between fatty acids and the glycerol backbone of membrane phospholipids. Lipases release free fatty acids, destroy the membrane, and empty the cytoplasmic contents of its prey. Additionally, fatty acids themselves are rich sources of energy for myxobacteria (Lau *et al.*, 2002; Loebeck and Klein, 1956). *M. xanthus* has a large number of genes that could encode lipases belonging to three main families.

GDSL lipases are a family of bacterial esterases with varied and different properties (Carinato *et al.*, 1998). Esterases cleave, and sometimes form, ester bonds. Esterases are active on either insoluble molecules, such as phospholipids, or on soluble compounds, such as nitrophenol-, naphthyl-, hydroxypyrene trisulfonic fatty acid esters and polymeric acyl-substituted compounds (Talker-Huiber *et al.*, 2003). There is very little overlap in the substrate specificites. It is difficult to determine if a newly identified GDSL esterase can hydrolyze membrane phospholipids from the primary amino acid sequence. Instead the protein must be purified and biochemically tested. Lipases only become active when in the presence of a water/oil interface (Turner, 1995). Such proteins are inactive against soluble compounds. GDSL esterases can be found in a number of plant and animal pathogens, including *Pseudomonas aeruginosa* (Martinez and Soberon-Chavez, 2001), *Salmonella typhimurium* (Carinato *et al.*, 1998), *Xanthomonas vesicatoria* (Talker-Huiber *et al.*, 2003) and *Legionella pneumophila* (Flieger *et al.*, 2002).

*M. xanthus* contains two GDSL lipase homologs (MXAN5500 and MXAN4569) that contain all the conserved residues of other GDSL proteins in approximately the same spacing (Figure B-1). It is speculated that GDSL esterases have a Ser-His-Asp catalytic triad (Wilhelm

*et al.*, 1999). However, it is not known which of the two conserved aspartates functions in catalysis. The N-terminal portion of the proteins can be variable in length; the function of this N-terminal excess is unknown. After the proteins have been secreted into the periplasm, the C-terminal sequences of the outer membrane esterases from *P. aeruginosa* and *S. typhimurium* enter the outer membrane facilitated by an aromatic residue as the last amino acid (Schulz, 2000). The C-terminal portion then forms an 11-14 stranded beta-barrel pore in the outer membrane (Loveless and Saier, 1997). It is speculated that this pore causes autotranslocation of the N-terminal catalytic domain to the outside of the cell where it is anchored in the membrane facing away from the cell's surface (Wilhelm *et al.*, 1999). An opposing theory holds that the beta-barrel domain anchors the protein in the outer membrane but never mediates translocation (Talker-Huiber *et al.*, 2003). This would result in the catalytic domain residing in the periplasm. Compounds commonly degraded by GDSL esterases are soluble but can readily pass through membranes, suggesting that the catalytic domain need not face the outside medium to hydrolyze substrates.

The *M. xanthus* homologs lack the C-terminal sequences, suggesting they are different from the other members of the family. However, EstA in *Burkholderia gladioli* also lacks the C-terminal domain but is anchored to the outer membrane by acylation at the N- terminus (Klingsbichel, 1996). The *M. xanthus* MXAN4569 has a cysteine residue after the putative signal sequence and is likely acylated, suggesting that MXAN4569 may be anchored to the outer membrane in the same fashion as EstA. MXAN5500 lacks the cysteine acylation residue. This protein may be anchored to the membrane in by another fashion, such as protein-protein interactions, or may be secreted into the extracellular medium. Deletion of MXAN4569 has no effect on aggregation or sporulation on TPM starvation agar, however on CF agar, aggregation

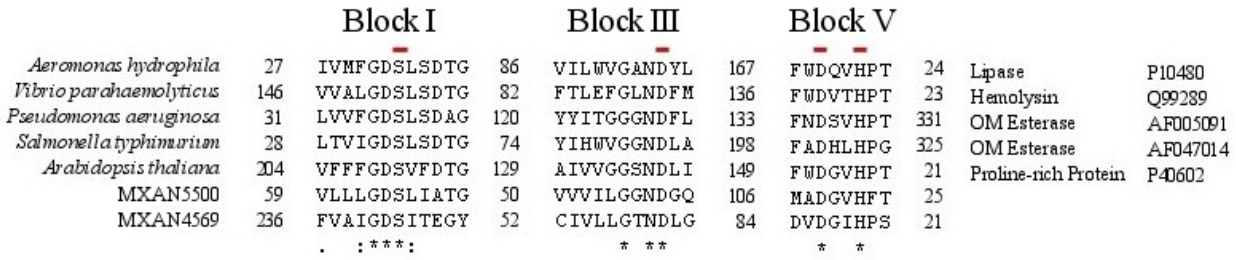


**Figure B-1.** Conserved sequence blocks in GDSL esterases. *Aeromonas hydrophila* GCAT: P10480. *Vibrio parahaemolyticus* LDH: Q99289. *Pseudomonas aeruginosa* EstA: AF005091. *Salmonella typhimurium* ApeE: AF047014. *Arabidopsis thaliana* APG: P40602. *Myxococcus xanthus* MXAN5500 and MXAN4569. Conserved catalytic site residues are marked with bars. Numbers between columns indicate number of amino acids between each block.

shows a mild fruiting body morphology defect and sporulation proceeds approximately 24 hours faster than WT (Moraleda-Munoz and Shimkets, 2007). MXAN4569 demonstrates activity towards substrates with small acyl chains.

Autoannotion of the *M. xanthus* genome indicates a number of homologs related to patatins, a family of proteins found in eukaryotes. The name derives from the fact that they are the major storage protein in the potato tuber, constituting up to 40% of the total soluble protein (Racusen and Foote, 1980). These proteins have non-specific acyl hydrolase activity towards multiple substrates, including mono- and diacyl phospholipids, glycerolipids and long chain fatty acid esters (Galliard, 1971). They have the conserved G-X-S-X-G active site motif characteristic of hydrolases, and crystallography has shown that they have structural similarity to eukaryotic phospholipase $A_2$ ($PLA_2$) (Rydel *et al.*, 2003). *M. xanthus* has six genes annotated as patatins, but five are either missing or have a mis-located conserved oxyanion hole (G-G-X-R) required for catalysis. However, MXAN3852 the conserved catalytic site motif, oxyanion hole, and a number of aspartate residues that could serve as the other half of the Ser-Asp catalytic dyad. It also contains the conserved His109, a residue important for structural integrity (Rydel *et al.*, 2003). MXAN3852 is only expressed during starvation. Deletion of MXAN3852 results in no aggregation or sporulation defect on TPM agar, but on CF agar there is a 24 hour delay to both aggregation and sporulation, and the fruiting bodies are unusually large and amorphous (Moraleda-Munoz and Shimkets, 2007).

Patatins are thought to be inactive against membrane phospholipids as they do not demonstrate interface activation due to the absence of a flexible lid region over the active site (Rydel *et al.*, 2003). In eukaryotic $PLA_2$, a helix covers the lipase active site; the hydrophobic side facing the active site and the hydrophilic side facing the solution. When the enzyme

encounters a membrane, the lid flips open so that the hydrophobic side of the helix becomes exposed to the phospholipids, forming the basis of interface activation. Patatins lack this flexible lid and thus do not become activated by the interface, indicating that they can act only on lipids that have become solubilized, such as in the small intestine. Therefore it is unsurprising that MXAN3852 demonstrates hydrolase activity towards substrates with shorter acyl chains, making them more soluble (Moraleda-Munoz and Shimkets, 2007).

The third family of lipases represented in the *M. xanthus* genome is the alpha/beta hydrolase group, characterized by an eight-stranded beta sheet formed of two antiparallel beta strands followed by six parallel beta strands (Ollis *et al.*, 1992). The beta sheet is stabilized by intervening alpha helices, and interface activation is achieved by the same flexible hinge region as described for the patatins. The alpha-beta hydrolase fold is the major fold for most bacterial lipases. Unfortunately, much the same as GDSL esterases, alpha/beta hydrolases are active against many other substrates and the catalytic domain is common to many other enzymes, most notably proteases. Therefore, the activity of individual putative lipases must be determined biochemically.

*M. xanthus* has at least six proteins that significantly match the pfam for alpha/beta hydrolases and have the conserved active site motif of G-X-S-X-G. Two of these proteins are likely lipases. MXAN5522 has significant identity to triacyl glycerol lipases from organisms such as *Pseudomonas mendocina* (57% identical, 71% similar), *P. aeruginosa* (58% identical, 71% similar) and *Acinetobacter calcoaceticus* (47% identical, 63% similar). Triacyl glycerol lipases cleave ester bonds on all three positions of phospholipids. Bacterial alpha/beta hydrolases are divided into two primary groups based on the codon encoding the catalytic serine (AGY or TCN) (Anthonsen *et al.*, 1995). MXAN5522 falls into the first group; the catalytic

serine codon is AGC. This first group is further divided into four sub-groups. The first sub-group is characterized by Xcp-dependent secretion and the presence of the lipase chaperone in an operon with the lipase itself. The chaperone functions in proper folding of the lipase in the periplasm; without proper folding, the lipase is not secreted into the extracellular medium. MXAN5522 falls into this first sub-group as it is separated by 27 base pairs from MXAN5523, encoding a lipase chaperone. Separations up to 35 base pairs between lipases and their cognate chaperones is not uncommon (Sullivan *et al.*, 1999). Conserved active site residues are found in the MXAN5522 (Figure B-2), in addition to two Asp residues conserved for coordinating a $Ca^{2+}$ ion. Both the *M. xanthus* lipase and lipase chaperone have strong predicted signal secretion sequences, and the lipase chaperone has a predicted transmembrane helix at the N-terminus used to anchor lipase chaperones to the inner membrane. The evidence suggests that this predicted lipase is strongly related to other well characterized bacterial lipases.

MXAN5522 is expressed during both vegetative growth and development, but demonstrates a sharp spike in expression 24 hours after starvation (Moraleda-Munoz and Shimkets, 2007). Deletion of MXAN5522 results in a 3-fold increase in spore yield on both TPM and CF, and the mutant aggregates 24 hours faster than WT on CF agar. This mutant may be unable to utilize triacyl-glycerol storage lipids for energy, thereby starving faster than WT, causing it to proceed through development faster. However, like the two previous lipases tested, MXAN5522 also prefers substrates with shorter acyl chains (Moraleda-Munoz and Shimkets, 2007).

The second likely alpha/beta lipase is MXAN4638. This predicted protein is closely related to characterized lysophospholipases from *Leptospira interrogans* (29% identical, 50% similar) and *Mycobacterium bovis* (30% identical, 44% similar). Lysophospholipases are

general lipases, cleaving fatty acids from phospholipids that have at least one fatty acid removed (lysophospholipids). Disruption of the gene upstream and operonic with MXAN4638 generates an A motility defect (Youderian *et al.*, 2003). Other putative alpha/beta hydrolases in *M. xanthus* have no significant homologies to characterized alpha/beta lipases, but match the pfam above the cut-off. Therefore, they may be hydrolases and/or lipases, but can only be determined biochemically.

It is interesting to note that all of the putative lipases described are predicted to lack regiospecificity. Many well-characterized lipases, especially eukaryotic lipases, specifically hydrolyze fatty acids from one position on the glycerol backbone. These lipases often serve other functions besides lipid degradation. Eukaryotic $PLA_2$ is well studied and has been tied to the release of lipid hormones and the inflammation response (Farooqui *et al.*, 2000). Conversely, lipase activity in *M. xanthus* is predicted to release fatty acids mainly for metabolic purposes instead of signaling capacities. Utilizing general lipases instead of two regiospecific lipases may be more efficient.

The study of these lipases may have further implications other than metabolism. LipA in *Acinetobacter* sp. RAG-1 is expressed when the culture enters stationary phase, suggesting a role for this enzyme in the starvation response (Snellman *et al.*, 2002). Lipases in *M. xanthus* may be tied to starvation and therefore development. LipC in *P. aeruginosa* is dependent on the presence of the lipase chaperone LipB (Martinez *et al.*, 1999). In a random mutagenesis screen, two mutations were found to increase expression from the LipC promoter: *pilX* and *pilY1* (Martinez *et al.*, 1999). Proteins encoded by these genes are involved in pilus biogenesis, a necessary component of biofilm formation in *P. aeruginosa*. This result suggests that there may be connections between pilus synthesis, lipase expression, and biofilm formation. Lipases, as

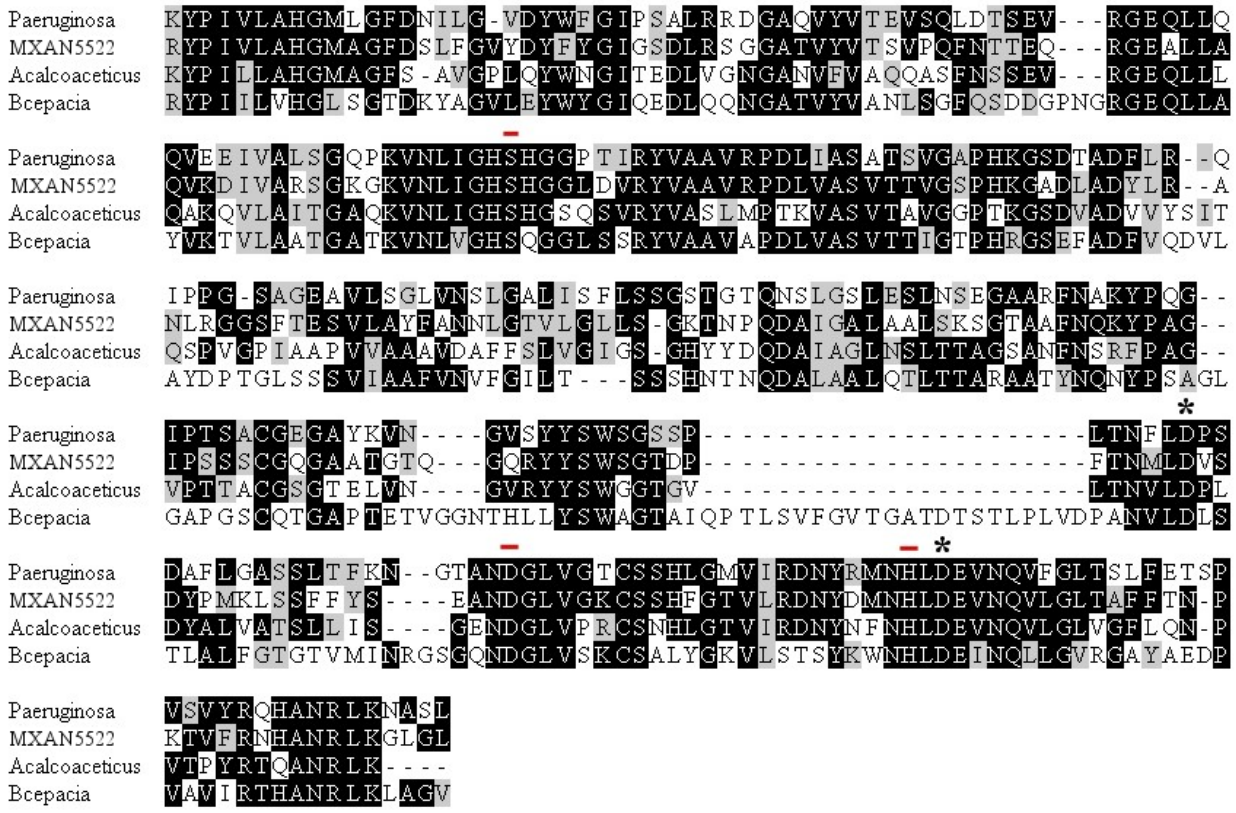


**Figure B-2.** Comparison of MXAN5522 to known Group I proteobacterial lipases. *Pseudomonas aeruginosa* LipA: P26876 (Paeruginosa). *Myxococcus xanthus* MXAN5522 (MXAN5522). *Acinetobacter calcoaceticus* LipA: AF047691 (Acalcoaceticus). *Burkholderia capacia* LipA: P22088 (Bcepacia). Conserved catalytic site residues are marked with bars. Conserved aspartate residues required for coordination of a $Ca^{2+}$ ion are marked with asterisks.

devastating toxic enzymes, are likely intimately tied to population sensing and predator-prey relationships. The study of lipases may lead to greater understanding of the behavior of *M. xanthus* and other biofilm-forming predatory bacteria.

**References**


Anthonsen, H.W., Baptista, A., Drablos, F., Martel, P., Petersen, S.B., Sebastiao, M., and Vaz, L. (1995) Lipases and esterases: a review of their sequences, structure and evolution. *Biotechnol Annu Rev* **1**: 315-371.

Carinato, M.E., Collin-Osdoby, P., Yang, X., Knox, T.M., Conlin, C.A., and Miller, C.G. (1998) The *apeE* gene of *Salmonella typhimurium* encodes an outer membrane esterase not present in *Escherichia coli*. *J Bacteriol* **180**: 3517-3521.

Farooqui, A.A., Horrocks, L.A., and Farooqui, T. (2000) Glycerophospholipids in brain: their metabolism, incorporation into membranes, functions, and involvement in neurological disorders. *Chem Phys Lipids* **106**: 1-29.

Flieger, A., Neumeister, B., and Cianciotto, N.P. (2002) Characterization of the gene encoding the major secreted lysophospholipase A of *Legionella pneumophila* and its role in detoxification of lysophosphatidylcholine. *Infect Immun* **70**: 6094-6106.

Galliard, T. (1971) The enzymic deacylation of phospholipids and galactolipids in plants. Purification and properties of a lipolytic acyl-hydrolase from potato tubers. *Biochem J* **121**: 379-390.

Klingsbichel, E. (1996) Esterase EstA from Pseudomonas marginata: heterologous expression, biological, biochemical, and biocatalytical characterization. Graz: Technical University of Graz.

Lau, J., Frykman, S., Regentin, R., Ou, S., Tsuruta, H., and Licari, P. (2002) Optimizing the heterologous production of epothilone D in *Myxococcus xanthus*. *Biotechnol Bioeng* **78**: 280-288.

Loebeck, M.E., and Klein, H.P. (1956) Substrates for *Myxococcus virescens* with special reference to eubacterial fractions. *J Gen Microbiol* **14**: 281-289.

Loveless, B.J., and Saier, M.H., Jr. (1997) A novel family of channel-forming, autotransporting, bacterial virulence factors. *Mol Membr Biol* **14**: 113-123.

Martinez, A., Ostrovsky, P., and Nunn, D.N. (1999) LipC, a second lipase of *Pseudomonas aeruginosa*, is LipB and Xcp dependent and is transcriptionally regulated by pilus biogenesis components. *Mol Microbiol* **34**: 317-326.

Martinez, A., and Soberon-Chavez, G. (2001) Characterization of the *lipA* gene encoding the major lipase from *Pseudomonas aeruginosa* strain IGB83. *Appl Microbiol Biotechnol* **56**: 731-735.

Moraleda-Munoz, A., and Shimkets, L.J. (2007) Lipolytic enzymes in *Myxococcus xanthus*. *J Bacteriol*.

Ollis, D.L., Cheah, E., Cygler, M., Dijkstra, B., Frolow, F., Franken, S.M., Harel, M., Remington, S.J., Silman, I., Schrag, J., and et al. (1992) The alpha/beta hydrolase fold. *Protein Eng* **5**: 197-211.

Racusen, D., and Foote, M. (1980) A major soluble glycoprotein of potato tubers. *J. Food Biochem* **4**: 43-52.

Rydel, T.J., Williams, J.M., Krieger, E., Moshiri, F., Stallings, W.C., Brown, S.M., Pershing, J.C., Purcell, J.P., and Alibhai, M.F. (2003) The crystal structure, mutagenesis, and

activity studies reveal that patatin is a lipid acyl hydrolase with a Ser-Asp catalytic dyad. *Biochemistry* **42**: 6696-6708.

Schulz, G.E. (2000) Beta-barrel membrane proteins. *Curr Opin Struct Biol* **10**: 443-447.

Snellman, E.A., Sullivan, E.R., and Colwell, R.R. (2002) Purification and properties of the extracellular lipase, LipA, of *Acinetobacter* sp. RAG-1. *Eur J Biochem* **269**: 5771-5779.

Sullivan, E.R., Leahy, J.G., and Colwell, R.R. (1999) Cloning and sequence analysis of the lipase and lipase chaperone-encoding genes from *Acinetobacter calcoaceticus* RAG-1, and redefinition of a proteobacterial lipase family and an analogous lipase chaperone family. *Gene* **230**: 277-286.

Talker-Huiber, D., Jose, J., Glieder, A., Pressnig, M., Stubenrauch, G., and Schwab, H. (2003) Esterase EstE from *Xanthomonas vesicatoria* ( *Xv*_EstE) is an outer membrane protein capable of hydrolyzing long-chain polar esters. *Appl Microbiol Biotechnol* **61**: 479-487.

Turner, M. (1995) Advances in the use of enzyme-catalyzed reactions in organic synthesis. *Trends Biotechnol* **13**: 253-258.

Wilhelm, S., Tommassen, J., and Jaeger, K.E. (1999) A novel lipolytic enzyme located in the outer membrane of *Pseudomonas aeruginosa*. *J Bacteriol* **181**: 6977-6986.

Youderian, P., Burke, N., White, D.J., and Hartzell, P.L. (2003) Identification of genes required for adventurous gliding motility in *Myxococcus xanthus* with the transposable element *mariner*. *Mol Microbiol* **49**: 555-570.